Concept study to develop a platform process for the production of antimicrobial peptides/proteins

Dissertation

Zur

Erlangung des akademischen Grades der Doktorin der Ingenieurwissenschaften

(Dr.-Ing.)

Dem Promotionszentrum für Ingenieurwissenschaften am Forschungscampus Mittelhessen

vorgelegt von

Carolin Anna Lappöhn, M.Sc.

Gießen, den 11.12.2023

Acknowledgments

I would like to express my sincere appreciation to those who have accompanied and supported me on my doctoral journey.

I would like to express my sincere thanks to my supervisors, Prof. Dr. Michael Wolff and Prof. Dr.-Ing. Peter Czermak. Their support and the opportunity to gain this experience were very important to me. I also appreciate the time they took to evaluate the results of my work.

Special thanks to Prof. Dr. Michael Wolff for giving me the opportunity to use his laboratories as part of his research group. My extensive research at the Technische Hochschule Mittelhessen (THM) - University of Applied Sciences - Institute of Bioprocess Engineering and Pharmaceutical Technology would not have been possible without the good cooperation of the various working groups. Therefore, I would like to acknowledge Prof. Dr.-Ing. Peter Czermak, the head of the institute, who made it possible for me to work in these well-structured laboratories, and provided me with numerous technical possibilities and resources. Furthermore I would like to acknowledge support from the working groups of Prof. Dr.-Ing. Denise Salzig, Prof. Dr.-Ing. Dirk Holtmann and Prof. Dr. Frank Runkel, for resources and exchange of knowledge. This exchange extended beyond the institute, as close collaboration with the Fraunhofer-Gesellschaft under the guidance of Prof. Dr. Andreas Vilcinskas provided me with valuable insights and allowed me to broaden my horizons.

In addition to the financial support of the THM from the strategic research fund, I would like to express my sincere thanks to the Johannes Hübner Foundation for giving me the opportunity to complete my thesis in a timely and independent manner. In this context, I would also like to acknowledge Richard M. Twyman's support and extend my gratitude.

I would like to thank Michaela Gilbert, Catherine Meckel-Oschmann, Dr. Sina Weidenweber and Dr. Janina Rojek for their help with administrative tasks throughout my work.

Many thanks also to all my colleagues for the great support and fruitful discussions throughout my work. Here I would like to especially thank the Downstream Group for

their support and regular exchanges, in particular my former colleagues in the office, Keven Lothert and Friederike Eilts, for the discussions and their support. Throughout my working group, I received tremendous professional and emotional support from Lisa-Marie Sittek and Lena Stillger, to whom I would like to express my sincere thanks. Furthermore, my huge thanks to the Bioprocess Engineering Group for the helpful exchanges, the pleasant cooperation, and especially for the friendly support in all phases of my work. Special thanks to Arne Oestreich, Oliver Birrenbach, Nicolas Maguire, Dustin Eckhardt, Joel Eichmann, Jan Philipp Burghardt, Oscar Kruppa, Stefan Schwarz and Hanna Dambeck. Your support and insights have more than enriched and embellished my long working days.

It has been a particular pleasure to supervise the thesis work of my students Robin Stei, Lea Maerz, Linus Georg Weber and Daria Dudnik. Helping these students to successfully complete their thesis has helped me to gain valuable insights myself. I would like to once again express my sincere gratitude to Lea. Her support for this project did not conclude with her thesis. She has proven to be a valuable discussion partner and my most discerning critic, even to this day.

I would like to take this opportunity to thank my boyfriend Jan for his understanding, his patience, but also for his distractions. Furthermore, I would like to thank my friends, especially Mareike, Vivian and Nicole for always being a source of motivation and joy for me. Lastly, I wish to express my gratitude to my family, including my parents and siblings, for their unwavering support and affection during my entire journey. They have instilled in me the importance of advocating for my own needs and believing in myself and my abilities.

Eidesstattliche Erklärung / Declaration of authorship

Ich erkläre: Ich habe die vorgelegte Dissertation selbstständig und ohne unerlaubte fremde Hilfe und nur mit den Hilfen angefertigt, die ich in der Dissertation angegeben habe. Alle Textstellen, die wörtlich oder sinngemäß aus veröffentlichten Schriften entnommen sind, und alle Angaben, die auf mündlichen Auskünften beruhen, sind als solche kenntlich gemacht. Ich stimme einer evtl. Überprüfung meiner Dissertation durch eine Antiplagiat-Software zu. Bei den von mir durchgeführten und in der Dissertation erwähnten Untersuchungen habe ich die Grundsätze guter wissenschaftlicher Praxis, wie sie in der entsprechenden Satzung der federführenden Hochschule niedergelegt sind und die mir ausgehändigt wurde, eingehalten.

I declare that I have completed this dissertation single-handedly without the unauthorized help of a second party and only with the assistance acknowledged therein. I have appropriately acknowledged and cited all text passages that are derived verbatim from or are based on the content of published work of others, and all information relating to verbal communications. I consent to the use of anti-plagiarism software to check my thesis. I have abided by the principles of good scientific conduct laid down in the regulations of the leading university, which were delivered to me in carrying out the investigations described in the dissertation.

Gießen, 23.01.2024

Carolin Lappöhn

Abstract

The increasing prevalence of antibiotic-resistant pathogens has created a demand for alternative treatments. However, the production of antimicrobial peptides and proteins (AMPs) in sufficient quantities for therapeutic use remains a significant bottleneck.

This study introduces an innovative platform technology for the heterologous production, purification, and detection of AMPs. The technology is based on a small fusion tag, called the C-tag, composed of four amino acids (EPEA) fused to the C-terminus of AMPs. Notably, using a complex model AMP, we demonstrated for the first time that the C-tag enhances the expression of this AMP in *Escherichia coli* compared to the unmodified peptide. Further process intensification increased the yield by nearly 30-fold compared to previous attempts with the same AMP. The primary advantage of the tag is apparent during product purification, leading to > 85% recovery and ~80% purity in a single step without compromising product activity, thus eliminating the need to remove the tag in a cost-intensive additional process step.

In the subsequent parts of this study, we introduce, for the first time, an analytical immunoaffinity chromatography based on the C-tag. A detailed exploration of the critical process parameters using statistical optimization techniques enabled us to achieve 98.8 ± 0.1% analyte recovery. Validation of the method indicated high specificity, linearity, accuracy, and precision, underscored by a short sample analysis time, enabling high-throughput sample screening. Further characterization of the method revealed its limited ability to detect AMPs in acidic samples (pH < 2). Pretreatment strategies to overcome these limitations are discussed. Consequently, this study introduces a quantitative C-tag platform for the in-process monitoring of AMPs.

Zusammenfassung

Die zunehmende Verbreitung von antibiotikaresistenten Pathogenen hat einen Bedarf an alternativen Behandlungsmöglichkeiten geschaffen. Die Produktion von antimikrobiellen Peptiden und Proteinen (AMPs) in ausreichenden Mengen für den therapeutischen Einsatz stellt jedoch nach wie vor einen erheblichen Engpass dar.

In dieser Studie wird eine innovative Plattformtechnologie für die heterologe Produktion, Aufreinigung und Detektion von AMPs vorgestellt. Die Technologie basiert auf einem kleinen Fusions-Tag, dem sogenannten C-Tag, der aus vier Aminosäuren (EPEA) besteht, die an den C-Terminus von AMPs fusioniert sind. Anhand eines komplexen AMP-Modells konnte erstmals gezeigt werden, dass der C-Tag die Expression dieses AMPs in *Escherichia coli* im Vergleich zum unmodifizierten Peptid erhöht. Durch eine weitere Prozessintensivierung konnte die Ausbeute im Vergleich zu früheren Arbeiten mit dem gleichen AMP um fast das 30-fache gesteigert werden. Der Hauptvorteil des Tags zeigt sich bei der Produktaufreinigung, die in einem einzigen Schritt zu einer Ausbeute von > 85% und einer Reinheit von ~80% führt, ohne die Produktaktivität zu beeinträchtigen, wodurch die Notwendigkeit entfällt, den Tag in einem kostenintensiven zusätzlichen Prozessschritt zu entfernen.

In den folgenden Teilen dieser Studie wird zum ersten Mal eine analytische Immunoaffinitätschromatographie auf der Basis des C-Tags vorgestellt. Durch eine detaillierte Untersuchung der kritischen Prozessparameter mit Hilfe statistischer Optimierungstechniken konnte eine Wiederfindung des Analyten von 98,8 ± 0,1% erreicht werden. Die Validierung der Methode zeigte eine hohe Spezifität, Linearität, Genauigkeit und Präzision, die durch eine kurze Probenanalysezeit unterstrichen wurde und ein Hochdurchsatz-Screening ermöglicht. Die weitere Charakterisierung der Methode zeigte, dass diese nur begrenzt in der Lage ist, AMPs in sauren Proben (pH < 2) nachzuweisen. Vorbehandlungsstrategien zur Überwindung dieser Einschränkungen werden diskutiert. Im Ergebnis wird eine quantitative C-Tag-Plattform für das In-Prozess-Monitoring von AMPs vorgestellt.

Table of contents

List of Abbreviations

AMP	antimicrobial peptide or protein
BiP	binding immunoglobulin protein
cDNA	complementary deoxyribonucleic acid
C-tag	C-terminal fusion tag of four amino acids (EPEA)
DNA	deoxyribonucleic acid
ELISA	enzyme-linked immunosorbent assay
ELP	elastin-like polypeptide
FDA	Food and Drug Administration
GST	glutathione S-transferase
His_6	fusion tag comprising six consecutive histidine residues
HPLC	high performance liquid chromatography
ICH	International Council for Harmonisation
IC50	half maximal inhibitory concentration
IMAC	immobilized metal-ion affinity chromatography
IMPI	insect metalloproteinase inhibitor
LPS	lipopolysaccharide
MBC	minimum bactericidal concentration
MDR	multidrug-resistant
MIC	minimum inhibitory concentration
PEG	polyethylene glycol
PTM	post-translational modification
TIMP	tissue inhibitor of metalloproteinase
Trx	thioredoxin
WHO	World Health Organization

CHAPTER 1: Introduction

The World Health Organization (WHO) warns that antibiotic resistance is on the rise, bringing us closer to a future where infections may no longer respond to antibiotics. Current broad-spectrum antibiotics are becoming less effective, leading to longer treatment durations, increased hospitalization rates, and a staggering 4.95 million deaths worldwide in 2019 from multidrug-resistant (MDR) infections.[1–3] This increase in MDR bacterial strains has intensified the demand for new antimicrobial agents.[4] Antimicrobial peptides and proteins (AMPs), with their diverse mechanisms of action, could offer a solution. However, economical processes that produce sufficient quantities of AMPs are needed, including purification, analytical control, and process monitoring.[5,6]

Chapter 1 explores the potential of AMPs, particularly those originating from insects. It considers heterologous production methods, focusing on a structurally complex model AMP and current challenges, followed by an overview of current analytical methods for product quantification. Chapters 2 and 3 describe a novel approach for the production and analysis of AMPs, and concluding perspectives are provided in Chapter 4.

1. Antimicrobial peptides and proteins

AMPs are antimicrobial oligopeptides or proteins that contribute to the innate immune system of all groups of organisms. Importantly, AMPs are encoded by genes and synthesized by ribosomes.[7] This sets them aside from the non-ribosomal defense peptides produced by bacteria and some fungi, which are usually described as bacteriocins.[8,9]

Classification of AMPs

AMPs are short peptides with fewer than 100 amino acids.[10] They vary greatly in size, amino acid composition and structure, allowing classification by source, activity, structural characteristics or amino acid enrichment (e.g., AMPs can be rich in arginine, glycine, histidine, proline or tryptophan).[11] The following sections provide an insight into the diversity and variability of AMP classifications, further summarized in Table 1.

The most common classification based on secondary structure (α-helical, β-sheet, mixed or linear).[12] The α-helical AMPs tend to be unstructured in aqueous solutions but become structured in contact with micelles and liposomes.[13] AMPs with a predominantly β-sheet structure often contains cysteine residues that are conserved and form disulfide bridges, providing stability and protection against protease degradation.[14]

Mechanisms of action

AMPs have diverse functions, including antibacterial, antifungal, antiviral, antiparasitic, anticancer, antibiofilm, immunomodulatory and anti-inflammatory activities.[11,15] These effects are highly selective because they depend on the composition and concentration of the AMP. For example, some antimicrobial activities are associated with membrane-directed AMPs, and this is advantageous because activity is dependent on the type of membrane, thus allowing the targeting of bacteria while leaving human cells unaffected.[16] Eukaryotic membranes tend to be positively charged due to the presence of zwitterions, phospholipids and cholesterol, whereas Gram-negative bacteria feature an outer membrane with abundant negatively charged lipopolysaccharides, and Gram-positive bacteria have peptidoglycans linked to the cytoplasmic membrane via negatively charged teichoic acids. The distinction between fungi and other eukaryotic membranes is thought to lie in the different sterol compositions of their membranes.[17] Depending on the interaction with the membrane, the AMP can affect membrane stability by building up peptide carpets or by forming pores, leading to depolarization, membrane disruption and cell lysis.[16] The formation of pores can facilitate the transport of additional AMPs into the cell, bringing them into contact with intracellular targets.[18] The latter are not membrane directed, and instead inhibit nucleic acid synthesis, key enzymes or other essential proteins.[16]

Potential and advantages of AMPs over common antibiotics

The advantages of AMPs reflect their diverse modes of action, targeting different microbial targets simultaneously, which reduces the likelihood of emerging microbial resistance.[19] The absence of distinct receptors presents a formidable challenge for microorganisms in terms of their ability to evolve resistance mechanisms.[10] The likelihood of resistance is further reduced by the similar minimum inhibitory concentration (MIC) and minimum bactericidal concentration (MBC) of many AMPs.[19]

The concentrations are comparable to conventional antibiotics, but in terms of molarity far fewer AMP molecules are needed.[13,19] These advantages underscore the motivation to discover and harness more AMPs for therapeutic applications.

Table 1: Overview of AMP classifications by source, structure, activity, and amino acid enrichment (*the focus of the study described in this dissertation).

Source	Structure	Activity	Amino acid enrichment
Amphibians	α-helical	Antibacterial*	Arginine
Aquatic organisms	β-sheet	Anticancer	Glycine
Insects*	Linear	Antifungal	Histidine
Mammals	Mixed*	Anti-inflammatory*	Proline
Microorganisms		Antiparasitic	Tryptophan
Plants		Antiviral	

1.1 AMPs originating from insects

The extraordinary diversity of AMPs could lead to new therapeutic approaches for a wide range of diseases. Insects provide an excellent source of potentially therapeutic AMPs because they account for ~75% of all animal species and have evolved numerous defense mechanisms to survive in many different environments.[20] Key factors that contribute to their remarkable success include their relatively short lifespan, their ability to adapt to new ecological niches and utilize a wide range of plants and animals as food, and their efficient innate immune system, making them remarkably resistant to microbial pathogens.[21,22] Unlike vertebrates, insects do not possess adaptive immunity but their innate immune system has both cellular and humoral components. The humoral responses involve the production of potent AMPs that act directly against invading microorganisms.[23,24] The production of AMPs is much more energy efficient and therefore almost 100 times faster than adaptive immune responses,[25,26] allowing the rapid resolution of infections.[27] AMPs can be detected in the hemolymph only a few hours after microbial exposure.[28,29] This rapid production of potent AMPs makes insects a valuable resource for the discovery of these molecules.[30]

Classification and antimicrobial activity of insect-derived AMPs

Insect AMPs were first identified in the 1950s,[31] but they were not comprehensively described until the 1970s, based on research focusing on *Drosophila melanogaster* and cecropid moths.[32] More than 350 insect-derived AMPs have now been identified (AMP Database, University of Nebraska, January 2023) and they have been assigned to five distinct groups: cecropins, insect defensins, glycine-rich peptides, proline-rich peptides and lysozymes.[33] Cecropins or cecropin-like peptides are linear AMPs with an amphipathic α-helical structure lacking cysteine residues. These properties confer strong activity against Gram-negative bacteria,[22,34] but they have also been shown to inhibit the growth of yeasts and filamentous fungi such as *Aspergillus* spp. and *Fusarium* spp.[30] Defensins are larger than cecropins, with a mixture of secondary structures stabilized by disulfide bridges. They are further divided into antifungal and antibacterial defensins, the latter showing strong activity against Gram-positive bacteria and weaker activity against Gram-negative bacteria.[22,35] The proline-rich and glycine-rich AMPs have selective effects depending on their composition and structure. The proline and glycine residues can be distributed in groups of two or three within specific motifs throughout the peptide or concentrated in different subdomains.[22,36,37] Finally, lysozymes are subdivided according to their amino acid sequence and tertiary structure, and can act as antibacterial enzymes by hydrolyzing peptideglycan.[38,39] This broad spectrum of AMPs enables insects to eliminate or inhibit many different types of pathogen.

2. Applications of AMPs

In the following sections, the versatility of AMPs is demonstrated through several examples covering the challenges and potential applications summarized in Table 2.

AMPs on the market

AMPs have already been developed as commercial products due to their diverse mechanisms of action, broad-spectrum antimicrobial activity, rapid effects, and the low likelihood of resistance.[40] They have long been used in the food industry as natural preservatives to inhibit the growth of microorganisms and extend product shelf life.[11,41] One example is the bacteriocin nisin, which was discovered in *Lactococcus lactis* and has been used as a food preservative for more than 60 years.[42] AMPs are also used in

agriculture, aquaculture and veterinary medicine to promote animal health and prevent infections in livestock, such as the peptide antibiotic bacitracin.[12,43] AMPs have also been used as antimicrobial drugs.[11,41] For example, colistin is used to treat serious infections with Gram-negative bacteria, and daptomycin is used to treat skin and soft tissue infections caused by Gram-positive bacteria.[44,45] Human AMPs such as LL-37 can prevent infection in chronic wounds, promoting tissue regeneration and healing.[46]

Challenges and possibilities of therapeutic AMPs

Despite the therapeutic potential of AMPs and the increasing number of candidates that have been discovered and characterized, only few have been approved for human use by the US Food and Drug Administration (FDA).[16] This reflects a number of challenges affecting the delivery, stability and safety of AMPs as drugs.

The administration of AMPs is the first challenge. For example, peptides have limited oral bioavailability due to enzymatic degradation in the gastrointestinal tract prior to systemic absorption and their limited ability to penetrate the intestinal mucosa. Intravenous administration of AMPs is limited by a short half-life due to enzymatic degradation in the bloodstream and rapid hepatic and renal clearance.[47,48] Furthermore, although many AMPs show no toxicity toward eukaryotic cells *in vitro*, systemic toxicity is rarely assessed and therefore cannot be excluded.[49] Efforts to address these challenges include PEGylation (attachment of polyethylene glycol) to prevent uptake into non-target tissues, minimize cellular toxicity, prolong the half-life of AMPs in the bloodstream, and mitigate proteolytic degradation.[50,51] Given these hurdles, most of the AMPs that have been marketed thus far have been approved for topical applications.[52] Additionally, it is noteworthy that the majority of these approvals are for analogues of natural AMPs (none from insects so far) and pertain to the treatment of infectious diseases.[48,53] These AMPs tend to be comparable in efficacy to conventional antibiotics, but one of their main advantages is their ability to kill MDR bacteria at comparable concentrations.[13] Combining antimicrobials, especially those with different targets, is a proven strategy to suppress further resistance and can also help reduce side effects and increase selectivity.[54–56] Combinations of AMPs are particularly interesting because they often demonstrate synergistic effects.[57] This synergy is a key factor in their effectiveness against resistance mechanisms in pathogenic bacteria.[58,59] The combination of AMPs with conventional antibiotics can also improve the efficacy of both antimicrobial

classes. Indeed, the high efficacy of some antimicrobial agents *in vivo* may reflect synergistic interactions with host AMPs. Here, the immune system is supported by other AMPs in its defense against pathogens.[60,61] This means that AMPs without bactericidal activity can be used as an alternative treatment for infections caused by MDR bacteria, avoiding the acquisition of further resistance traits due to strong and direct selection pressure.[62] For example, AMPs can be used in wound infections to inhibit virulence factors such as toxins, adhesion molecules or invasion factors secreted by pathogens.[63]

Table 2: Overview of potential fields of AMP application (*the focus of the study described in this dissertation).

Application				
Agriculture	Animal husbandry and aquaculture	Cosmetics	Food and feed	Medicine*

2.1 Therapeutic use of an insect metalloproteinases inhibitor

The development of topical AMP formulations should focus on the treatment of skin and soft tissue infections, which are among the most common bacterial infections in humans. The bacteria responsible for these infections are becoming increasingly resistant to common antibiotics.[64,65]

Metalloproteinases in chronic wound infections

The WHO is particularly concerned about the growing prevalence of the so called ESKAPE pathogens (*Enterococcus faecium*, *Staphylococcus aureus*, *Klebsiella pneumoniae*, *Acinetobacter baumannii*, *Pseudomonas aeruginosa* and *Enterobacter* species). These bacteria adapt rapidly and are already resistant to many common antibiotics, making them the leading cause of hospital-acquired infections.[2,66] Chronic and post-operative wounds are often colonized by *P. aeruginosa*.[67,68] The key virulence factors are M4 family metalloproteinases, which require zinc as a cofactor.[69] The *P. aeruginosa* metalloproteinase, an extracellular elastase called pseudolysin, breaks down proteins in wound fluids, skin tissue and the extracellular matrix.[70] This leads to tissue decomposition and the release of nutrients that promote bacterial growth and invasion.[70,71] Pseudolysin also inactivates components of the host immune system and induces the production of pro-inflammatory cytokines such as interleukin (IL)-8.[71–73] Its ability to digest the extracellular matrix increases the permeability of cell layers,

causing further colonization by pathogens.[74–76] The important and versatile function of pseudolysin suggests that metalloproteinase inhibitors may be promising therapeutic candidates for the treatment of chronic wound infections.

Discovery and characterization of an insect metalloproteinase inhibitor

The remarkable immune response of insects has led to the analysis of hemolymph as a source of antimicrobial compounds. Accordingly, the injection of soluble elicitors such as lipopolysaccharide (LPS) or suspensions of bacterial and fungal cells into larvae of the greater wax moth *Galleria mellonella* results in a humoral immune response in which a metalloproteinase inhibitor, known as insect metalloproteinase inhibitor (IMPI), is released into the hemolymph along with other AMPs. IMPI is a glycosylated peptide 69 amino acids in length with a molecular mass of 8364 Da. It contains 10 cysteine residues that form five disulfide bonds, increasing its chemical and thermal stability.[77,78] To identify and clone the IMPI gene, a complementary DNA (cDNA) library was prepared using immunocompetent hemocytes isolated from the hemolymph.[63,79,80] The IMPI amino acid sequence shared no similarities with vertebrate tissue inhibitors of metalloproteinases (TIMPs) or other natural metalloproteinase inhibitors.[77] This is useful because TIMPs and matrix metalloproteinases play an important role in the remodeling of the extracellular matrix during wound healing and are not inhibited by IMPI.[63] In further studies, IMPI showed activity against microbial metalloproteinases such as thermolysin and pseudolysin, making it an attractive drug candidate.[77,81,82]

The efficacy of IMPI is demonstrated by its ability to bind the active site of metalloproteinases, functioning as a molecular wedge. This leads to the cleavage of the IMPI molecule as a substrate. The IMPI structure is stabilized by five disulfide bonds plus molecular interactions with the bound zinc ion and the general β-sheet structure. IMPI therefore retains its shape and reversibly blocks the active site of the protease. The hydrolysis of the IMPI peptide bond by thermolysin is reversible. This allows the IMPI molecule to serve as a substrate for hydrolysis multiple times, explaining why the IC_{50} (half maximal inhibitory concentration) against thermolysin is only 0.6 nM.[81] The glycosylation of IMPI is not necessary for its activity, and the peptide has a molecular weight of 7679 Da in the absence of this modification.[77]

The efficacy of IMPI has been tested against *P. aeruginosa* infections *in vitro* and *ex vivo* using a thermosensitive hydrogel, revealing the ability of the peptide to restore skin cell viability, prevent necrosis in porcine wound models, and inhibit M4 metalloproteinases.[76,83] IMPI's specificity, minimal cytotoxicity, and strong inhibitory activity position it as a promising treatment for *P. aeruginosa*-infected wounds. Moreover, its potential extends to the prevention of other *Pseudomonas* infections, biofilm formation, and possibly the control of infections caused by bacteria such as *S. aureus* that also utilize M4 metalloproteinases as virulence factors.[76,83]

Challenges related to IMPI therapy

The development of IMPI as a drug candidate will require sufficient quantities of the purified product for pre-clinical and subsequent clinical tests, which is currently a bottleneck. Greater wax moth larvae do not produce enough IMPI for economically viable extraction, and the chemical synthesis of large peptides with multiple disulfide bonds is also expensive and inefficient.[84] The most promising approach is therefore the heterologous expression of IMPI, as discussed in the next section.

3. Heterologous production

In the 1980s, the expression of human insulin in *E. coli* was a milestone in genetic engineering. This made it possible to produce therapeutic proteins and laid the foundations for industrial-scale biotechnology based on the transfer of genes between organisms, allowing heterologous expression in different host cells.[85] This technology has been further developed and is now used to produce a variety of proteins in different expression systems. Many AMPs have been successfully produced in *E. coli*,[86,87] as well as other bacteria, yeast and insect cells. Each of these organisms has advantages and disadvantages that must be weighed in terms of product yield, product quality and production costs.[88,89]

3.1 Host cells for the heterologous production of IMPI

Proteins with complex post-translational modifications, like IMPI, are often produced in eukaryotic cell lines. Examples include Chinese hamster ovary (CHO) cells and insect cells, the latter often producing higher yields.[90] The following sections describe in more

detail the host cells for heterologous IMPI production described in the literature to date. Their advantages and disadvantages are discussed. These findings are summarized at the end in Table 3.

IMPI production in insect cell lines

Insect cells are the most logical choice for the production of insect proteins because the biological processes involved (transcription, mRNA processing, protein synthesis, protein folding and post-translational modifications such as glycosylation) are likely to resemble their native counterparts very closely. One of the most widely used platforms is the *D. melanogaster* Schneider 2 (S2) cell line, which is advantageous due to the availability of high-quality cell stocks, optimized media, and vectors with appropriate secretion signals and fusion tags. The latter facilitate product purification from the medium. However, the IMPI yields achieved in S2 cells have not been reported.[63] Furthermore, the discovery that glycosylation is not necessary for IMPI activity[63,77,78,91] makes it possible to use simpler and less expensive platforms based on yeast and bacteria. The activity of IMPI in the absence of glycosylation is consistent with reports showing that only proline-rich AMPs require specific glycosylation patterns for full activity.[92]

IMPI production in yeast

Yeasts such as *Pichia pastoris* are easier and less expensive to cultivate than insect and mammalian cell lines, scaling up production is more straightforward, and the robust cell growth often translates into higher product yields.[93] This capitalizes on the inherent ability of yeasts to secrete large amounts of correctly folded proteins. Differences in glycosylation mean that yeast platforms are not always suitable for the production of animal proteins because the product may not fold correctly and/or may be inactive.[91] A significant drawback is the proteolytic degradation of secreted products at high cell densities, which is particularly challenging for small, proteolytically sensitive AMPs.[94] Accordingly, a genetically modified *P. pastoris* strain (SuperMan5) was used for IMPI production, engineered to reduce protease activity and hyper-glycosylation. However, such strains tend of produce lower product yields and to be less efficient in terms of secretion, necessitating cell disruption. The yield of IMPI per gram of biomass was therefore only 0.02 mg in SuperMan5 cells.[95]

IMPI production in bacteria

Because *E. coli* is one of the most widely used production hosts, there are many strains and expression constructs available, as well as a wealth of experience and knowledge relating to cultivation, scale-up, and automation, which are simple and inexpensive. One significant drawback is the potential for process-related contamination of the product with the immunogenic bacterial LPS. A further disadvantage by using bacteria as host cells is the absence of eukaryotic post-translational modifications and the inefficient formation of disulfide bonds, which can lead to protein misfolding. In the context of AMPs, another major issue is the possibility that the product will kill the host cell.[84,93] Neither post-translational modifications nor antimicrobial activity are relevant in the case of IMPI, but the presence of multiple disulfide bonds is problematic. Signal peptides can be used to direct IMPI to the periplasm, the space between the outer and inner membranes that contains more chaperones than the cytoplasm, thus promoting folding and in theory resulting in higher yields and a simple purification process.[96] However, the production of IMPI with the corresponding signal peptide resulted in low yields of soluble product (~3 mg L^{-1}). Although solubilized IMPI was present in the periplasm, a large proportion was insoluble, possibly unfolded or misfolded, and accumulated as inclusion bodies in the cytoplasm.[97] The same approach was tested in a commercial strain of *Vibrio natriegens*. This Gram-negative marine bacterium is able to utilize low-cost carbon sources and has a high growth rate, making it ideal for biotechnological applications.[98] But even in this strain, with its high metabolic capacity, IMPI was insoluble.[97] The outcome of the periplasmic secretion approach has been inconsistent.[99] Using this strain of *V. natriegens* to secrete soluble IMPI into the medium achieved a yield of ~8.5 mg L^{-1}, which is still relatively low.[100]

Another strategy to produce peptides with multiple disulfide bonds in *E. coli* is to use genetically modified strains such as Rosetta-gami, which has mutations in the thioredoxin reductase (*trxB*) and glutathione reductase (*gor*) genes, creating an oxidative cytoplasmic milieu that promotes the formation of disulfide bonds.[84,101] Rosetta-gami strains have been able to produce active IMPI, although solubility of the product was largely attributed to the fusion tags.[83,102–105]

Overview of the IMPI expression hosts

Table 3: Comprehensive list of advantages (+) and disadvantages (–) for the use of insect cells, yeast and bacteria for the heterologous production of AMPs, including the highest reported IMPI yields.

Insect cells	Yeast	Bacteria
+ Protein folding	+ Protein folding	+ Fast growth rate
+ PTM (disulfide bonds)	+ PTM (disulfide bonds)	+ Low overall costs
+ Secretion	+ Secretion	+ Simple genetic manipulation
+ AMP activity low against host	+ Fast growth rate	+ High production yield
	+ Medium overall costs	+ (Disulfide bonds in modified
	+ AMP activity low against host	strains)
	+ Low contamination risk	+ Low contamination risk
- Slow growth rate	- Medium production yield	- Protein folding
- Long production time	- Hyper-glycosylation	- PTM
- High cultivation costs	- High protease activity	- Endotoxin (LPS)
- Low production yields		- Secretion
- High contamination risk		- AMP activity could be high
		against host
Undefined IMPI yields in *D. melanogaster* S2 cells[63]	Highest IMPI yield in *P. pastoris* SuperMan5 cells ~0.6 mg L^{-1} (0.02 mg g^{-1} biomass)[95]	Highest IMPI yield 102.4 ± 8.8 mg L^{-1} in *E. coli* BL21(DE3) cells[104,105]

(AMP, antimicrobial peptide/protein; IMPI, insect metalloproteinase inhibitor; LPS, lipopolysaccharide; PTM, post-translational modification)

4. Fusion tags for the heterologous production of proteins

A fusion tag is a short sequence that is cloned in-frame with a gene of interest so that they are translated as a single polypeptide. Fusion tags can have many different purposes, including to improve the solubility or stability of the fusion partner, to make it easier to detect and/or purify, to target a particular subcellular compartment, or to modulate functional properties such as toxicity.[89]

Fusion tags that influence product solubility

A thioredoxin fusion tag is often used to improve product solubility by providing a template for correct folding, and this is generally commensurate with product activity.[86,89] In contrast, elastin-like polypeptides (ELPs) can be used to promote the formation of protein aggregates, which can inactivate a protein and make it less toxic, but this necessitates a complex and empirical refolding process. However, many AMPs

have been expressed as soluble fusion proteins, indicating that it is not absolutely necessary to force AMPs into aggregates (inclusion bodies) to protect the host cell.[84,102,106,107]

Selecting a purification method using fusion tags

Fusion tags can also help to optimize the purification of AMPs during downstream processing, which is by far the most expensive step of the production process. The goal of downstream processing is to recover the product from the feed stream (cells and/or cultivation medium) by separating the product from process-related impurities, while maintaining its quality and activity. Various methods are used to separate the product from impurities, exploiting different physicochemical properties. For example, centrifugation exploits differences in density, filtration exploits differences in size, extraction/precipitation capitalizes on differences in solubility, and chromatography facilitates the separation of molecules based on specific interactions between the sample, stationary phase and mobile phase.[108,109]

AMPs are difficult to purify because they share many physicochemical properties with small cellular metabolites. For this reason, purification is often facilitated using fusion tags.[110] AMPs fused to ELPs transition from a soluble state to an aggregated state in response to variations in temperature or salt concentration. Consequently, aggregated fusion products can be inexpensively separated from impurities by centrifugation or filtration.[84,111] However, this approach often fails to achieve high purity and recovery. For example, only ~70% of the IMPI-ELP fusion protein was recovered after filtration and with only ~70% purity.[103] Nevertheless, in cases where endotoxins might act as potential process-related contaminants, ensuring high purity becomes imperative. Affinity chromatography is therefore preferred for the recovery of AMPs with fusion tags, even though it is a more expensive method.[84,106,111]

Fusion tags for affinity chromatography

Affinity chromatography is based on specific interactions between a target molecule (in this case a fusion tag) and an affinity ligand that is coupled to a chromatography matrix (stationary phase). This ensures that only molecules with the tag bind to the column. Importantly, the interaction is always reversible. In the initial step, a mixture containing the desired target, which has a high affinity for the ligand, is applied to the column. The

target molecule binds to the immobilized ligands while other molecules pass through the column in the flow-through fraction. Some impurities may bind weakly to the column, so a washing step is used to remove them. Finally, the buffer conditions are changed to weaken the interaction between the fusion tag and the affinity ligand, allowing the target product to be collected in the elution fraction. This can be achieved by changing the buffer pH, ionic strength, or by introducing competitive agents. The simplicity and selectivity of affinity chromatography make it the method of choice for product purification, particularly as a capture step immediately after cell harvesting and clarification.[112,113] Antibodies or antibody-based molecules are often immobilized on the column as the capture agent (immunoaffinity chromatography) because antibodies naturally have a very high affinity for their specific antigens. However, if the binding affinity is too high it may be necessary to use harsh elution conditions that risk damaging the product. Immunoaffinity chromatography columns are also expensive and sensitive to fouling by certain impurities.[114]

Fusion tags and affinity chromatography provide a useful platform for the purification of AMPs because the same set of optimized methods can be used for any target protein. The aim of platform technology is to make the production of heterologous proteins more efficient and cost-effective, and to reduce the effort required to optimize the production and purification process.[115,116]

Common fusion tags and limitations

The best known and most widely used fusion tags are glutathione S-transferase (GST) and hexahistidine (His_6).[117] Like thioredoxin, GST is used to improve the solubility of its fusion partners, although some GST fusion proteins are nevertheless insoluble.[117,118] One of the main benefits of the GST tag is the ease of product purification, because the tag binds with high affinity to glutathione immobilized on the stationary phase. This binding can be reversed by adding reduced glutathione under mild conditions, releasing the fusion product from the matrix.[119] The GST tag is also easy to detect and quantify using antibodies or enzyme assays.[118] One disadvantage of the GST tag for AMP production is that it is much larger (~26 kDa) than its peptide fusion partner, which can reduce the AMP yield compared to other tags. For example, the yield of GST-IMPI (35 kDa) was 6 mg L^{-1}, but IMPI accounted for only a quarter of the total.[105] The large

size of the GST tag can also increase the susceptibility of the product to proteolytic degradation.[117,120,121]

The His_6 tag (six consecutive histidine residues) overcomes the size-related issues discussed above and its small size rarely influences the folding or activity of its fusion partner. Although this means the His_6 tag does not generally improve product solubility or stability, it does facilitate detection using antibodies and purification using antibodies or, more commonly, chelated metal ions as affinity ligands, the latter method known as immobilized metal ion affinity chromatography (IMAC).[122,123] The binding of His_6 to metal ions can be reversed by adding imidazole to the elution buffer.[106] However, despite these mild elution conditions, product aggregation is often reported and purification is moderately efficient at best.[124] The later reflects the contamination of products with copurified histidine-containing host cell proteins.[122,125,126] IMAC resins are less expensive than glutathione resins, but the leaching of toxic metal ions such as nickel into the product solution (and during regeneration into the waste water), as well as poor batch-to-batch reproducibility, make it unsuitable for large-scale production.[123,127]

The main disadvantage of most tags is that they have to be removed. The GST tag is so large that leaving it in place would impair the function of the product.[119,122] In contrast, the limited impact of the His_6 tag means that it is often left on the product for laboratory research and preclinical development, but for clinical testing and in marketed products it must be removed due to the risk of adverse immunological reactions.[116,127,128]

Tags can be removed by chemical treatment, but the effects are nonspecific and may therefore damage other parts of the product.[118,129] The typical approach is therefore enzymatic cleavage using specific proteases, but this requires long incubation times and the enzymes are expensive, and subsequent purification is necessary to separate the product from the free tag and the enzyme.[130] In addition, even specific proteases may have some activity at non-target sites, resulting in product degradation and lower yields.[131] This is another reason why tags are rarely used for large-scale production.[111] With market pressure for shorter production times and more economical manufacturing, companies will be forced to implement effective strategies to ensure the high purity and efficient recovery of target proteins. It would be advantageous if a tag could be used as a manufacturing platform without the need to separate it from the product.

4.1 The C-tag as a platform technology for the purification of AMPs

C-tag advantages and usage

The C-tag consists of only four amino acids: glutamic acid, proline, glutamic acid and alanine (EPEA). It is attached to the C-terminus of its fusion partner (hence its name) and its small size does not affect the activity, stability or solubility of the final product.[132,133] This would be highly beneficial for the expression of very small AMPs, although there have been no reports of such an application thus far. However, the C-tag has been extensively explored with larger proteins, including vaccine candidates. It had no effect on the immunogenicity of the RH5.1 malaria vaccine, implying that the C-tag can be retained on the final product without deviating from current good manufacturing practice (cGMP).[134,135] Accordingly, the C-tag was used in vaccine candidates developed during the COVID-19 pandemic, demonstrating its potential as a platform technology for commercial large-scale production.[136,137] The C-tag not only eliminates the need for cleavage and a post-cleavage purification step, but facilitates product purification directly from a supernatant or crude bacterial lysate by immunoaffinity chromatography with yields exceeding 80%, achieving more than 70% purity in a single step.[135,138]

Challenges of immunoaffinity chromatography

For a long time, immunoaffinity chromatography was rarely used at the industrial scale due to high costs, the large size of the equipment and the low stability of the resins.[138] However, the large-scale production of many therapeutic proteins now relies on this method for product capture and for the removal of specific impurities such as endotoxins.[105,127,140]

Single-chain antibody resins are now being used in cGMP production campaigns because they overcome many of the limitations of conventional monoclonal antibodies.[135,141,142] Unlike typical immunoglobulin G (IgG) antibodies, which consist of two identical heavy (H)-chains and two identical light (L)-chains, camelid antibodies consist only of two H-chains and are therefore also known as nanobodies or H-chain antibodies (HCAbs), as shown in Figure 1.[143] They are easily purified from serum because the antigen-binding fragment interacts with parts of the target that are less antigenic to conventional antibodies. This is because the Fab fragment responsible for

epitope recognition is reduced to a single variable domain (VHH).[144,145] Nanobodies are also easy to express in microbial systems because, unlike conventional antibodies, there is only one type of polypeptide and therefore no need to assemble complex multiprotein complexes.[144] They also show excellent solubility, stability even under challenging environmental conditions, high affinity and specificity for the target antigen, compact size and strictly monomeric behavior, which makes them ideal as long-lasting selective ligands for affinity chromatography.[139,144]

C-tag purified by immunoaffinity chromatography

To develop an affinity matrix for the C-tag, a dromedary was immunized with α-synuclein and the resulting nanobodies (NbSyn2) were developed into the CaptureSelect C-tag affinity resin by BAC B.V., Netherlands (now part of Thermo Fisher Scientific), as schematically illustrated in Figure 1. This resin is used for the purification of C-tagged proteins, with high affinity and selectivity, even in the presence of urea and guanidine HCl, from complex mixtures such as cytoplasmic and periplasmic fractions in a single step.[132,135,139] The C-tagged product is eluted under mild conditions at neutral pH using magnesium chloride, propylene glycol or competitive peptides with the SEPEA sequence. This ensures the recovery of pH-sensitive target proteins and retains their activity. For products that are not pH sensitive, such as IMPI and many other AMPs, elution can also be achieved by lowering the pH using citric acid or glycine.[137,138,146] This doubles as a low-pH virus inactivation step, which is required for products from animal cell lines.[147]

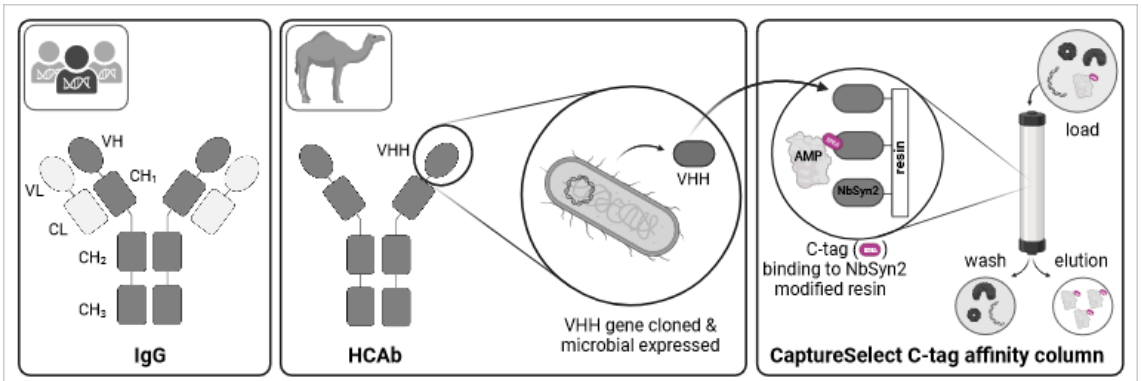

Figure 1: A schematic representation of a classical IgG antibody. The dark-colored heavy chains (H) and bright-colored light chains (L) each comprise rectangular constant domains (C) and oval variable domains (V). In comparison, a camelid HCAb contains only heavy chains. The antigen-binding, single-domain fragment (VHH) from HCAb can be cloned, expressed and immobilized on a matrix to produce CaptureSelect C-Tag resin, which can be used to capture AMPs carrying a C-tag. (Created with BioRender.com)

5. Analytical methods for AMP detection

The production of AMPs requires effective analytical methods to evaluate the efficiency of the process, including product detection and quantification. The amount of protein can be determined by weighing the solid product or by quantitative amino acid analysis but these methods are time consuming and too expensive for routine sample analysis. Methods that allow the approximate content to be determined against a defined standard are sufficient and the most common methods used during the heterologous production of AMPs are evaluated below. We distinguish between protein quantification and product quantification. Some methods measure the total protein content of the sample, whereas others measure the specific product content in a protein mixture.

5.1 Protein quantification

Spectrophotometry

Proteins can be quantified by spectrophotometry, although this is an insensitive method and therefore only suitable for concentrated solutions. It is typically used after protein purification to determine the total protein content of a sample. The spectral absorption or emission properties of proteins are measured at a defined wavelength in a light path, and this can be used to determine the concentration of a protein solution relative to a set of standards. Absorbance is often measured at 280 nm because the aromatic amino acids tryptophan and tyrosine (and to a lesser extent phenylalanine) absorb at this wavelength. This is useful for mixed protein solutions, but care must be taken when measuring a specific protein because the absorbance is dependent on the amino acid sequence. Appropriate standards must therefore be selected for comparison. Absorbance can also be measured at 205 nm, which is based on the absorption properties of peptide bonds. However, a large number of buffer substances and some amino acids also absorb at this wavelength, which can cause interference.[148–150]

Colorimetry

Colorimetry is more sensitive and less susceptible to interference than spectrophotometry. Examples include the bicinchoninic acid (BCA) assay and the Bradford assay, where the protein content of a solution is quantified by measuring the color intensity produced by color-forming reagents when they react with the functional

groups of proteins. The color intensity is correlated with the concentration of the reacting group, which can be measured using a spectrophotometer. However, problems with these methods include the protein-specific variation, which can reach 20% with more complex protein mixtures, and the presence of interfering substances that can produce incorrect measurements. It is important to specify the stain or method used and to provide information on the amino acid sequence of the standard protein. Other process parameters, such as pH and temperature, may also affect the results. Due to the subjective nature of these staining assays and the non-specific quantification of total proteins, they should only be used for product quantification with pure samples that are similar to the standard.[151,152]

Densitometry

Densitometry is based on a similar principle to colorimetry, but in this case the proteins in a sample are separated by gel electrophoresis according to their size and/or charge before staining, and the densitometer then measures the light absorption at different points on the gel. Generally, a moving light source is passed over the gel and the readings at different positions are converted into values representing the color intensity of bands or spots. The number of steps involved makes this method less suitable for large sample numbers and all the disadvantages of colorimetric methods also apply. However, it does not necessarily require a pure product because the impurities are separated from the product during electrophoresis.[153–155]

5.2 Product quantification

Enzyme-linked immunosorbent assay

The enzyme-linked immunosorbent assay (ELISA) is a quantitative analytical method that uses antibodies conjugated to enzymes as a means to measure the concentration of a specific target protein. The conjugated enzyme catalyzes a colorimetric reaction, allowing the protein concentration to be determined by spectrophotometry. The preferred ELISA format is the sandwich ELISA, which requires two specific antibodies that recognize different epitopes on the target, increasing the sensitivity up to 5-fold by reducing the likelihood of interference. In a sandwich ELISA, the first antibody is immobilized on a surface and captures the antigen from the sample, allowing impurities to be washed away. The second antibody, which is conjugated to the enzyme, is then

used to detect the antigen. After another wash to remove unbound antibody, the substrate for the colorimetric reaction is added, and the intensity of the colored product is used to determine the product concentration relative to a set of standards.[156,157]

A major advantage of the sandwich ELISA is that it is suitable for high-throughput screening without sacrificing sensitivity and specificity, resulting in low detection limits and fast results.[157] Antibodies are available for common fusion tags, and can be combined with antibodies against the product, which are in any case necessary if the tag is removed. However, the production of such antibodies is expensive and time consuming, often requiring the immunization of animals. Furthermore, sandwich ELISAs may not be suitable for many AMPs because the small size of the product makes it difficult for two antibodies to bind simultaneously.[158–160] The C-tag is advantageous in this context because there is no need to remove it from the AMP, enabling the use of one antibody recognizing the C-tag and another recognizing the AMP product.[134,135]

Analytical immunoaffinity with high performance liquid chromatography

The principle is similar to affinity purification (described above) but the resins used for high-performance liquid chromatography (HPLC) consist of smaller particles, allowing higher pressures to be applied and improving the resolution and speed of separation. Only small sample volumes (a few microliters) are applied to the column but the binding capacity is never reached. Harsh elution conditions can be applied because the samples are discarded post-analysis and functional products are not required. Accurate quantification requires a high-affinity ligand to ensure that all product molecules are captured, as well as efficient elution to ensure the complete release of all product molecules. The product can be detected by in-line spectroscopy, in which the absorption over time is recorded at a specific wavelength, and quantification is based on the elution peak area.[161,162] This method has yet to be used for the quantification of AMPs, but protein A analytical chromatography is often used for the high-throughput quantification of antibodies due to its precision, selectivity and low limits of quantitation. Compared to the ELISA, fewer steps are required, interactions are less sensitive to matrix effects, and there is no need for two product-specific antibodies. In both methods, it is essential to ensure strong interactions between the ligand and product for accurate quantification. The HPLC method requires complete elution for accurate quantification, whereas both

the ligand and product are discarded following an ELISA. However, analytical HPLC columns are very expensive. One reason for the success of protein A columns is that they can be used for the detection of most classical antibodies during large-scale commercial production. This advantage is seldom found with fusion tags, which are often used for smaller-scale experiments.[163–165]

6. Scope of the presented studies

The potential of insect-derived AMPs to treat a wide range of microbial diseases has long been recognized and is an integral part of many research efforts. However, the large-scale production of these AMPs is required for further studies and therapeutic applications. Some approaches, such as the enzymatic cleavage of fusion tags, are not economically viable for large-scale production. The detection and quantification of these AMPs is also challenging, but crucial for the assessment of process efficiency and product quality.

The aim of this dissertation project is to develop and establish a platform technology for the production, purification and quantification of AMPs. This technology will be based on the C-tag and will be demonstrated using IMPI, a complex and difficult-to-produce model AMP. The work will be divided into three parts: first, the production of IMPI, focusing on how to produce sufficient quantities of the active product when using the C-tag; secondly, demonstration of IMPI purification using the C-tag; and third, the comprehensive platform will be used to accurately quantify C-tagged AMPs throughout the production process using analytical immunoaffinity chromatography and the C-tag for the first time.

References

1. WHO. Prioritization of Pathogens to Guide Discovery, Research and Development of New Antibiotics for Drug-Resistant Bacterial Infections, Including Tuberculosis. (2017) ISBN: 9789240026438 https://apps.who.int/iris/handle/10665/311820 (retrieved Aug 2019).

2. Mestrovic, T. *et al.* The burden of bacterial antimicrobial resistance in the WHO European region in 2019: a cross-country systematic analysis. *Lancet Public Heal.* **7**, e897–e913 (2022) doi:10.1016/S2468-2667(22)00225-0.

3. Naghavi, M. Global burden of bacterial antimicrobial resistance in 2019: a systematic analysis. *Lancet* **399**, 629–655 (2022) doi:10.1016/S0140-6736(21)02724-0.

4. Neubauer, D. *et al.* Retro analog concept: comparative study on physico-chemical and biological properties of selected antimicrobial peptides. *Amino Acids* **49**, 1755–1771 (2017) doi:10.1007/s00726-017-2473-7.

5. Zhang, L. & Gallo, R. L. Antimicrobial peptides. *CellPress Curr. Biol.* **26**, 14–19 (2016) doi:10.1007/978-3-319-29785-9_6.

6. Arash, I. & Gallo, R. L. Antimicrobial peptides. *Am. Acad. Dermatology* **52**, 381–390 (2005) doi:10.1007/978-3-319-29785-9_6.

7. Ganz, T. The role of antimicrobial peptides in innate immunity. *Integr. Comp. Biol.* **43**, 300–304 (2003) doi:10.1093/icb/43.2.300.

8. Hazam, P. K., Goyal, R. & Ramakrishnan, V. Peptide based antimicrobials: Design strategies and therapeutic potential. *Prog. Biophys. Mol. Biol.* **142**, 10–22 (2019) doi:10.1016/j.pbiomolbio.2018.08.006.

9. Wiesner, J. & Vilcinskas, A. Antimicrobial peptides: The ancient arm of the human immune system. *Virulence* **1**, 440–464 (2010) doi:10.4161/viru.1.5.12983.

10. Laverty, G., Gorman, S. P. & Gilmore, B. F. The potential of antimicrobial

peptides as biocides. *Int. J. Mol. Sci.* **12**, 6566–6596 (2011) doi:10.3390/ijms12106566.

11. Huan, Y., Kong, Q., Mou, H. & Yi, H. Antimicrobial Peptides: Classification, Design, Application and Research Progress in Multiple Fields. *Front. Microbiol.* **11**, 1–21 (2020) doi:10.3389/fmicb.2020.582779.

12. Erdem Büyükkiraz, M. & Kesmen, Z. Antimicrobial peptides (AMPs): A promising class of antimicrobial compounds. *J. Appl. Microbiol.* **132**, 1573–1596 (2022) doi:10.1111/jam.15314.

13. Brogden, K. A. Antimicrobial peptides: pore formers or metabolic inhibitors in bacteria? *Nat. Rev. Microbiol.* **3**, 238–250 (2005) doi:10.1038/nrmicro1098.

14. Dhople, V., Krukemeyer, A. & Ramamoorthy, A. The human beta-defensin-3, an antibacterial peptide with multiple biological functions. *Biochim. Biophys. Acta - Biomembr.* **1758**, 1499–1512 (2006) doi:10.1016/j.bbamem.2006.07.007.

15. Hancock, R. E. W., Haney, E. F. & Gill, E. E. The immunology of host defence peptides: beyond antimicrobial activity. *Nat. Rev. Immunol.* **16**, 321–334 (2016) doi:10.1038/nri.2016.29.

16. Kumar, P., Kizhakkedathu, J. N. & Straus, S. K. Antimicrobial peptides: Diversity, mechanism of action and strategies to improve the activity and biocompatibility in vivo. *Biomolecules* **8**, (2018) doi:10.3390/biom8010004.

17. Yeaman, M. R. & Yount, N. Y. Mechanisms of Antimicrobial Peptide Action and Resistance. *Pharmacol. Rev.* **55**, 27–55 (2003) doi:10.1124/pr.55.1.2.

18. Li, Y., Xiang, Q., Zhang, Q., Huang, Y. & Su, Z. Overview on the recent study of antimicrobial peptides: Origins, functions, relative mechanisms and application. *Peptides* **37**, 207–215 (2012) doi:10.1016/j.peptides.2012.07.001.

19. Marr, A. K., Gooderham, W. J. & Hancock, R. E. Antibacterial peptides for therapeutic use: obstacles and realistic outlook. *Curr. Opin. Pharmacol.* **6**, 468–472 (2006) doi:10.1016/j.coph.2006.04.006.

20. Ratcliffe, N. A., Mello, C. B., Garcia, E. S., Butt, T. M. & Azambuja, P. Insect natural products and processes: New treatments for human disease. *Insect Biochem. Mol. Biol.* **41**, 747–769 (2011) doi:10.1016/j.ibmb.2011.05.007.

21. Hoffmann, J. A., Kafatos, F. C., Janeway, C. A. & Ezekowitz, R. A. Phylogenetic perspectives in innate immunity. *Science* **284**, 1313–1318 (1999) doi:10.1126/science.284.5418.1313.

22. Bulet, P. & Stöcklin, R. Insect Antimicrobial Peptides: Structures, Properties and Gene Regulation. *Protein Pept. Lett.* **12**, 3–11 (2005) doi:10.3724/SP.J.1141.2010.01027.

23. Hoffmann, J. A. Innate immunity of insects. *Curr. Opin. Immunol.* **7**, 4–10 (1995) doi:10.1016/0952-7915(95)80022-0.

24. Gillespie, J. P., Kanost, M. R. & Trenczek, T. Biological mediators of insect immunity. *Annu. Rev. Entomol.* **42**, 611–643 (1997) doi:10.1146/annurev.ento.42.1.611.

25. Boman, H. G. Antibacterial peptides: Key components needed in immunity. *Cell* **65**, 205–207 (1991) doi:10.1016/0092-8674(91)90154-Q.

26. Boman, H. G. Peptide antibiotics and their role in innate immunity. *Annu. Rev. Immunol.* **13**, 61–92 (1995) doi:10.1146/annurev.iy.13.040195.000425.

27. Hultmark, D. Ancient relationships. *Nature* **367**, 116–117 (1994) doi:10.1038/367116a0.

28. Meister, M., Lemaitre, B. & Hoffmann, J. A. Antimicrobial peptide defense in Drosophila. *BioEssays* **19**, 1019–1026 (1997) doi:10.1002/bies.950191112.

29. Otvos, L. Antibacterial peptides isolated from insects. *J. Pept. Sci.* **6**, 497–511 (2000) doi:10.1002/1099-1387(200010)6:10<497::AID-PSC277>3.0.CO;2-W.

30. Bulet, P., Charlet, M. & Hetru, C. Antimicrobial Peptides in Insect Immunity. in *Innate Immunity* (eds. Ezekowitz, R. A. B. & Hoffmann, J. A.) 89–107 (Humana Press, 2003). doi:10.1007/978-1-59259-320-0_5.

31. Briggs, J. D. Humoral immunity in lepidopterous larvae. *J. Exp. Zool.* **138**, 155–188 (1958) doi:10.1002/jez.1401380106.

32. Boman, H. G., Nilsson, I. & Rasmuson, B. Inducible antibacterial defence system in Drosophila. *Nature* **237**, 232–235 (1972) doi:10.1038/237232a0.

33. Hwang, J.-S. *et al.* Isolation and Characterization of a Defensin-Like Peptide (Coprisin) from the Dung Beetle, Copris tripartitus. *Int. J. Pept.* **2009**, 1–5 (2009) doi:10.1155/2009/136284.

34. Brady, D., Grapputo, A., Romoli, O. & Sandrelli, F. Insect cecropins, antimicrobial peptides with potential therapeutic applications. *Int. J. Mol. Sci.* **20**, (2019) doi:10.3390/ijms20235862.

35. Tonk, M. *et al.* Tribolium castaneum defensins are primarily active against Gram-positive bacteria. *J. Invertebr. Pathol.* **132**, 208–215 (2015) doi:10.1016/j.jip.2015.10.009.

36. Ball, L. J., Kühne, R., Schneider-Mergener, J. & Oschkinat, H. Recognition of proline-rich motifs by protein-protein-interaction domains. *Angew. Chemie - Int. Ed.* **44**, 2852–2869 (2005) doi:10.1002/anie.200400618.

37. Tavares, L. S. *et al.* Antimicrobial activity of recombinant Pg-AMP1, a glycine-rich peptide from guava seeds. *Peptides* **37**, 294–300 (2012) doi:10.1016/j.peptides.2012.07.017.

38. Hultmark, D. Insect lysozymes. *EXS* **75**, 87–102 (1996) doi:10.1007/978-3-0348-9225-4_6.

39. Matsuura, K., Tamura, T., Kobayashi, N., Yashiro, T. & Tatsumi, S. The antibacterial protein lysozyme identified as the termite egg recognition pheromone. *PLoS One* **2**, (2007) doi:10.1371/journal.pone.0000813.

40. Wang, Z. & Wang, G. APD: The antimicrobial peptide database. *Nucleic Acids Res.* **32**, 590–592 (2004) doi:10.1093/nar/gkh025.

41. Johnson, E. M. *et al.* Bacteriocins as food preservatives: Challenges and

emerging horizons. *Crit. Rev. Food Sci. Nutr.* **58**, 2743–2767 (2018) doi:10.1080/10408398.2017.1340870.

42. Khan, I. & Oh, D.-H. Integration of nisin into nanoparticles for application in foods. *Innov. Food Sci. Emerg. Technol.* **34**, 376–384 (2016) doi:10.1016/j.ifset.2015.12.013.

43. Wang, Q. *et al.* Optimization of Inexpensive Agricultural By-Products as Raw Materials for Bacitracin Production in Bacillus licheniformis DW2. *Appl. Biochem. Biotechnol.* **183**, 1146–1157 (2017) doi:10.1007/s12010-017-2489-1.

44. Cirioni, O. *et al.* Colistin enhances therapeutic efficacy of daptomycin or teicoplanin in a murine model of multiresistant *Acinetobacter baumannii* sepsis. *Diagn. Microbiol. Infect. Dis.* **86**, 392–398 (2016) doi:10.1016/j.diagmicrobio.2016.09.010.

45. Ongey, E. L., Pflugmacher, S. & Neubauer, P. Bioinspired designs, molecular premise and tools for evaluating the ecological importance of antimicrobial peptides. *Pharmaceuticals* **11**, 1–28 (2018) doi:10.3390/ph11030068.

46. Tjabringa, G. S., Rabe, K. F. & Hiemstra, P. S. The human cathelicidin LL-37: A multifunctional peptide involved in infection and inflammation in the lung. *Pulm. Pharmacol. Ther.* **18**, 321–327 (2005) doi:10.1016/j.pupt.2005.01.001.

47. Vlieghe, P., Lisowski, V., Martinez, J. & Khrestchatisky, M. Synthetic therapeutic peptides: science and market. *Drug Discov. Today* **15**, 40–56 (2010) doi:10.1016/j.drudis.2009.10.009.

48. Vaara, M. New approaches in peptide antibiotics. *Curr. Opin. Pharmacol.* **9**, 571–576 (2009) doi:10.1016/j.coph.2009.08.002.

49. Seo, M. D., Won, H. S., Kim, J. H., Mishig-Ochir, T. & Lee, B. J. Antimicrobial peptides for therapeutic applications: A review. *Molecules* **17**, 12276–12286 (2012) doi:10.3390/molecules171012276.

50. Reinhardt, A. & Neundorf, I. Design and Application of Antimicrobial Peptide Conjugates. *Int. J. Mol. Sci.* **17**, (2016) doi:10.3390/ijms17050701.

51. Veronese, F. M. & Mero, A. The Impact of PEGylation on Biological Therapies. *BioDrugs* **22**, 315–329 (2008) doi:10.2165/00063030-200822050-00004.

52. Dijksteel, G. S., Ulrich, M. M. W., Middelkoop, E. & Boekema, B. K. H. L. Review: Lessons Learned From Clinical Trials Using Antimicrobial Peptides (AMPs). *Front. Microbiol.* **12**, (2021) doi:10.3389/fmicb.2021.616979.

53. Divyashree, M. *et al.* Clinical Applications of Antimicrobial Peptides (AMPs): Where do we Stand Now? *Protein Pept. Lett.* **26**, 1–15 (2019) doi:10.2174/0929866526666190925152957.

54. Zimmermann, G. R., Lehár, J. & Keith, C. T. Multi-target therapeutics: when the whole is greater than the sum of the parts. *Drug Discov. Today* **12**, 34–42 (2007) doi:10.1016/j.drudis.2006.11.008.

55. Turnidge, J. Drug-Drug Combinations. in *Fundamentals of Antimicrobial Pharmacokinetics and Pharmacodynamics* (eds. Vinks, A. A., Derendorf, H. & Mouton, J. W.) 153–198 (Springer New York, 2014). doi:10.1007/978-0-387-75613-4_8.

56. Chou, T.-C. Theoretical Basis, Experimental Design, and Computerized Simulation of Synergism and Antagonism in Drug Combination Studies. *Pharmacol. Rev.* **58**, 621–681 (2006) doi:10.1124/pr.58.3.10.

57. Chen, X. *et al.* Synergistic effect of antibacterial agents human β-defensins, cathelicidin LL-37 and lysozyme against *Staphylococcus aureus* and *Escherichia coli*. *J. Dermatol. Sci.* **40**, 123–132 (2005) doi:10.1016/j.jdermsci.2005.03.014.

58. Guilhelmelli, F. *et al.* Antibiotic development challenges: the various mechanisms of action of antimicrobial peptides and of bacterial resistance. *Front. Microbiol.* **4**, (2013) doi:10.3389/fmicb.2013.00353.

59. LaRock, C. N. & Nizet, V. Cationic antimicrobial peptide resistance mechanisms of streptococcal pathogens. *Biochim. Biophys. Acta - Biomembr.* **1848**, 3047–3054 (2015) doi:10.1016/j.bbamem.2015.02.010.

60. Zharkova, M. S. *et al.* Application of Antimicrobial Peptides of the Innate

Immune System in Combination With Conventional Antibiotics—A Novel Way to Combat Antibiotic Resistance? *Front. Cell. Infect. Microbiol.* **9**, (2019) doi:10.3389/fcimb.2019.00128.

61. Knappe, D., Kabankov, N., Herth, N. & Hoffmann, R. Insect-derived short proline-rich and murine cathelicidin-related antimicrobial peptides act synergistically on Gram-negative bacteria in vitro. *Future Med. Chem.* **8**, 1035–1045 (2016) doi:10.4155/fmc-2016-0083.

62. Travis, J. & Potempa, J. Bacterial proteinases as targets for the development of second-generation antibiotics. *Biochim. Biophys. Acta* **1477**, 35–50 (2000) doi:10.1016/s0167-4838(99)00278-2.

63. Clermont, A. *et al.* Cloning and expression of an inhibitor of microbial metalloproteinases from insects contributing to innate immunity. *Biochem. J.* **382**, 315–322 (2004) doi:10.1042/bj20031923.

64. Eckmann, C. & Dryden, M. Treatment of complicated skin and soft-tissue infections caused by resistant bacteria: value of linezolid, tigecycline, daptomycin and vancomycin. *Eur. J. Med. Res.* **15**, 554 (2010) doi:10.1186/2047-783X-15-12-554.

65. Shilpa Amara Robert T. Adamson, I. L. & Huang, X. Clinical response at Day 3 of therapy and economic outcomes in hospitalized patients with acute bacterial skin and skin structure infection (ABSSSI). *Curr. Med. Res. Opin.* **29**, 869–877 (2013) doi:10.1185/03007995.2013.803056.

66. Santajit, S. & Indrawattana, N. Mechanisms of Antimicrobial Resistance in ESKAPE Pathogens. *Biomed Res. Int.* **2016**, 2475067 (2016) doi:10.1155/2016/2475067.

67. Guillamet, C. V. & Kollef, M. H. How to stratify patients at risk for resistant bugs in skin and soft tissue infections? *Curr. Opin. Infect. Dis.* **29**, 116–123 (2016) doi:10.1097/QCO.0000000000000244.

68. Raffaele Serra Raffaele Grande, L. B. A. R. U. F. S. B. C. B. A. L. G. & de Franciscis, S. Chronic wound infections: the role of *Pseudomonas aeruginosa*

and *Staphylococcus aureus*. *Expert Rev. Anti. Infect. Ther.* **13**, 605–613 (2015) doi:10.1586/14787210.2015.1023291.

69. Hasan, R., Rony, M. N. H. & Ahmed, R. In silico characterization and structural modeling of bacterial metalloprotease of family M4. *J. Genet. Eng. Biotechnol.* **19**, (2021) doi:10.1186/s43141-020-00105-y.

70. Schmidtchen, A., Holst, E., Tapper, H. & Björck, L. Elastase-producing *Pseudomonas aeruginosa* degrade plasma proteins and extracellular products of human skin and fibroblasts, and inhibit fibroblast growth. *Microb. Pathog.* **34**, 47–55 (2003) doi:10.1016/S0882-4010(02)00197-3.

71. Van Delden, C. & Iglewski, B. H. Cell-to-cell signaling and *Pseudomonas aeruginosa* infections. *Emerg. Infect. Dis.* **4**, 551–560 (1998) doi:10.3201/eid0404.980405.

72. Azghani, A. O. *et al.* Mechanism of fibroblast inflammatory responses to *Pseudomonas aeruginosa* elastase. *Microbiology* **160**, 547–555 (2014) doi:10.1099/mic.0.075325-0.

73. Kon, Y. *et al.* The role of *Pseudomonas aeruginosa* elastase as a potent inflammatory factor in a rat air pouch inflammation model. *FEMS Immunol. Med. Microbiol.* **25**, 313–321 (1999) doi:10.1111/j.1574-695X.1999.tb01356.x.

74. Van Itallie, C. M. & Anderson, J. M. The Molecular Physiology of Tight Junction Pores. *Physiology* **19**, 331–338 (2004) doi:10.1152/physiol.00027.2004.

75. Jacobsen, J. N., Andersen, A. S. & Krogfelt, K. A. Impact of *Pseudomonas aeruginosa* quorum sensing on cellular wound healing responses in vitro. *Scand. J. Infect. Dis.* **44**, 615–619 (2012) doi:10.3109/00365548.2011.653583.

76. Eisenhardt, M. *et al.* The therapeutic potential of the insect metalloproteinase inhibitor against infections caused by *Pseudomonas aeruginosa*. *J. Pharm. Pharmacol.* **71**, 316–328 (2019) doi:10.1111/jphp.13034.

77. Wedde, M., Weise, C., Kopacek, P., Franke, P. & Vilcinskas, A. Purification and characterization of an inducible metalloprotease inhibitor from the hemolymph of

greater wax moth larvae, *Galleria mellonella*. *Eur. J. Biochem.* **255**, 535–543 (1998) doi:10.1046/j.1432-1327.1998.2550535.x.

78. Wedde, M., Weise, C., Nuck, R., Altincicek, B. & Vilcinskas, A. The insect metalloproteinase inhibitor gene of the lepidopteran *Galleria mellonella* encodes two distinct inhibitors. *Biol. Chem.* **388**, 119–127 (2007) doi:10.1515/BC.2007.013.

79. Schuhmann, B., Seitz, V., Vilcinskas, A. & Podsiadlowski, L. Cloning and expression of gallerimycin, an antifungal peptide expressed in immune response of greater wax moth larvae, *Galleria mellonella*. *Arch. Insect Biochem. Physiol.* **53**, 125–133 (2003) doi:10.1002/arch.10091.

80. Seitz, V. *et al.* Identification of immunorelevant genes from greater wax moth (*Galleria mellonella*) by a subtractive hybridization approach. *Dev. Comp. Immunol.* **27**, 207–215 (2003) doi:10.1016/S0145-305X(02)00097-6.

81. Arolas, J. L., Botelho, T. O., Vilcinskas, A. & Gomis-Rüth, F. X. Structural evidence for standard-mechanism inhibition in metallopeptidases from a complex poised to resynthesize a peptide bond. *Angew. Chemie - Int. Ed.* **50**, 10357–10360 (2011) doi:10.1002/anie.201103262.

82. Vilcinskas, A. & Wedde, M. Insect inhibitors of metalloproteinases. *IUBMB Life* **54**, 339–343 (2002) doi:10.1080/15216540216040.

83. Eisenhardt, M. *et al.* Development of an insect metalloproteinase inhibitor drug carrier system for application in chronic wound infections. *J. Pharm. Pharmacol.* **67**, 1481–1491 (2015) doi:10.1111/jphp.12452.

84. Müller, H., Salzig, D. & Czermak, P. Considerations for the process development of insect-derived antimicrobial peptide production. *Biotechnol. Prog.* **31**, 1–11 (2015) doi:10.1002/btpr.2002.

85. Baeshen, N. A. *et al.* Cell factories for insulin production. *Microb. Cell Fact.* **13**, 141 (2014) doi:10.1186/s12934-014-0141-0.

86. Ingham, A. B. & Moore, R. J. Recombinant production of antimicrobial peptides

in heterologous microbial systems. *Biotechnol. Appl. Biochem.* **47**, 1 (2007) doi:10.1042/ba20060207.

87. Li, Y. & Chen, Z. RAPD: A database of recombinantly-produced antimicrobial peptides. *FEMS Microbiol. Lett.* **289**, 126–129 (2008) doi:10.1111/j.1574-6968.2008.01357.x.

88. Deng, T. *et al.* The heterologous expression strategies of antimicrobial peptides in microbial systems. *Protein Expr. Purif.* **140**, 52–59 (2017) doi:10.1016/j.pep.2017.08.003.

89. Li, Y. Recombinant production of antimicrobial peptides in *Escherichia coli*: A review. *Protein Expr. Purif.* **80**, 260–267 (2011) doi:10.1016/j.pep.2011.08.001.

90. Schmidt, F. R. Recombinant expression systems in the pharmaceutical industry. *Appl. Microbiol. Biotechnol.* **65**, 363–372 (2004) doi:10.1007/s00253-004-1656-9.

91. Müller, H., Salzig, D. & Czermak, P. Considerations for the process development of insect-derived antimicrobial peptide production. *Biotechnol. Prog.* **31**, 1–11 (2015) doi:10.1002/btpr.2002.

92. Andreu, D. & Rivas, L. Animal Antimicrobial Peptides: An Overview. *Biopolymers* **47**, 415–433 (1998) doi:10.1002/(sici)1097-0282(1998)47:6<415::aid-bip2>3.0.co;2-d.

93. Schreiber, C. *et al.* A high-throughput expression screening platform to optimize the production of antimicrobial peptides. *Microb. Cell Fact.* **16**, 1–13 (2017) doi:10.1186/s12934-017-0637-5.

94. Sinha, J., Plantz, B. A., Inan, M. & Meagher, M. M. Causes of proteolytic degradation of secreted recombinant proteins produced in methylotrophic yeast *Pichia pastoris*: Case study with recombinant ovine interferon-τ. *Biotechnol. Bioeng.* **89**, 102–112 (2005) doi:10.1002/bit.20318.

95. Müller, H. *Development of an antimicrobial peptide production process platform in Pichia pastoris*. Shaker (2019) ISBN: 978-3-8440-6463-6.

96. Choi, J. H. & Lee, S. Y. Secretory and extracellular production of recombinant proteins using *Escherichia coli*. *Appl. Microbiol. Biotechnol.* **64**, 625–635 (2004) doi:10.1007/s00253-004-1559-9.

97. Eichmann, J., Oberpaul, M., Weidner, T., Gerlach, D. & Czermak, P. Selection of High Producers From Combinatorial Libraries for the Production of Recombinant Proteins in *Escherichia coli* and *Vibrio natriegens*. *Front. Bioeng. Biotechnol.* **7**, 1–13 (2019) doi:10.3389/fbioe.2019.00254.

98. Hoffart, E. *et al.* High Substrate Uptake Rates Empower *Vibrio natriegens* as Production Host for Industrial Biotechnology. *Appl. Environ. Microbiol.* **83**, e01614-17 (2017) doi:10.1128/AEM.01614-17.

99. Klint, J. K. *et al.* Production of Recombinant Disulfide-Rich Venom Peptides for Structural and Functional Analysis via Expression in the Periplasm of *E. coli*. *PLoS One* **8**, 1–12 (2013) doi:10.1371/journal.pone.0063865.

100. Schwarz, S., Gerlach, D., Fan, R. & Czermak, P. GbpA as a secretion and affinity purification tag for an antimicrobial peptide produced in *Vibrio natriegens*. *Electron. J. Biotechnol.* **56**, 75–83 (2022) doi:10.1016/j.ejbt.2022.01.003.

101. Richard, C., Drider, D., Elmorjani, K., Marion, D. & Prévost, H. Heterologous Expression and Purification of Active Divercin V41, a Class IIa Bacteriocin Encoded by a Synthetic Gene in *Escherichia coli*. *J. Bacteriol.* **186**, 4276–4284 (2004) doi:10.1128/jb.186.13.4276-4284.2004.

102. Joachim, M., Maguire, N., Schäfer, J., Gerlach, D. & Czermak, P. Process Intensification for an Insect Antimicrobial Peptide Elastin-Like Polypeptide Fusion Produced in Redox-Engineered *Escherichia coli*. *Front. Bioeng. Biotechnol.* **7**, 1–13 (2019) doi:10.3389/fbioe.2019.00150.

103. Joachim, M. *Prozessintensivierung der rekombinanten Herstellung und neuartigen membranbasierten Aufreinigung eines Elastin-Like-Polypeptid gekoppelten antimikrobiellen Peptids*. Shaker (2020) ISBN: 978-3-8440-7456-7.

104. Hoffmann, D., Eckhardt, D., Gerlach, D., Vilcinskas, A. & Czermak, P. Downstream processing of Cry4AaCter-induced inclusion bodies containing

insect-derived antimicrobial peptides produced in *Escherichia coli*. *Protein Expr. Purif.* **155**, 120–129 (2019) doi:10.1016/j.pep.2018.12.002.

105. Hoffmann, D. *Produktion des Insektenmetalloprotease Inhibitors in Escherichia coli Neuartige Plattformtechnologie für die inclusion body-basierte Produktaufarbeitung*. Shaker (2019) ISBN: 978-3-8440-6677-7.

106. Mahmoudi Gomari, M. *et al.* Opportunities and challenges of the tag-assisted protein purification techniques: Applications in the pharmaceutical industry. *Biotechnol. Adv.* **45**, 107653 (2020) doi:10.1016/j.biotechadv.2020.107653.

107. Birrenbach, O., Faust, F., Ebrahimi, M., Fan, R. & Czermak, P. Recovery and Purification of Protein Aggregates From Cell Lysates Using Ceramic Membranes: Fouling Analysis and Modeling of Ultrafiltration. *Front. Chem. Eng.* **3**, 1–11 (2021) doi:10.3389/fceng.2021.656345.

108. Flaschel, E. & Friehs, K. Improvement of downstream processing of recombinant proteins by means of genetic engineering methods. *Biotechnol. Adv.* **11**, 31–78 (1993) doi:10.1016/0734-9750(93)90409-G.

109. Roush, D. J. & Lu, Y. Advances in primary recovery: Centrifugation and membrane technology. *Biotechnol. Prog.* **24**, 488–495 (2008) doi:10.1021/bp070414x.

110. Sun, B., Wibowo, D., Middelberg, A. P. J. & Zhao, C. X. Cost-effective downstream processing of recombinantly produced pexiganan peptide and its antimicrobial activity. *AMB Express* **8**, (2018) doi:10.1186/s13568-018-0541-3.

111. Guan, D. & Chen, Z. Challenges and recent advances in affinity purification of tag-free proteins. *Biotechnol. Lett.* **36**, 1391–1406 (2014) doi:10.1007/s10529-014-1509-2.

112. Urh, M., Simpson, D. & Zhao, K. Affinity chromatography: general methods. *Methods Enzymol.* **463**, 417–438 (2009) doi:10.1016/S0076-6879(09)63026-3.

113. Rodriguez, E. L. *et al.* Affinity chromatography: A review of trends and developments over the past 50 years. *J. Chromatogr. B. Analyt. Technol. Biomed.*

Life Sci. **1157**, 122332 (2020) doi:10.1016/j.jchromb.2020.122332.

114. Moser, A. C. & Hage, D. S. Immunoaffinity chromatography: an introduction to applications and recent developments. *Bioanalysis* **2**, 769–790 (2010) doi:10.4155/bio.10.31.

115. Ki, M.-R. & Pack, S. P. Fusion tags to enhance heterologous protein expression. *Appl. Microbiol. Biotechnol.* **104**, 2411–2425 (2020) doi:10.1007/s00253-020-10402-8.

116. Kosobokova, E. N., Skrypnik, K. A. & Kosorukov, V. S. Overview of fusion tags for recombinant proteins. *Biochem.* **81**, 187–200 (2016) doi:10.1134/S0006297916030019.

117. Li, Y. Carrier proteins for fusion expression of antimicrobial peptides in Escherichia coli. *Biotechnol. Appl. Biochem.* **54**, 1–9 (2009) doi:10.1042/ba20090087.

118. Terpe, K. Overview of tag protein fusions: From molecular and biochemical fundamentals to commercial systems. *Appl. Microbiol. Biotechnol.* **60**, 523–533 (2003) doi:10.1007/s00253-002-1158-6.

119. Harper, S. & Speicher, D. W. Purification of Proteins Fused to Glutathione S-Transferase. *Protein Chromatography: Methods and Protocols* (eds. Walls, D. & Loughran, S. T.) 259–280 (Humana Press, 2011). doi:10.1007/978-1-60761-913-0_14.

120. Skosyrev, V. S., Kulesskiy, E. A., Yakhnin, A. V., Temirov, Y. V. & Vinokurov, L. M. Expression of the recombinant antibacterial peptide sarcotoxin IA in *Escherichia coli* cells. *Protein Expr. Purif.* **28**, 350–356 (2003) doi:10.1016/S1046-5928(02)00697-6.

121. Moon, J. Y., Henzler-Wildman, K. A. & Ramamoorthy, A. Expression and purification of a recombinant LL-37 from *Escherichia coli*. *Biochim. Biophys. Acta - Biomembr.* **1758**, 1351–1358 (2006) doi:10.1016/j.bbamem.2006.02.003.

122. Zhao, X., Li, G. & Liang, S. Several affinity tags commonly used in

chromatographic purification. *J. Anal. Methods Chem.* **2013**, (2013) doi:10.1155/2013/581093.

123. Pina, A. S., Lowe, C. R. & Roque, A. C. A. Challenges and opportunities in the purification of recombinant tagged proteins. *Biotechnol. Adv.* **32**, 366–381 (2014) doi:10.1016/j.biotechadv.2013.12.001.

124. Hefti, M. H., Van Vugt-Van Der Toorn, C. J. G., Dixon, R. & Vervoort, J. A novel purification method for histidine-tagged proteins containing a thrombin cleavage site. *Anal. Biochem.* **295**, 180–185 (2001) doi:10.1006/abio.2001.5214.

125. Lichty, J. J., Malecki, J. L., Agnew, H. D., Michelson-Horowitz, D. J. & Tan, S. Comparison of affinity tags for protein purification. *Protein Expr. Purif.* **41**, 98–105 (2005) doi:10.1016/j.pep.2005.01.019.

126. Zitzmann, J., Weidner, T. & Czermak, P. Optimized expression of the antimicrobial protein Gloverin from *Galleria mellonella* using stably transformed *Drosophila melanogaster* S2 cells. *Cytotechnology* **69**, 371–389 (2017) doi:10.1007/s10616-017-0068-5.

127. Gaberc-Porekar, V. & Menart, V. Potential for using histidine tags in purification of proteins at large scale. *Chem. Eng. Technol.* **28**, 1306–1314 (2005) doi:10.1002/ceat.200500167.

128. Randolph, T. W. The two faces of His-tag: immune response versus ease of protein purification. *Biotechnol. J.* **7**, 18–19 (2012) doi:10.1002/biot.201100459.

129. Rais-Beghdadi, C., Roggero, M. A., Fasel, N. & Reymond, C. D. Purification of recombinant proteins by chemical removal of the affinity tag. *Appl. Biochem. Biotechnol.* **74**, 95–103 (1998) doi:10.1007/BF02787176.

130. Arnau, J., Lauritzen, C., Petersen, G. E. & Pedersen, J. Current strategies for the use of affinity tags and tag removal for the purification of recombinant proteins. *Protein Expr. Purif.* **48**, 1–13 (2006) doi:10.1016/j.pep.2005.12.002.

131. Jenny, R. J., Mann, K. G. & Lundblad, R. L. A critical review of the methods for cleavage of fusion proteins with thrombin and factor Xa. *Protein Expr. Purif.* **31**,

1–11 (2003) doi:10.1016/s1046-5928(03)00168-2.

132. De Genst, E. J. *et al.* Structure and properties of a complex of α-synuclein and a single-domain camelid antibody. *J. Mol. Biol.* **402**, 326–343 (2010) doi:10.1016/j.jmb.2010.07.001.

133. Djender, S., Beugnet, A., Schneider, A. & de Marco, A. The Biotechnological Applications of Recombinant Single-Domain Antibodies are Optimized by the C-Terminal Fusion to the EPEA Sequence (C Tag). *Antibodies* **3**, 182–191 (2014) doi:10.3390/antib3020182.

134. Jin, J. *et al.* Production, quality control, stability, and potency of cGMP-produced *Plasmodium falciparum* RH5.1 protein vaccine expressed in *Drosophila* S2 cells. *npj Vaccines* **3**, 1–13 (2018) doi:10.1038/s41541-018-0071-7.

135. Jin, J. *et al.* Accelerating the clinical development of protein-based vaccines for malaria by efficient purification using a four amino acid C-terminal 'C-tag'. *Int. J. Parasitol.* **47**, 435–446 (2017) doi:10.1016/j.ijpara.2016.12.001.

136. Fougeroux, C. *et al.* Capsid-like particles decorated with the SARS2-CoV-2 receptor-binding domain elicit strong virus neutralization activity. *Nat. Commun.* **12**, (2021) doi:10.1038/s41467-020-20251-8.

137. Khan, M. S. *et al.* Adenovirus-vectored SARS-CoV-2 vaccine expressing S1-N fusion protein. *Antib. Ther.* **5**, 177–191 (2022) doi:10.1093/abt/tbac015.

138. Ren, J., Zhang, C., Ji, F. & Jia, L. Characterization and comparison of two peptide-tag specific nanobodies for immunoaffinity chromatography. *J. Chromatogr. A* **1624**, (2020) doi:10.1016/j.chroma.2020.461227.

139. De Genst, E., Saerens, D., Muyldermans, S. & Conrath, K. Antibody repertoire development in camelids. *Dev. Comp. Immunol.* **30**, 187–198 (2006) doi:10.1016/j.dci.2005.06.010.

140. Jang, H. *et al.* Effects of protein concentration and detergent on endotoxin reduction by ultrafiltration. *BMB Rep.* **42**, 462–466 (2009) doi:10.5483/bmbrep.2009.42.7.462.

141. Wang, L., Blouin, V., Brument, N., Bello-Roufai, M. & Francois, A. Production and Purification of Recombinant Adeno-Associated Vectors. *Methods Mol. Biol. 807* **807**, 361–404 (2011) doi:10.1007/978-1-61779-370-7.

142. Wang, Q. *et al.* Identification of an adeno-associated virus binding epitope for AVB sepharose affinity resin. *Mol. Ther. - Methods Clin. Dev.* **2**, 15040 (2015) doi:10.1038/mtm.2015.40.

143. Hamers-Casterman, C. *et al.* Naturally occurring antibodies devoid of light chains. *Nature* **363**, 446–448 (1993) doi:10.1038/363446a0.

144. Muyldermans, S. *et al.* Camelid immunoglobulins and nanobody technology. *Vet. Immunol. Immunopathol.* **128**, 178–183 (2009) doi:10.1016/j.vetimm.2008.10.299.

145. Holliger, P. & Hudson, P. J. Engineered antibody fragments and the rise of single domains. *Nat. Biotechnol.* **23**, 1126–1136 (2005) doi:10.1038/nbt1142.

146. life technologies. *Product Information Sheet: CaptureSelect ™ C-tag Affinity Matrix*. (2014) Catalog Number 191307005, 191307010, and 191307050 with Pub. No. MAN0010706 https://assets.thermofisher.com/TFS-Assets/LSG/manuals/MAN0010706_CapSelect_Ctag_PI.pdf (retrieved May 2019).

147. Mattila, J. *et al.* Retrospective evaluation of Low-pH viral inactivation and viral filtration data from a multiple company collaboration. *PDA J. Pharm. Sci. Technol.* **70**, 293–299 (2016) doi:10.5731/pdajpst.2016.006478.

148. Edelhoch, H. Spectroscopic determination of tryptophan and tyrosine in proteins. *Biochemistry* **6**, 1948–1954 (1967) doi:10.1021/bi00859a010.

149. Stoscheck, C. M. Quantitation of protein. *Methods Enzymol.* **182**, 50–68 (1990) doi:10.1016/0076-6879(90)82008-p.

150. Anthis, N. J. & Clore, G. M. Sequence-specific determination of protein and peptide concentrations by absorbance at 205 nm. *Protein Sci.* **22**, 851–858 (2013) doi:10.1002/pro.2253.

151. Shen, C.-H. Quantification and analysis of proteins. in *Diagnostic Molecular Biology (Second Edition)* (ed. Shen, C.-H.) 231–257 (Academic Press, 2023). doi:10.1016/B978-0-323-91788-9.00002-8.

152. Cortés-Ríos, J. *et al.* Protein quantification by bicinchoninic acid (BCA) assay follows complex kinetics and can be performed at short incubation times. *Anal. Biochem.* **608**, 113904 (2020) doi:10.1016/j.ab.2020.113904.

153. Holzmüller, W. & Kulozik, U. Protein quantification by means of a stain-free SDS-PAGE technology without the need for analytical standards: Verification and validation of the method. *J. Food Compos. Anal.* **48**, 128–134 (2016) doi:10.1016/j.jfca.2016.03.003.

154. Congdon, R. W., Muth, G. W. & Splittgerber, A. G. The binding interaction of Coomassie blue with proteins. *Anal. Biochem.* **213**, 407–413 (1993) doi:10.1006/abio.1993.1439.

155. Alonso Villela, S. M. *et al.* A protocol for recombinant protein quantification by densitometry. *Microbiologyopen* **9**, 1175–1182 (2020) doi:10.1002/mbo3.1027.

156. Aydin, S. A short history, principles, and types of ELISA, and our laboratory experience with peptide/protein analyses using ELISA. *Peptides* **72**, 4–15 (2015) doi:10.1016/j.peptides.2015.04.012.

157. Engvall, E. The ELISA, Enzyme-Linked Immunosorbent Assay. *Clin. Chem.* **56**, 319–320 (2010) doi:10.1373/clinchem.2009.127803.

158. Sakamoto, S. *et al.* Enzyme-linked immunosorbent assay for the quantitative/qualitative analysis of plant secondary metabolites. *J. Nat. Med.* **72**, 32–42 (2018) doi:10.1007/s11418-017-1144-z.

159. Corrales, J., Gordon, W. L. & Noga, E. J. Development of an ELISA for quantification of the antimicrobial peptide piscidin 4 and its application to assess stress in fish. *Fish Shellfish Immunol.* **27**, 154–163 (2009) doi:10.1016/j.fsi.2009.02.023.

160. Jordan, M., Fraboulet, D., Fourmestraux, G., Wurm, F. M. & Freitag, R.

Sandwich Elisa Today: Limits for Sensitivity, Speed, Precision and Throughput. in *Animal Cell Technology: Products from Cells, Cells as Products: Proceedings of the 16th ESACT Meeting April 25--29, 1999, Lugano, Switzerland* (eds. Bernard, A., Griffiths, B., Noé, W. & Wurm, F.) 483–485 (Springer Netherlands, 2002). doi:10.1007/0-306-46875-1_103.

161. Santucci, A *et al.* High performance liquid chromatography immunoaffinity purification of antibodies and antibody fragments. *J. Immunol. Methods* **114**, 181–5 (1988) doi:10.1016/0022-1759(88)90171-8.

162. Vidal-Madjar, C. & Jaulmes, A. Theoretical Aspects of Quantitative Affinity Chromatography. *Theoretical Advancement in Chromatography and Related Separation Techniques* (eds. Dondi, F. & Guiochon, G.) 481–511 (Springer Netherlands, 1992). doi:10.1007/978-94-011-2686-1_17.

163. Grotefend, S. *et al.* Protein quantitation using various modes of high performance liquid chromatography. *J. Pharm. Biomed. Anal.* **71**, 127–138 (2012) doi:10.1016/j.jpba.2012.08.024.

164. Horak, J., Ronacher, A. & Lindner, W. Quantification of immunoglobulin G and characterization of process related impurities using coupled Protein A and size exclusion high performance liquid chromatography. *J. Chromatogr. A* **1217**, 5092–5102 (2010) doi:10.1016/j.chroma.2010.06.007.

165. Castegnaro, M. *et al.* Advantages and drawbacks of immunoaffinity columns in analysis of mycotoxins in food. *Mol. Nutr. Food Res.* **50**, 480–487 (2006) doi:10.1002/mnfr.200500264.

CHAPTER 2: Production and purification of an insect-derived AMP

The ultimate goal during the heterologous production of AMPs is to obtain a sufficient yield of a highly pure and active product. In this context, numerous attempts have been made to produce and purify the complex model AMP known as IMPI using a variety of approaches.

This chapter presents an innovative method for the production of IMPI using a C-tag. IMPI was expressed in a genetically modified *E. coli* strain, followed by a comparative analysis of expression with and without the C-tag to investigate its influence on the yield and functionality of IMPI.

The product yield was increased by intensifying the parameters of an uncontrolled shake-flask system, and purification was achieved using the CaptureSelect C-tag affinity resin, the characterization of which is an essential part of this study.

Furthermore, the heterologous expression and purification of C-tagged IMPI was comprehensively compared to previous IMPI production approaches, considering quantitative differences in yield as well as qualitative aspects of functionality and structural integrity.

This work contributes to a deeper understanding of the suitability of C-tags for AMP production and provides insights into the intensification of production processes for complex peptides. The findings in this chapter could help to improve the efficiency and effectiveness of AMP production, thus enabling innovative therapeutic approaches based on AMPs. This work is the first step toward the development of a platform technology that could enable the production and purification of other AMPs using the C-tag in the future.

Production and purification of an insect-derived AMP

Lappöhn, C.A., Oestreich, A.M., Stei, R., Weber, L.G., Maerz, L., Wolff, M.W. Process intensification for the production of a C-tagged antimicrobial peptide in *Escherichia coli* - First steps toward a platform technology. J. Biosci. Bioeng. 136, 5 (2023) doi:10.1016/j.jbiosc.2023.09.003

Journal of Bioscience and Bioengineering
VOL. 136 No. 5, 358–365, 2023

www.elsevier.com/locate/jbiosc

Process intensification for the production of a C-tagged antimicrobial peptide in *Escherichia coli* – First steps toward a platform technology

Carolin A. Lappöhn,[1] Arne M. Oestreich,[1] Robin Stei,[1] Linus G. Weber,[1] Lea Maerz,[1] and Michael W. Wolff[1,2,*]

Institute of Bioprocess Engineering and Pharmaceutical Technology, University of Applied Sciences Mittelhessen (THM), Wiesenstr. 14, 35390 Giessen, Germany[1] and Fraunhofer Institute for Molecular Biology and Applied Ecology (IME), Ohlebergsweg 12, 35392 Giessen, Germany[2]

Received 5 May 2023; accepted 6 September 2023
Available online 26 September 2023

The production of antimicrobial peptides/proteins (AMPs) in sufficient quantities for clinical evaluation is challenging because complex peptides are unsuitable for chemical synthesis, natural sources have low yields, and heterologous systems often have low expression levels or require product-specific process adaptations. Here we describe the production of a complex AMP, the insect metalloproteinase inhibitor (IMPI), by adding a C-terminal C-tag to increase the yield compared to the unmodified peptide. We used a design of experiments approach for process intensification in *Escherichia coli* Rosetta-gami 2(DE3)pLysS cells and achieved a yield of 260 mg L^{-1}, which is up to 30-fold higher than previously reported. The C-tag also enhanced product purity but had no effect on IMPI activity, making tag removal unnecessary and therefore simplifying process analytics and downstream processing. We have confirmed that the C-tag is compatible with the peptide and could form the basis of a platform technology for the expression, purification and detection of diverse AMPs produced in *E. coli*.

[**Keywords:** Antimicrobial peptide/protein; Recombinant peptide; Insect metalloproteinase inhibitor; *Escherichia coli*; Small molecular fusion tag; C-tag]

The widespread and irresponsible use of antibiotics has promoted the emergence and spread of resistant bacterial strains (1,2). This leads to longer hospital stays, more deaths, and higher healthcare costs (3). Accordingly, there is an urgent demand for antimicrobials with novel mechanisms of action, such as antimicrobial peptides/proteins (AMPs) (4). These molecules form part of the innate immune response in organisms, selectively preventing or inhibiting the reproduction and growth of bacteria, viruses or fungi (5). Insects are promising sources of AMPs because they have conquered many microbe-rich environments and therefore produce diverse AMPs that target a broad range of pathogens (6).

Insect AMPs can be extracted from natural sources, produced by chemical synthesis or expressed as recombinant peptides in heterologous systems. However, the natural abundance of AMPs is too low for efficient extraction, and chemical synthesis is only suitable for structurally simple peptides less than 40 amino acids in length (7). Heterologous production is therefore the preferred approach for more complex AMPs, but expression levels tend to be low and product-specific process adaptations are required, consuming time and resources.

Low recombinant protein expression levels can be overcome using fusion tags, which increase protein stability while also providing a convenient ligand for single-step affinity purification (7–9). Fusions tags therefore reduce the time and cost of production, but they must not interfere with the structure, interactions or functionality of the native protein (10,11). Accordingly, small peptide tags are preferred because they generally allow the native protein to fold independently (12–14). One of the smallest available peptide tags is the C-tag, which consists of only four amino acids (Glu-Pro-Glu-Ala, EPEA) and is fused to the C-terminus of the recombinant protein (15,16). Single-step purification involves immunoaffinity chromatography with a camelid single-chain antibody (16,17). Experience with the C-tag thus far indicates that it is compatible with large proteins (17,18) and smaller ones such as 15-kDa single-domain antibodies (19), preserving their functionality while still allowing efficient purification. Therefore, the C-tag does not need to be removed during the manufacturing process, saving time and costs and avoiding the risk of product loss caused by inefficient cleavage or precipitation (17,20).

Here we investigated the suitability of the C-tag for the purification of a complex AMP, the 7.7-kDa insect metalloproteinase inhibitor (IMPI). This is naturally produced by larvae of the greater wax moth (*Galleria mellonella*) and is 69 amino acids in length, with several disulfide bridges (21–23). Previous attempts to produce recombinant IMPI in bacteria have resulted in low yields, and typically involved the use of N-terminal purification tags (8,9,24,25). IMPI has shown significant therapeutic potential, particularly for the treatment of wounds infected with *Pseudomonas aeruginosa* and *Staphylococcus aureus* (23,26), where it inhibits bacterial M4-type metalloproteinases, as demonstrated in a porcine skin wound model (27). If a C-tag could be used to improve

* Corresponding author at: University of Applied Sciences Mittelhessen (THM), Wiesenstr. 14, 35390 Giessen, Germany.
E-mail address: Michael.Wolff@lse.thm.de (M.W. Wolff).

1389-1723/$ – see front matter
https://doi.org/10.1016/j.jbiosc.2023.09.003

the yield of IMPI and preserves its activity, this would allow the development of a robust platform technology for the production of many other AMPs.

MATERIALS AND METHODS

Bacterial strain and plasmid constructs *Escherichia coli* strain Rosetta-gami 2(DE3)pLysS (ΔtrxB/Δgor mutant, described hereafter as RG2) was obtained from Merck (Darmstadt, Germany) and was transformed with vector pGG117 (4516 bp), originally constructed by Golden Gate cloning (28). This plasmid contains the IMPI coding sequence with N-terminal thioredoxin (Trx) and His_6 tags separated from IMPI by a thrombin cleavage site (Thr). Fusion protein expression is controlled by the inducible T7 promoter and terminator (T7/lac+His_6-Trx-Thr-IMPI+T7).

Vector pGG117 was modified by directly adding a C-terminal C-tag to the IMPI sequence without an intervening cleavage site, resulting in vector pGG117C (4528 bp, Fig. 1). The modifications were achieved by using the Q5 Site-directed Mutagenesis Kit (New England Biolabs, Frankfurt, Germany) with 0.5 μM of each primer and 1 ng of pGG117 plasmid DNA. The reaction was carried out with a melting temperature of 66°C (New England BioLabs Tm Calculator, Version 1.16.5, http://tmcalculator.neb.com/#!/) and the vector was circularized using the KLD-Mastermix (kinase, ligase and endonuclease DpnI). More detailed information is provided in the Supplementary Materials Fig. S1 and Text S1.

DNA amplification and bacterial transformation Chemically competent *E. coli* NEB10-β cells (New England Biolabs) were recovered from glycerol stocks at an optical density at 600 nm (ΔOD_{600}) of 10 in 100 mM $CaCl_2$ with 15% glycerol. The cells were transformed with pGG117 and pGG117C by adding 5 μL of the KLD mixture to 80 μL of cells, incubating on ice for 1 h, heat shocking the cells at 42°C for 60 s, and incubating on ice for a further 5 min. The mixture was then spread on preheated lysogeny broth (LB) agar plates supplemented with 15 μg L^{-1} gentamycin (Carl Roth, Karlsruhe, Germany), and incubated overnight at 37°C. Single colonies were transferred to liquid LB medium containing gentamycin as above, and the cultures were incubated at 37°C overnight, shaking at 250 rpm. Plasmid DNA was isolated using the NucleoSpin Plasmid EasyPure kit (Macherey-Nagel, Düren, Germany) and verified by sequencing. Plasmids with the correct sequence were introduced into chemically competent RG2 cells as described above, in LB medium supplemented with 34 μg L^{-1} chloramphenicol (Carl Roth).

Cultivation and IMPI expression Untransformed RG2 cells as well as cells transformed with pGG117 and pGG117C were cultivated in terrific broth (TB) medium (Carl Roth) supplemented with 5 g L^{-1} glycerol (Carl Roth) and appropriate antibiotics (see above) at 37°C, shaking at 250 rpm. The 1-L flasks were filled to only 10% capacity to maximize the oxygen transfer rate. In scouting experiments, we compared the growth rate and productivity of the cells (the latter based on the IMPI concentration in the cleared lysate). We induced IMPI expression by adding various concentrations of isopropyl-β-D-galactopyranoside (IPTG) at $\Delta OD_{600} = 1.0$ followed by incubation for 4 h. We also tested different growth temperatures from 22°C to 42°C.

The production parameters for RG2 pGG117C cultures were investigated and intensified in 1-L shake flask cultures using a Design of Experiments (DoE) approach, with critical process parameters and the design space defined according to literature data (24,29) and scouting experiments. Temperature (32–44°C) and induction conditions (time 0.5–5 h, IPTG concentration 0.1–2.1 mM) were optimized using an I-optimal randomized quadratic response surface methodology design in Design Expert v11 (Stat-Ease, Minneapolis, MI, USA). The samples were cultivated for 4 h post-induction before harvesting.

C-tag purification process RG2 pGG117C cells were cultivated under the enhanced growth conditions described above and harvested by centrifugation (16,000 *g*, 4°C, 5 min). The pellet was resuspended in phosphate-buffered saline (PBS, 20% w/v biomass/PBS; Sigma–Aldrich, St Louis, MO, USA) and disrupted by two cycles of high-pressure homogenization (approximately 2000 bar). After clarification by centrifugation (16,000 *g*, 4°C, 1 h), IMPI was captured on a 1-mL CaptureSelect C-tagXL column (Thermo Fisher Scientific, Waltham, MA, USA) installed on an ÄKTA Pure 25 system (Cytiva, Marlborough, MA, USA) running UNICORN v7.3. The processing steps and buffers are summarized in Table 1.

Purification and digestion for activity tests RG2 pGG117 and RG2 pGG117C cultures were harvested by centrifugation (16,000 *g*, 4°C, 5 min) 4 h post-induction and were disrupted by high-pressure homogenization as described above. The lysate was passed through a 1-mL HisTrap FF crude column (Cytiva) equilibrated in 20 mM sodium phosphate buffer (pH 7.4) containing 0.5 M sodium chloride and 20 mM imidazole, and IMPI was eluted by increasing the imidazole concentration to 500 mM. The eluate was further purified by size-exclusion chromatography using a 5-mL Bio-Scale Mini Bio-Gel P-6 column (Bio-Rad Laboratories, Hercules, CA, USA) simultaneously exchanging the buffer for 50 mM Tris–HCl (pH 8) containing 0.1 M NaCl. We mixed 10 μg of the fusion protein with 7.5 μg thrombin Sepharose beads (1 g L^{-1} ligand density; BioVision, Waltham, MA, USA) for 24 h at room temperature to cleave off the N-terminal tags. The beads were then removed by centrifugation (16,000 *g*, 3 min, room temperature) followed by passing the supernatant through a 0.2-mL HisPur Ni-NTA spin-column (Thermo Fisher Scientific) at 700 *g* for 2 min at room temperature. The flow-through fractions were stored at −80°C for further analysis.

Bacterial cell growth Cell growth was monitored by measuring the OD_{600} with a BioSpectrometer kinetic (Eppendorf, Hamburg, Germany). OD_{600} samples >1 were diluted with 0.9% NaCl. The ΔOD_{600} was calculated using the following equation:

$$\Delta OD_{600} = (OD_{600,sample} - OD_{600,blank})^{*}\text{dilution factor} \quad (1)$$

Measurements were taken in biological triplicates each with technical triplicates. The relative standard deviation of the technical triplicates was ≤5%.

Sample preparation Cells were harvested using a centrifuge (16,000 *g*, 4°C, 5 min) and the pellets were stored at −20°C overnight. The pellets were disrupted in BugBuster Mastermix (Merck) using 2.5 mL of the mix per 0.1 g of cells (not less than 100 μL per pellet). The resuspended lysate was incubated for 45 min at room temperature, and clarified by centrifugation as above. The supernatant was stored at −20°C.

ELISA IMPI concentrations in cell lysates were determined by enzyme-linked immunosorbent assay (ELISA) using plates coated with the monoclonal THE anti-His-tag antibody (GenScript Biotech, Piscataway, NJ, USA) (24). The 5.0-kDa synthetic peptide BR029H with a His_6 tag (KWKIFKKIEKAGRNIRDGIIKAGPA VSVVGEAATIYKTGHHHHHH; GenScript Biotech) was used as a standard. Due to the size difference, correlations were first established using a weighed recombinant in-house IMPIC standard (Supplementary Material Text S2) and BR029H, and the ELISA method was then declared suitable. The standard peptide, IMPI-containing samples and antibody were diluted in 0.4% bovine serum albumin (Carl Roth) before analysis. The bound primary antibody was detected with the horseradish peroxidase (HRP)-conjugated secondary antibody anti-His_5-HRP (Qiagen, Hilden, Germany) diluted 1:5000, and the signal was developed using the 1-Step Ultra TMB-ELISA substrate (Thermo Fisher Scientific). We measured the reaction kinetics at 370 nm for 45 min at 1-min intervals using a Synergy HTX multimode reader with Gen5 software (BioTek Instruments, Winooski, VT, USA). The measurements were taken in triplicates, and the relative standard deviation of technical triplicates was ≤20%.

Sodium dodecylsulfate polyacrylamide gel electrophoresis Samples were mixed with 4× Laemmli sample buffer (Bio-Rad Laboratories) containing 5% 2-mercaptoethanol. After heating to 95°C for 5 min, 10 μL of each sample per lane was loaded onto a 4–20% TGX Stain-Free gel (Bio-Rad Laboratories) alongside 3 μL of the Precision Plus Protein Unstained Standard (Bio-Rad Laboratories). Gels were visualized and assessed by densitometry using the ChemiDoc MP system (Software Image Lab v5.2). Gels were stained using the Pierce Silver Stain Kit (Thermo Fisher Scientific) with aprotinin (≥3.0 PEU mg^{-1}; Carl Roth) as the quantification standard.

Western blot Proteins were transferred from gels to a TransferPac Midi 0.2 μm polyvinylidene diflouride (PVDF) membrane (Bio-Rad Laboratories) using the Trans-Blot Turbo Transfer System (Bio-Rad Laboratories) at 2.5 A and 25 V for 7 min. The membrane was then blocked with 5% bovine serum albumin in PBS for 2 h and washed three times in 0.1% (v/v) Tween-20/PBS. We then incubated the membrane for 2 h in the HRP-conjugated anti-His_5 primary antibody (diluted 1:5000) or HRP-conjugated anti-IMPI(I38V) (Bio-Rad Laboratories, diluted 1:10,000) and the Precision Protein StrepTactin alkaline phosphatase (AP) conjugate (Bio-Rad

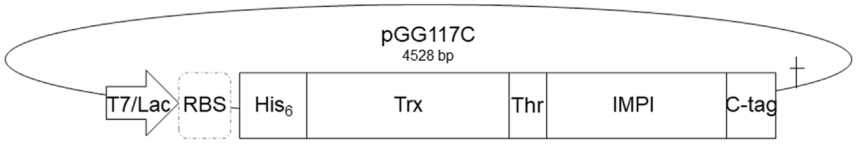

FIG. 1. Schematic representation of vector pGG117C for the production of IMPI with a C-terminal C-tag (IMPIC). The expression cassette comprises the T7 promoter with operon (T7/Lac) and ribosomal binding site (RBS), followed by N-terminal His_6 and thioredoxin (Trx) tags for purification and solubilization, respectively, a thrombin cleavage side (Thr), and the IMPI coding region directly fused to the C-terminal C-tag. The T7 terminator (+) is downstream of the stop codon adjacent to the C-tag.

TABLE 1. Steps in the purification of insect metalloproteinase inhibitor (IMPI) from the cell lysate purification using C-tag CaptureSelect C-tagXL resin.

Step	Buffer or solution	Flow rate (cm h^{-1})	Column volumes (CV)
Equilibration	PBS	200	10 CV
Loading	Cell lysate	100	3.5 mg IMPIC (mL column)$^{-1}$
Wash	PBS	200	15 CV
Elution	115 mM glycine, pH 2.0	170	10 CV
Strip	1 M acetic acid	200	10 CV

PBS, phosphate-buffered saline; IMPIC, insect metalloproteinase inhibitor with C-tag.

Laboratories) in 0.05% (v/v) Tween-20/PBS. The signal was visualized using the ChemiDoc MP system as described above.

Activity assay IMPI activity against the metalloproteinase thermolysin (30,31) was quantified in a fluorescence-based assay using 1 μg of the substrate fluorescein thiocarbamoyl casein (FTC-casein) and 1 μg phosphoramidon as a positive control. The substrate concentration in the samples was determined using a Synergy HTX multimode reader after 20 min, with an excitation wavelength of 485 nm and an emission peak wavelength of 528 nm. The relative standard deviation of the technical triplicates was ≤15%.

RESULTS AND DISCUSSION

Effect of the C-tag on cell growth and IMPI production The density of RG2 cell cultures transformed with pGG117 and pGG117C was compared 4 h post-induction with and without IPTG (Fig. 2A). This revealed no significant difference between the non-induced cultures ($\alpha = 0.05$, $p = 0.79$, $t = 0.27$) but a substantial decline in cell density following induction, which was significantly more severe for RG2 pGG117C ($\alpha = 0.05$, $p = 2.86 \times 10^{-12}$, $t = 18.63$). Despite the low cell density, the concentration of the IMPIC product in the RG2 pGG117C cultures was significantly higher than the IMPI concentration in the RG2 pGG117 cultures after 1 h post-induction ($\alpha = 0.05$, $p = 2.95 \times 10^{-3}$, $t = 6.46$), and was 5.8-fold higher in absolute terms and 7.6-fold higher when corrected for differences in cell density after 4 h post-induction (Fig. 2B). This result was confirmed by the differences in band density observed in sodium dodecylsulfate polyacrylamide gel electrophoresis (SDS-PAGE) and Western blot experiments (Fig. S2A and B).

The slow cell growth during the production phase was expected because the expression of recombinant proteins causes elevated stress (32,33). The severity of the stress depends on the rates of transcription and translation and any conditions necessary to maintain the system, such as the presence of antibiotics to ensure selection pressure (33). Furthermore, even single amino acid additions to recombinant proteins can influence bacterial cell growth and product yield (34). Accordingly, the C-terminal extension of four amino acids has the potential to affect cell growth, although this has not been reported thus far and attention naturally focuses on the product yield rather than cell density. The C-tag has not been reported to increase the yield of other recombinant proteins, but the phenomenon is well known for larger protein tags such as glutathione S-transferase (GST; 211 amino acids, 26 kDa) and the maltose-binding protein (MBP; 370 amino acids, 40 kDa) (35–37). Fourteen small peptide tags ranging from 6 to 15 amino acids in length have also been shown to improve protein expression in *E. coli*. Several of these tags are self-assembling amphipathic peptides composed of alternating hydrophobic and hydrophilic residues, with emphasis on hydrophobicity and net charge (38–40). An alternative strategy is to append sequences of highly expressed proteins to the start codon (41,42). However, the mechanism of enhanced protein expression remains unclear and could reflect a combination of properties such as isoelectric point (pI), grand average of hydropathy (GRAVY value) and tag position (38,43). Only a few of these expression-enhancing peptide tags can also be used for product purification. One example is the S-tag (15 amino acids, 1.8 kDa), which was attached to the NtrX protein and overexpressed in *E. coli*, followed by purification using the S.Tag rEK Purification Kit (Novagen, Darmstadt, Germany) (44,45). Another is the human influenza virus hemagglutinin (HA) tag (12 amino acids, 1.4 kDa), which was attached to the nuclear receptor-binding SET domain (NSD), which is otherwise difficult to produce in *E. coli*, resulting in a 22.4-fold increase in yield (46). The HA tag was not used for purification in this case, but can be captured using commercial anti-HA monoclonal antibody resins (11,12).

Experimental design for process intensification The initial expression levels of IMPI/IMPIC were at the lower end typically reported for recombinant proteins in bacteria, suggesting intensification was necessary (47). Preliminary screening experiments defined the induction time (X_1), IPTG concentration (X_2), and cell

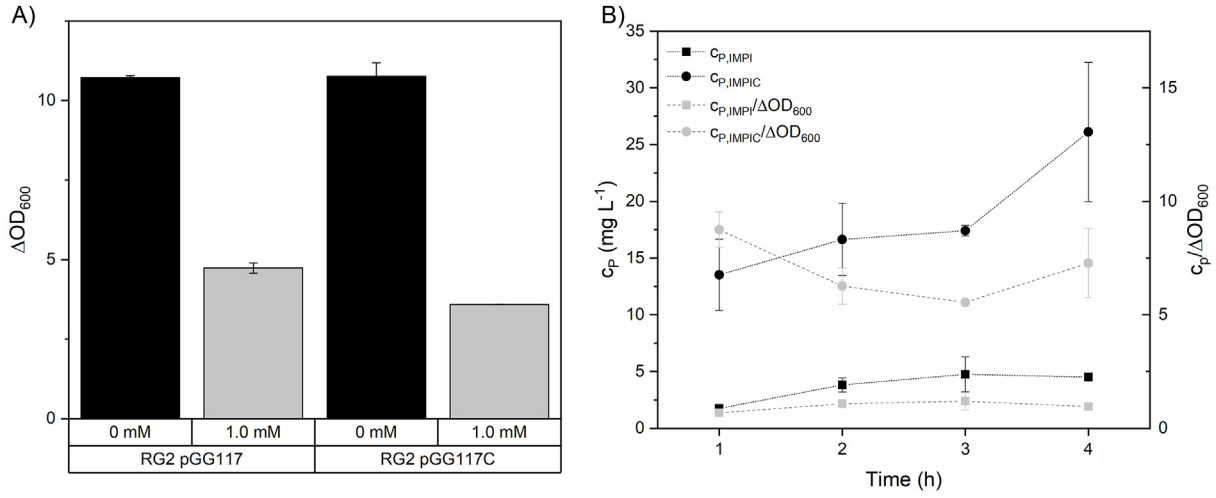

FIG. 2. Comparison of cell density and product concentration for the RG2 cultures pGG117 expressing IMPI (no C-tag) and pGG117C expressing IMPIC (with C-tag). (A) Strains RG2 pGG117 and RG2 pGG117C were grown without induction (0 mM IPTG, black bars) or with induction (1 mM IPTG, gray bars). The cell density (ΔOD_{600}) was determined 4 h post-induction. (B) Concentrations of IMPI (squares) and IMPIC (dots) were determined hourly after IPTG induction (black). These concentrations were correlated with cell densities using the factor $c_p/\Delta OD_{600}$ (gray). Product concentrations were analyzed by ELISA. All measurements were taken in biological triplicates each with technical triplicates. Data are means ± standard deviations.

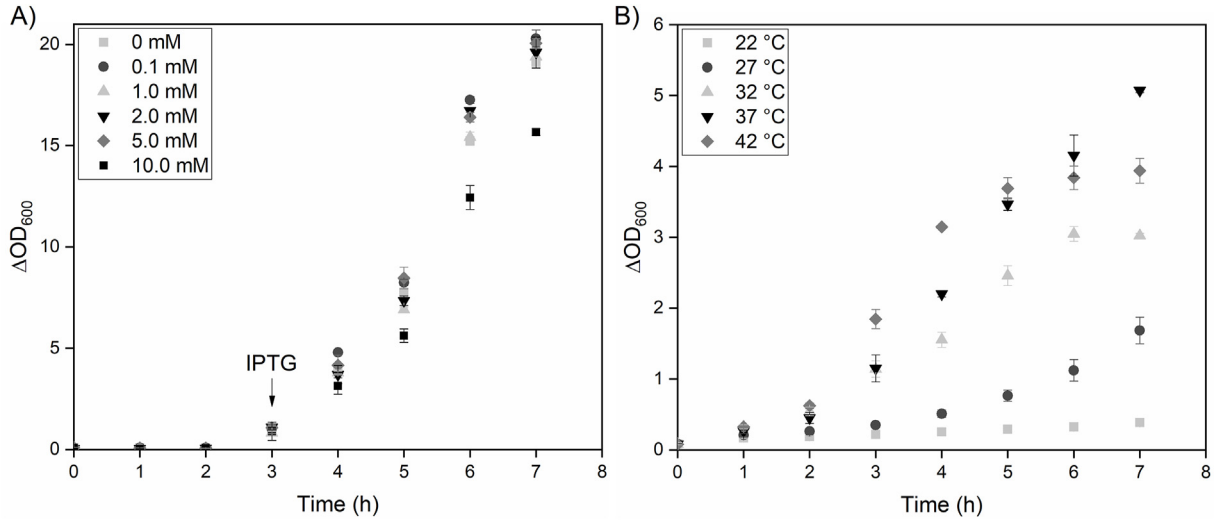

FIG. 3. Preliminary experiments to define the design space. (A) Preliminary growth analysis of native RG2 cells induced at $\Delta OD_{600} = 1$ with different concentrations of IPTG. (B) Preliminary growth analysis of the RG2 pGG117C cells at temperatures of 22–42°C. All measurements were taken in biological triplicates each with technical triplicates. Data are means ± standard deviations.

density reached after an IPTG induction as critical process parameters for IMPIC production in RG2 pGG117C cells. We set out a design space in which the IPTG concentration ranged from 0.1 to 2.1 mM, and carried out further preliminary experiments to ensure this was not toxic toward the cells. We found that IPTG concentrations up to 10 mM had no detrimental effect on cell growth (Fig. 3A), which is consistent with the literature (48). The cultivation temperature (X_3) was also included as a critical process parameter based on previous attempts to produce IMPI in the same bacterial strain, where a temperature range of 31.3–44.7°C was tested (24). We elected to test the range 22–42°C in preliminary experiments and found that growth was enhanced at temperatures >32°C (Fig. 3B), so we set the range 32–44°C for the DoE model.

We assigned the product concentration as the DoE response and set the harvesting time as 4 h post-induction based on the earlier scouting experiments. At this time point, the product concentration was analyzed in the supernatant after cell disruption and clarification. Inclusion bodies, which are often observed in *E. coli* during heterologous protein expression (49), were not considered in this study due to the low product concentration and activity in the insoluble cell fraction (data not shown). The DoE model and response factors are summarized in Table 2.

To ensure a homogeneous distribution of the externally studentized residuals in the experimental design, the product concentration was transformed to a natural logarithm value. In reference to the experiments, the reduced quadratic model was significant ($p < 0.0001$) with a non-significant lack of fit ($p = 0.2206$). The model coefficient of determination was $R^2 = 0.9536$. Given the predicted R^2 of 0.8852 (reasonable agreement with the adjusted R^2 of 0.9320) and an adequate precision of 21.026, the initial measurements are close to the model's prediction, arguing that the model provides reliable data within the defined design space. Additional descriptive data for the model and factor interactions are provided in the Supplementary Material Tables S1 and S2.

Numerical optimization was used to identify settings for the critical process parameters within the design space (Fig. 4). The resulting model predicted that a cultivation temperature of 32.0°C would achieve the maximum product concentration within the tested parameters. The optimal induction conditions were 1.4 mM IPTG after cultivation for 6.72 h, which in our case corresponded to an ΔOD_{600} of 2.8. After further cultivation for 4 h post-induction, these settings resulted in a product yield of 260 mg L^{-1}, which is 10-fold higher than the initial process conditions we investigated. This was supported by the comparison of densitometric analysis in SDS-PAGE and Western blot experiments representing the initial and enhanced conditions (Fig. S3A and B). The intensification of product yield was sufficient for further investigation to develop a single-step purification strategy based on the C-tag, which recovered 86.4 ± 5.0% of the product at a purity of 77 ± 10% (based on densitometric analysis following SDS-PAGE). Similar high yields (>80%) and purities (>70%) have been reported in the supernatant of insect cell lines and in crude bacterial lysates following a single chromatography step (15,17).

Our IMPI yields were up to 29.4-fold higher than previously reported (8,24,25,46,47) and were at least 2.5-fold higher than in a

TABLE 2. Response surface design to investigate the influence of critical process parameters on IMPIC product concentration in RG2 pGG117C cells.

Run	X_1: time of induction (h)	X_2: IPTG concentration (mM)	X_3: temperature (°C)	Product concentration (mg L^{-1})
1	0.5	0.1	32	18.4
2	5.1	2.1	44	20.8
3	10.5	1.1	44	34.0
4	0.5	1.6	41	59.2
5*	5.5	1.1	38	145.3
6	7.7	1.6	32	268.0
7	10.5	1.1	44	48.1
8	7.8	0.1	41	47.6
9	0.5	0.6	38	77.6
10	10.5	1.1	38	53.2
11	3.0	1.6	35	139.1
12	10.5	2.1	38	30.9
13	7.8	0.1	41	43.5
14*	5.5	1.1	38	186.9
15	5.1	2.1	44	18.0
16	5.5	0.1	35	52.4
17	0.5	2.1	32	63.0
18*	5.5	1.1	38	132.3
19	10.5	2.1	38	38.2
20	7.7	1.6	32	207.3
21	4.3	1.1	44	71.9
22	10.5	0.1	32	40.8
23	0.5	0.1	44	35.2

The paramours are induction time (X_1, h), IPTG concentration (X_2, mM) and temperature (X_3, °C). Center points are marked with an asterisk.

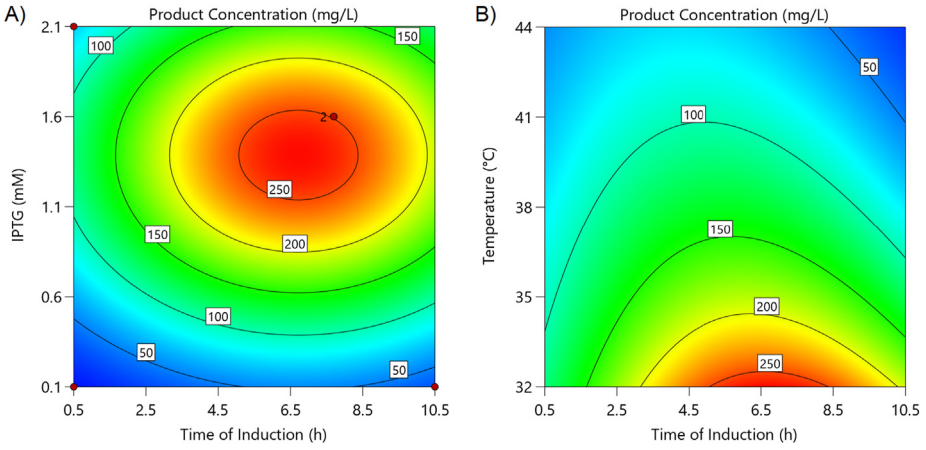

FIG. 4. Contour plots of the reduced quadratic response surface model for the enhanced expression of IMPIC in RG2 pGG117C cells. (A) IPTG concentration and time of induction at 32°C. (B) Temperature and time of induction at an IPTG concentration of 1.39 mM.

fully controlled fed-batch process (9). The C-tag was used for the first time as a purification strategy for IMPI, increasing the product recovery by 10–70% compared to previous reports (Table 3). IMPI has previously been expressed as a GST fusion in RG2 cells, resulting in the recovery of 28.65 ± 9.19 mg of GST-GS-IMPI from 5 L of culture (approximately 1.3 mg L^{-1}) (50), which is approximately 200-fold lower than the optimized process discussed here. The authors compared multiple strategies with the same product, and differences in performance were attributed to the type of tag and its positioning, and the culture conditions. For example, they compared C-terminal and N-terminal positioning for the Cry4AaCter pull-down tag, which had no impact on the yield of IMPI but showed that a fusion partner is generally required for IMPI expression in *E. coli* (9). Furthermore, they described the negative impact of the His_6 tag on the solubility of IMPI in *E. coli* (50,51), which is a common challenge for His_6-tagged recombinant proteins in this system (52). We also included a His_6 tag to facilitate product detection and further chromatography steps, but this was paired with a Trx fusion to improve solubility, as previously described (8).

Regardless of the recombinant protein and expression system, the positioning and amino acid sequence of the tag, as well as the overall expression strategy, can affect product solubility and yield. One of many examples is the expression of recombinant aspartic proteinase in *E. coli* (53). It is unclear how the fusion partner influences protein solubility, but one potential explanation is that the tag provides an intrinsic chaperone-like activity, in which hydrophobic regions of the tag interact with the partially-folded fusion partner to prevent aggregation (54). Another hypothesis is that strongly acidic tags prevent aggregation of the fusion partner by electrostatic repulsion (54). Empirically, a pI of 4–5 and a GRAVY value between 0 and −1 has been shown to improve the solubility of a fusion partner by increasing hydrophilicity (38). A higher proportion of hydrophilic amino acids in the tag makes the GRAVY value more negative and improves the solubility and yield of other recombinant proteins (55).

If this hypothesis is transferred to our model IMPIC, the addition of two negatively charged residues shifts the theoretical pI from 5.67 to 5.41, and the GRAVY value changed from −0.269 to −0.298 (calculated using ProtParam, Expasy). The GRAVY value becomes smaller, but the overall change is marginal suggesting that the effects on protein solubility are relatively small. In contrast, C-terminal modifications with single amino acids had a significant effect on the yield of recombinant pleurocidin in *E. coli* although the impact was highly dependent on the specific change, with the addition of glycine triggering a 15-fold increase whereas the addition of aspartate had no effect (34).

The expression of IMPI with an N-terminal Cry4AaCter pull-down tag in BL21(DE3) cells resulted in a yield of 102.4 ± 8.8 mg L^{-1}, based on a 5-L batch process at 37°C using TB medium and controlled cultivation conditions (9). Although this is about half of the yield we obtained, purification by precipitation in the previous study was simpler and less expensive than the affinity chromatography method we used. However, the reported recovery of 13.2 ± 1% in the previous study (9) is seven times lower than ours. A further disadvantage is the use of *E. coli* BL21(DE3) cells rather than the *E. coli* RG2 strain we selected, because BL21(DE3) cells cannot form disulfide bridges and a further processing step is required to induce product oxidation with trichloroacetic acid, thus compromising overall process efficiency (9).

IMPI has been expressed before in *E. coli* RG2 cells but Joachim et al. (24) used the self-aggregating elastin-like polypeptide (ELP) as a

TABLE 3. Comparison of parameters for recombinant IMPI production using different expression systems and fusion tags for expression and purification.

Expression construct	Expression strain	Soluble or insoluble	Medium	Cultivation scale	Expressed IMPI concentration (mg L^{-1})	Purification technique	Recovery after purification (%)	References
His-Trx-IMPI-C	Rosetta-gami 2(DE3)pLysS	Sol.	TB	1-L shake flask with 10% culture volume	Approximately 260	Chromatography	86.4 ± 5.0	This study
GbpA-IMPI	*Vibrio natriegens*	Sol.	Chem. def.	1-L shake flask with 10% culture volume	Approximately 8.5	Chromatography	n/a	25
Cry4AaCter-IMPI	*E. coli* BL21(DE3)	Insol.	TB	5-L working volume bioreactor	102.4 ± 8.8	Precipitation	13.2 ± 1	9,46
GST-IMPI	Rosetta-gami 2(DE3)pLysS	Sol.	TB	5-L working volume bioreactor	1.3 ± 1.8	Chromatography	14.5 ± 3.6	9,46
His-ELP-IMPI	Rosetta-gami B(DE3)pLysS	Sol./Insol.	Chem. def.	6.5-L working volume bioreactor	2.2 ± 0.2	Filtration	72.6 ± 2.7	24,47

Chem.def., chemically defined medium; Cry4AaCter, pull-down tag promotes the formation of inclusion bodies; C, C-tag; ELP, elastin-like polypeptide; GbpA, glucosamine-binding protein A; GST, glutathione-S-transferase; His, His6-tag; IMPI, insect metalloproteinase inhibitor; TB, terrific broth medium; Trx, thioredoxin; n/a, not applicable.

fusion partner and cultured the cells expressing this His-ELP-Trx-intein-IMPI construct in a 6.5-L multi-cascaded fed-batch process based on minimal medium. The highest IMPI yield was 2.2 ± 0.2 mg L^{-1} compared to 260 mg L^{-1} reported here for IMPIC in an uncontrolled batch process. Interestingly, Joachim et al. (24) found that a temperature of 40°C improved the production of ELP-IMPI, which differs from the 32°C optimal temperature predicted by our model. We have yet to include more elaborate process strategies and assume that controlled process conditions, will further improve IMPIC yields. Another group has expressed IMPI in *Vibrio natriegens*, achieving a yield of approximately 8.5 mg L^{-1} (25). The construct they used featured an N-terminal gluxosamine-binding protein A (GbpA) fusion, and the bacterial cells were cultured in a minimal medium.

Comparison of IMPI activity with and without C-terminal modification The higher yield associated with the C-tag modification is promising for the development of a future production platform technology. However, it would be even more significant for the entire manufacturing process, as well as process monitoring, if the efficacy of the target AMP was not impaired by the tag. We therefore tested the activity of IMPIC and unmodified IMPI prepared under comparable conditions (Figs. S4–S6A,B). We found that IMPI and IMPIC inhibited the cleavage of FTC-casein by thermolysin to a similar extent ($\alpha = 0.05$, $p = 0.212$, $t = 1.485$), reducing metalloproteinase activity by 86.0 ± 9.0% and 88.4 ± 6.8%, respectively (Fig. 5). The activity of IMPI and IMPIC also correlated with the ability of the positive control phosphoramidon to inhibit thermolysin. Notably, phosphoramidon is considered to be more active than other metalloproteinase inhibitors (56,57). Our results confirm that the small C-terminal C-tag has no significant influence on IMPI activity and can therefore remain on the product, which simplifies monitoring efforts during the production process and its development. Similarly, the C-tag had no effect on the activity, stability or solubility of the 60-kDa full-length RfRH5 protein expressed in *Drosophila melanogaster* S2 cells, and also did not affect immunogenicity, allowing the C-tagged RH5.1 protein to be used for cGMP-compliant production (17,18). The fusion of the C-tag to a 15-kDa recombinant single-domain antibody also had no effect on its functionality (19). We show that the same is true for even smaller proteins such as IMPI (7.7 kDa). The C-tag could therefore be developed as a platform technology to screen for pharmaceutically relevant AMPs, although it will be important to check its compatibility with AMPs that rely on free C-terminal residues for activity. In such cases, molecular models based on comparable N-terminal tags may be more suitable.

In summary, scalable production platforms and universal purification strategies are necessary to produce sufficient quantities of AMPs for the augmentation or replacement of antibiotics. We used IMPI as a model complex AMP, which has only been expressed at low levels thus far, to demonstrate the potential of the C-tag as a strategy to increase AMP yields and recovery. We expressed the modified IMPIC peptide in *E. coli* RG2 cells, increasing the concentration by 7.6-fold after normalizing for cell density compared the RG2 cells expressing the untagged IMPI peptide. This is the first report in which the C-tag has been shown to increase product yields. We used a DoE approach to intensify the cultivation parameters, reaching a maximum IMPIC yield of 260 mg L^{-1} (a 29.4-fold increase over previous uncontrolled production processes (8,9,24,25,50,51)). We anticipate further yield increases under controlled cultivation conditions, but this requires further investigation. Having expressed sufficient amounts of IMPIC, we demonstrated that direct product purification using the C-tag for immunoaffinity capture chromatography achieves efficient product recovery and high purity in a single step. Furthermore, the C-tag did not affect IMPI activity, and can therefore be retained on the product unlike most other tags. This streamlines the process by eliminating the need for an enzymatic tag removal step, thus improving process efficiency and economics. The presence of the C-tag throughout the manufacturing process will also enable product monitoring by ELISA or affinity chromatography. The principle discussed here can potentially be applied to any peptide or small protein, and thus represents the first stage in the development of a platform technology for the production of AMPs.

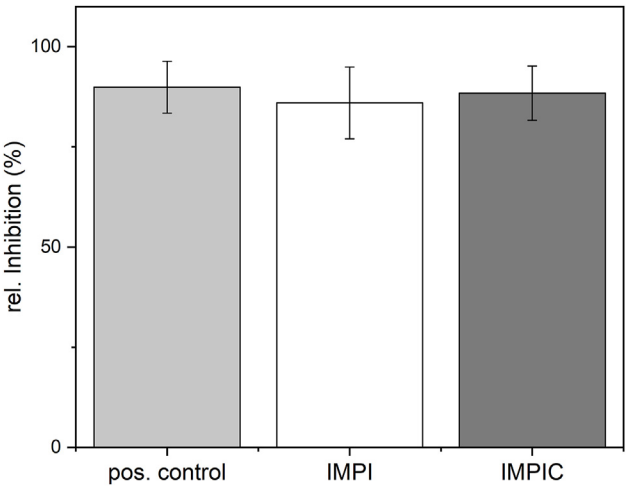

FIG. 5. IMPI activity assay based on the inhibition of the metalloproteinase thermolysin with FTC-casein as the substrate, and phosphoramidon as positive control. The bars show the inhibition of thermolysin relative to the non-inhibiting negative control. Data are means of biological triplicates ± standard deviations.

Supplementary data to this article can be found online at https://doi.org/10.1016/j.jbiosc.2023.09.003.

ACKNOWLEDGMENTS

The authors would like to thank Peter Czermak for technical support and Richard M. Twyman for editing the manuscript. The manuscript is part of Carolin A. Lappöhn's dissertation at the Graduate Centre for Engineering Sciences under the aegis of Justus-Liebig-University Giessen, Germany, in cooperation with the University of Applied Sciences Mittelhessen, Giessen, Germany. C. Lappoehn was financially supported by the Johannes Hübner Foundation with a doctoral scholarship. This work was financially supported by the strategic research fund of the University of Applied Sciences Mittelhessen, Giessen, Germany. The authors declare no conflict of interest.

References

1. **Ventola, C. L.:** The antibiotic resistance crisis, part 1: causes and threats, PT, **40**, 277–283 (2015).
2. **Ben, Y., Fu, C., Hu, M., Liu, L., Wong, M. H., and Zheng, C.:** Human health risk assessment of antibiotic resistance associated with antibiotic residues in the environment: a review, Environ. Res., **169**, 483–493 (2019).
3. **Bartlett, J. G., Gilbert, D. N., and Spellberg, B.:** Seven ways to preserve the miracle of antibiotics, Clin. Infect. Dis., **56**, 1445–1450 (2013).
4. **Reddy, K. V. R., Yedery, R. D., and Aranha, C.:** Antimicrobial peptides: premises and promises, Int. J. Antimicrob. Agents, **24**, 536–547 (2004).
5. **Koo, H. B. and Seo, J.:** Antimicrobial peptides under clinical investigation, Pept. Sci., **111** (2019).
6. **Tonk, M., Vilcinskas, A., and Rahnamaeian, M.:** Insect antimicrobial peptides: potential tools for the prevention of skin cancer, Appl. Microbiol. Biotechnol., **100**, 7397–7405 (2016).
7. **Müller, H., Salzig, D., and Czermak, P.:** Considerations for the process development of insect-derived antimicrobial peptide production, Biotechnol. Prog., **31**, 1–11 (2015).

8. **Eichmann, J., Oberpaul, M., Weidner, T., Gerlach, D., and Czermak, P.:** Selection of high producers from combinatorial libraries for the production of recombinant proteins in *Escherichia coli* and *Vibrio natriegens*, Front. Bioeng. Biotechnol., **7**, 254 (2019).
9. **Hoffmann, D., Eckhardt, D., Gerlach, D., Vilcinskas, A., and Czermak, P.:** Downstream processing of Cry4AaCter-induced inclusion bodies containing insect-derived antimicrobial peptides produced in *Escherichia coli*, Protein Expr. Purif., **155**, 120–129 (2019).
10. **Guan, D. and Chen, Z.:** Challenges and recent advances in affinity purification of tag-free proteins, Biotechnol. Lett., **36**, 1391–1406 (2014).
11. **Mahmoudi Gomari, M., Saraygord-Afshari, N., Farsimadan, M., Rostami, N., Aghamiri, S., and Farajollahi, M. M.:** Opportunities and challenges of the tag-assisted protein purification techniques: applications in the pharmaceutical industry, Biotechnol. Adv., **45**, 107653 (2020).
12. **Zhao, X., Li, G., and Liang, S.:** Several affinity tags commonly used in chromatographic purification, J. Anal. Methods Chem., **2013**, 581093 (2013).
13. **Nguyen, T. K. M., Ki, M. R., Son, R. G., and Pack, S. P.:** The NT11, a novel fusion tag for enhancing protein expression in *Escherichia coli*, Appl. Microbiol. Biotechnol., **103**, 2205–2216 (2019).
14. **Carson, M., Johnson, D. H., McDonald, H., Brouillette, C., and DeLucas, L. J.:** His-tag impact on structure, Acta Crystallogr. Sect. D Biol. Crystallogr., **63**, 295–301 (2007).
15. **Ren, J., Zhang, C., Ji, F., and Jia, L.:** Characterization and comparison of two peptide-tag specific nanobodies for immunoaffinity chromatography, J. Chromatogr. A, **1624**, 461227 (2020).
16. **De Genst, E. J., Guilliams, T., Wellens, J., Day, E. M., Waudby, C. A., Meehan, S., Dumoulin, M., Hsu, S. T. D., Cremades, N., Verschueren, K. H. G., and other 5 authors:** Structure and properties of a complex of α-synuclein and a single-domain camelid antibody, J. Mol. Biol., **402**, 326–343 (2010).
17. **Jin, J., Hjerrild, K. A., Silk, S. E., Brown, R. E., Labbé, G. M., Marshall, J. M., Wright, K. E., Bezemer, S., Clemmensen, S. B., Biswas, S., and other 7 authors:** Accelerating the clinical development of protein-based vaccines for malaria by efficient purification using a four amino acid C-terminal 'C-tag', Int. J. Parasitol., **47**, 435–446 (2017).
18. **Jin, J., Tarrant, R. D., Bolam, E. J., Angell-Manning, P., Soegaard, M., Pattinson, D. J., Dulal, P., Silk, S. E., Marshall, J. M., Dabbs, R. A., and other 22 authors:** Production, quality control, stability, and potency of cGMP-produced *Plasmodium falciparum* RH5.1 protein vaccine expressed in *Drosophila* S2 cells, npj Vaccines, **3**, 32 (2018).
19. **Djender, S., Beugnet, A., Schneider, A., and De Marco, A.:** The biotechnological applications of recombinant single-domain antibodies are optimized by the C-terminal fusion to the EPEA sequence (C tag), Antibodies, **3**, 182–191 (2014).
20. **Waugh, D. S.:** An overview of enzymatic reagents for the removal of affinity tags, Protein Expr. Purif., **80**, 283–293 (2011).
21. **Wedde, M., Weise, C., Kopacek, P., Franke, P., and Vilcinskas, A.:** Purification and characterization of an inducible metalloprotease inhibitor from the hemolymph of greater wax moth larvae, *Galleria mellonella*, Eur. J. Biochem., **255**, 535–543 (1998).
22. **Vilcinskas, A.:** Anti-infective therapeutics from the Lepidopteran model host *Galleria mellonella*, Curr. Pharm. Des., **17**, 1240–1245 (2011).
23. **Vilcinskas, A. and Wedde, M.:** Insect inhibitors of metalloproteinases, IUBMB Life, **54**, 339–343 (2002).
24. **Joachim, M., Maguire, N., Schäfer, J., Gerlach, D., and Czermak, P.:** Process intensification for an insect antimicrobial peptide elastin-like polypeptide fusion produced in redox-engineered *Escherichia coli*, Front. Bioeng. Biotechnol., **7**, 150 (2019).
25. **Schwarz, S., Gerlach, D., Fan, R., and Czermak, P.:** GbpA as a secretion and affinity purification tag for an antimicrobial peptide produced in *Vibrio natriegens*, Electron. J. Biotechnol., **56**, 75–83 (2022).
26. **Wedde, M., Weise, C., Nuck, R., Altincicek, B., and Vilcinskas, A.:** The insect metalloproteinase inhibitor gene of the lepidopteran *Galleria mellonella* encodes two distinct inhibitors, Biol. Chem., **388**, 119–127 (2007).
27. **Eisenhardt, M., Schlupp, P., Höfer, F., Schmidts, T., Hoffmann, D., Czermak, P., Pöppel, A. K., Vilcinskas, A., and Runkel, F.:** The therapeutic potential of the insect metalloproteinase inhibitor against infections caused by *Pseudomonas aeruginosa*, J. Pharm. Pharmacol., **71**, 316–328 (2019).
28. **Schreiber, C., Müller, H., Birrenbach, O., Klein, M., Heerd, D., Weidner, T., Salzig, D., and Czermak, P.:** A high-throughput expression screening platform to optimize the production of antimicrobial peptides, Microb. Cell Fact., **16**, 29 (2017).
29. **Beigi, L., Karbalaei-Heidari, H. R., and Kharrati-Kopaei, M.:** Optimization of an extracellular zinc-metalloprotease (SVP2) expression in *Escherichia coli* BL21 (DE3) using response surface methodology, Protein Expr. Purif., **84**, 161–166 (2012).
30. **Eisenhardt, M., Dobler, D., Schlupp, P., Schmidts, T., Salzig, M., Vilcinskas, A., Salzig, D., Czermak, P., Keusgen, M., and Runkel, F.:** Development of an insect metalloproteinase inhibitor drug carrier system for application in chronic wound infections, J. Pharm. Pharmacol., **67**, 1481–1491 (2015).
31. **Twining, S. S.:** Fluorescein isothiocyanate-labeled casein assay for proteolytic enzymes, Anal. Biochem., **143**, 30–34 (1984).
32. **Collins, T., Azevedo-Silva, J., da Costa, A., Branca, F., Machado, R., and Casal, M.:** Batch production of a silk-elastin-like protein in *E. coli* BL21(DE3): key parameters for optimisation, Microb. Cell Fact., **12**, 21 (2013).
33. **Li, Z. and Rinas, U.:** Recombinant protein production associated growth inhibition results mainly from transcription and not from translation, Microb. Cell Fact., **19**, 83 (2020).
34. **Bryksa, B. C., MacDonald, L. D., Patrzykat, A., Douglas, S. E., and Mattatall, N. R.:** A C-terminal glycine suppresses production of pleurocidin as a fusion peptide in *Escherichia coli*, Protein Expr. Purif., **45**, 88–98 (2006).
35. **Harper, S. and Speicher, D. W.:** Purification of proteins fused to glutathione S-transferase, pp. 259–280, in: Walls, D. and Loughran, S. (Eds.), Protein chromatography. Methods in molecular biology, vol 681. Humana Press, Totowa (2011).
36. **Tessema, M., Simons, P. C., Cimino, D. F., Sanchez, L., Waller, A., Posner, R. G., Wandinger-Ness, A., Prossnitz, E. R., and Sklar, L. A.:** Glutathione-S-transferase-green fluorescent protein fusion protein reveals slow dissociation from high site density beads and measures free GSH, Cytometry A, **69**, 326–334 (2006).
37. **Bernier, S. C., Cantin, L., and Salesse, C.:** Systematic analysis of the expression, solubility and purification of a passenger protein in fusion with different tags, Protein Expr. Purif., **152**, 92–106 (2018).
38. **Ki, M. R. and Pack, S. P.:** Fusion tags to enhance heterologous protein expression, Appl. Microbiol. Biotechnol., **104**, 2411–2425 (2020).
39. **Zhao, W., Liu, L., Du, G., and Liu, S.:** A multifunctional tag with the ability to benefit the expression, purification, thermostability and activity of recombinant proteins, J. Biotechnol., **283**, 10 (2018).
40. **Zhao, W., Liu, S., Du, G., and Zhou, J.:** An efficient expression tag library based on self-assembling amphipathic peptides, Microb. Cell Fact., **18**, 91 (2019).
41. **Ojima-Kato, T., Nagai, S., and Nakano, H.:** N-terminal SKIK peptide tag markedly improves expression of difficult-to-express proteins in *Escherichia coli* and *Saccharomyces cerevisiae*, J. Biosci. Bioeng., **123**, 540–546 (2017).
42. **Ritthisan, P., Ojima-Kato, T., Damnjanović, J., Kojima, T., and Nakano, H.:** SKIK-zipbody-alkaline phosphatase, a novel antibody fusion protein expressed in *Escherichia coli* cytoplasm, J. Biosci. Bioeng., **126**, 705–709 (2018).
43. **Marblestone, J. G., Edavettal, S. C., Lim, Y., Lim, P., Zuo, X., and Butt, T. R.:** Comparison of SUMO fusion technology with traditional gene fusion systems: enhanced expression and solubility with SUMO, Protein Sci., **15**, 182–189 (2006).
44. **Grunina, T. M., Demidenko, A. V., Lyaschuk, A. M., Poponova, M. S., Galushkina, Z. M., Soboleva, L. A., Cherepushkin, S. A., Polyakov, N. B., Grumov, D. A., Solovyev, A. I., and other 6 authors:** Recombinant human erythropoietin with additional processable protein domains: purification of protein synthesized in *Escherichia coli* heterologous expression system, Biochemistry, **82**, 1285–1294 (2017).
45. **Assumpção, M. C., de Souza, E. M., Yates, M. G., De Oliveira Pedrosa, F., and Benelli, E. M.:** Purification and characterisation of *Azospirillum brasilense* N-truncated NtrX protein, Protein Expr. Purif., **53**, 302–308 (2007).
46. **Shen, Y., Morishita, M., and di Luccio, E.:** High yield recombinant expression and purification of oncogenic NSD1, NSD2, and NSD3 with human influenza hemagglutinin tag, Protein Expr. Purif., **166**, 105506 (2020).
47. **Terpe, K.:** Overview of bacterial expression systems for heterologous protein production: from molecular and biochemical fundamentals to commercial systems, Appl. Microbiol. Biotechnol., **72**, 211–222 (2006).
48. **Chen, Y. L., Tuan, H. Y., Tien, C. W., Lo, W. H., Liang, H. C., and Hu, Y. C.:** Augmented biosynthesis of cadmium sulfide nanoparticles by genetically engineered *Escherichia coli*, Biotechnol. Prog., **25**, 1260–1266 (2009).
49. **Kopp, J., Bayer, B., Slouka, C., Striedner, G., Dürkop, M., and Spadiut, O.:** Fundamental insights in early-stage inclusion body formation, Microb. Biotechnol., **16**, 5 (2023).
50. **Hoffmann, D.:** Produktion des Insektenmetalloprotease Inhibitors in *Escherichia coli* Neuartige Plattformtechnologie für die inclusion body-basierte Produktaufarbeitung, Band 12, Shaker Verlag, Gießen (2019).
51. **Joachim, M.:** Prozessintensivierung der rekombinanten Herstellung und neuartigen membranbasierten Aufreinigung eines Elastin-Like-Polypeptid gekoppelten antimikrobiellen Peptids, Band 16, Shaker Verlag, Gießen (2020).
52. **Köppl, C., Lingg, N., Fischer, A., Kröß, C., Loibl, J., Buchinger, W., Schneider, R., Jungbauer, A., Striedner, G., and Cserjan-Puschmann, M.:** Fusion tag design influences soluble recombinant protein production in *Escherichia coli*, Int. J. Mol. Sci., **23**, 7678 (2022).
53. **Sachdev, D. and Chirgwin, J. M.:** Order of fusions between bacterial and mammalian proteins can determine solubility in *Escherichia coli*, Biochem. Biophys. Res. Commun., **244**, 933–937 (1998).

54. **Costa, S., Almeida, A., Castro, A., and Domingues, L.:** Fusion tags for protein solubility, purification, and immunogenicity in *Escherichia coli*: the novel Fh8 system, Front. Microbiol., **5**, 63 (2014).
55. **Verma, R. R., Sriraman, R., Rana, S. K., Ponnanna, N. M., Rajendar, B., Ghantasala, P., Rajendra, L., Matur, R. V., and Srinivasan, V. A.:** E6 protein of human papillomavirus 16 (HPV16) expressed in *Escherichia coli* sans a stretch of hydrophobic amino acids, enables purification of GST-ΔE6 in the soluble form and retains the binding ability to p53, Protein Expr. Purif., **92**, 41–47 (2013).
56. **Kam, C. M., Nishino, N., and Powers, J. C.:** Inhibition of thermolysin and carboxypeptidase A by phosphoramidates, Biochemistry, **18**, 3032–3038 (1979).
57. **Suda, H., Aoyagi, T., Takeuchi, T., and Umezawa, H.:** A thermolysin inhibitor produced by actinomycetes: phosphoramidon, J. Antibiot. (Tokyo), **26**, 621–623 (1973).

CHAPTER 3: Detection and quantification of AMPs

The successful evaluation of a manufacturing process depends on the corresponding analytical methods. Product detection and quantification throughout the manufacturing process are critical aspects of production, and are particularly challenging in the case of AMPs due to their small size. This chapter focuses on the detection and quantification of three different AMPs (including IMPI, further named AMP α_c) throughout the manufacturing process.

The method used in this study is based on a newly developed resin designed specifically for C-tag analytical affinity chromatography. This innovative approach allowed the characterization of critical process parameters, a pioneering effort that contributed to protocol optimization. The intended application of this method is process analysis during the production of pharmaceutically-relevant AMPs, and it was therefore validated according to established guidelines.

The primary objective of this work is to demonstrate the versatility of the C-tag as a platform technology for the detection and quantification of different AMPs. This study represents a significant improvement over conventional analytical methods such as the widely used ELISA, which is evaluated in comparison.

The results presented here confirm the superiority of C-tag analytical affinity chromatography in terms of sensitivity, specificity and efficiency when compared to the current ELISA method for AMP detection and quantification. The implications of these advances extend beyond the specific AMPs studied herein, positioning the C-tag as a promising platform technology for the production of AMPs with diverse applications.

Detection and quantification of AMPs

Lappöhn, C.A., Maerz, L., Stei, R., Weber, L.G., Wolff, M.W. Optimization and validation of analytical affinity chromatography for the in-process monitoring and quantification of peptides containing a C-tag. J. Chromatogr. B, Anal. Technol. Biomed. life Sci. 1229, 123899 (2023) doi:10.1016/j.jchromb.2023.123899

Journal of Chromatography B 1229 (2023) 123899

Contents lists available at ScienceDirect

Journal of Chromatography B

journal homepage: www.elsevier.com/locate/jchromb

Optimization and validation of analytical affinity chromatography for the in-process monitoring and quantification of peptides containing a C-tag

Carolin A. Lappöhn [a], Lea Maerz [a], Robin Stei [a], Linus G. Weber [a], Michael W. Wolff [a,b,*]

[a] Institute of Bioprocess Engineering and Pharmaceutical Technology, University of Applied Sciences Mittelhessen (THM), Wiesenstr. 14, 35390 Giessen, Germany
[b] Fraunhofer Institute for Molecular Biology and Applied Ecology (IME), Ohlebergsweg 12, 35392 Giessen, Germany

ARTICLE INFO

Keywords:
Antimicrobial peptide
C-tag
Protein analysis
high performance liquid chromatography (HPLC)
Affinity chromatography
design of experiments (DoE)

ABSTRACT

Antimicrobial peptides and proteins (AMPs) are promising alternatives to conventional antibiotics for the treatment of infections caused by multidrug-resistant bacteria. The production of recombinant AMPs is facilitated by platform technologies such as the C-tag, a sequence of four C-terminal amino acids that allows immunoaffinity capture and purification. However, the detection and quantification of such products throughout the manufacturing process is a significant challenge. We therefore used a design of experiments approach to optimize a novel high-throughput analytical immunoaffinity chromatography method for the accurate quantification of AMPs containing a C-tag, resulting in minimal analyte carryover (98.8 ± 0.1 % product elution). We then validated the method in accordance with International Conference on Harmonisation guideline Q2(R2). Validation confirmed that the method achieves high specificity, linearity, accuracy, and precision. We implemented in-process control and quantification throughout the manufacturing process, from cell lysis to the final purified product. We found that the lysate and acidic samples (pH < 2) can lead to deviations. However, following sample pretreatment, C-tag quantification reduced the error to ≤ 4 %, which is potentially superior to current non-specific quantification methods such as UV absorbance and colorimetry. Implementing this method for in-process control and quantification throughout the manufacturing process achieves the reliable assessment of product quantity and quality. This method also offers improvements over the product-specific enzyme-linked immunosorbent assay currently used for C-tagged products because it has a higher precision, accuracy and throughput, with a measurement time of 2.5 min per sample. Our analytical affinity chromatography method is therefore a valuable tool for the quantification of AMPs as part of a novel platform technology approach for C-tagged products.

1. Introduction

Multidrug-resistant (MDR) bacteria pose a significant and escalating threat to global health [1,2]. The effectiveness of current broad-spectrum antibiotics is declining, resulting in longer treatment times, higher rates of hospitalization, and 4.95 million deaths worldwide from MDR infections in 2019 [2,3]. Antimicrobial peptides and proteins (AMPs) offer a promising alternative to small-molecule antibiotics because these naturally occurring components of the innate immune system have diverse mechanisms of action, targeting bacteria, fungi, parasites and viruses [4–6]. But the pharmaceutical use of AMPs is hindered by the insufficient quantity of AMPs available for clinical applications [7,8].

Although AMPs occur naturally, they are produced in such small quantities that extraction is economically impractical. Chemical synthesis is possible for small, simple AMPs, but not for longer structures with disulfide bonds. The only accessible strategy for complex AMPs is the expression of recombinant peptides in heterologous production hosts [8–11]. Typically, the production process must be tailored for each product, which is time-consuming and expensive. This can be

Abbreviations: **AMP**, antimicrobial peptide/protein; **AMP$_{XC}$**, AMP with a C-tag; **ANOVA**, analysis of variance; **BSA**, bovine serum albumin; **C-tag**, C-terminal fusion tag of the four amino acids EPEA; **DoE**, design of experiments; **ELISA**, enzyme-linked immunosorbent assay; **HPLC**, high–performance liquid chromatography; **ICH**, International Council for Harmonisation; **IMAC**, immobilized metal-chelate affinity chromatography; **LOD**, limit of detection; **LOQ**, limit of quantification; **PBS**, phosphate-buffered saline; **RSD**, relative standard deviation; **RSM**, response surface methodology; **RG2**, Rosetta-gami 2(DE3)pLysS; **TB**, terrific broth; **Thr**, thrombin cleavage site; **Trx**, thioredoxin.

* Corresponding author at: University of Applied Sciences Mittelhessen (THM), Wiesenstr. 14, 35390 Giessen, Germany.
E-mail address: Michael.Wolff@lse.thm.de (M.W. Wolff).

https://doi.org/10.1016/j.jchromb.2023.123899
Received 3 August 2023; Received in revised form 25 September 2023; Accepted 27 September 2023
Available online 28 September 2023

circumvented by using platform technologies, which enable uniform production methods for diverse proteins. An example of such a technology is the genetic fusion tag, a peptide or small protein that is fused to the target protein to increase its stability or solubility and/or to facilitate its detection and affinity-based purification [12]. One drawback of genetic fusion tags is that they can alter the properties or activity of the tagged protein, including immunogenicity, necessitating the addition of post-purification steps to cleave off the tag and purify the native protein product [11,12].

The C-tag is a genetic fusion tag that overcomes the issues discussed above by allowing the selective capture of tagged proteins without interfering with their activity or conferring immunogenicity [13,14]. This sequence of four C-terminal amino acids (Glu-Pro-Glu-Ala, EPEA) can therefore be left in place without affecting the product, and is even considered to be compliant with current good manufacturing practice (cGMP) [14,15]. Accordingly, the development of several COVID-19 vaccine candidates has been based on the expression of SARS-CoV-2 proteins carrying a C-tag to facilitate purification using CaptureSelect C-tag affinity resin [16,17].

Although C-tag purification has evolved into a platform technology, the analysis and quantification of products during manufacturing still involves a diverse set of methods. These include colorimetric analysis such as the Bradford assay [17], densitometric analysis based on gel electrophoresis [16,18], and enzyme-linked immunosorbent assays (ELISAs) [14,15]. The Bradford assay and gel electrophoresis are well-established research methods, but their low precision and inadequate quantification limits make them unsuitable for quality control [19,20]. Ideally, the method should be fast and simple with a high throughput, and the specificity and sensitivity should meet the challenges posed by low analyte concentrations and the presence of impurities [19,21]. Sandwich ELISA fulfils these criteria. For the 60-kDa PfRH5 protein, product-specific antibodies labeling different epitopes were developed to establish a highly selective and specific method [14,15,22–24]. However, the use of two different antibodies for small products, such as 15-kDa C-tagged single-domain antibodies [18] or AMPs, is challenging due to steric hindrance [25,26]. In such cases, an attractive alternative approach is affinity chromatography based on high-performance liquid chromatography (HPLC), which has a specificity and sensitivity comparable to ELISA [19,21,27,28]. A standardized approach to C-tag analysis and quantification would allow a platform approach to be used throughput the manufacturing process. The immobilization of a single-domain anti-C-tag camelid antibody on a resin suitable for HPLC would allow the rapid and easy detection of small C-tagged products as well as adequate quantification [29]. These camelid antibodies (nanobodies) are less expensive to produce than conventional antibodies, and have greater stability and longevity [30–32].

Here we describe the quantitative detection of diverse C-tagged AMPs using a novel analytical POROS CaptureSelect C-tag affinity resin (Thermo Fisher Scientific, Waltham, MA, USA). A statistical design of experiments (DoE) approach was used to optimize the method based on its critical process parameters, and we validated it according to International Council for Harmonisation (ICH) guideline Q2(R2). This will allow the detection, monitoring and quantification of AMPs throughout the manufacturing process using the C-tag as a novel platform technology.

2. Materials and methods

2.1. Standard peptide

Three C-tagged model AMPs were used in this study: recombinant AMP α_c, chemically synthesized AMP β_c (GenScript Biotech, Piscataway, NJ, USA), and chemically synthesized AMP γ_c (University of Applied Sciences Mittelhessen, Giessen, Germany). The amino acid sequences and production processes are described in detail in the Appendix A Text A1, A2.

2.2. HPLC instrumentation

The AMPs were analyzed by HPLC using an Ultimate 3000 UHPLC System RS (Thermo Fisher Scientific) equipped with an RS autosampler (injection volume 1–100 µL), RS diode array detector, and RS column compartment. We used Chromeleon v7.2 SR4 software (Thermo Fisher Scientific) for data analysis and instrument control. The AMPs were captured using analytical POROS CaptureSelect C-tag affinity resin (Thermo Fisher Scientific, in development and kindly provided prior to commercial release), which was packed into the column housing (PEEK 50 × 2.1 mm ID, 0.173 mL; Macherey-Nagel, Düren, Germany).

2.3. Optimization (design of experiments)

The experimental design was established by preliminary one-factor-at-a-time analysis, using the mobile phase, pH, flow rate, and column oven temperature as independent variables. The limits of the variables were determined based on the detectable changes in eluate AMP recovery. The aim was to ensure that the presumed optimum was within the factor range and that all experiments produced an evaluable response. The design space was defined according to the factor levels listed in Table 1. We used Design Expert v11 (Stat-Ease, Minneapolis, MN, USA) to optimize the method with an individual, randomized quadratic response surface methodology (RSM) design (I-optimal). Five center points were included to estimate the experimental error (Table 2). The constant conditions were phosphate-buffered saline (PBS; binding buffer) and glycine (elution buffer, concentration and pH determined by model) as fixed mobile phases, along with the injection volume (10 µL) and amount of AMP α_c (43 µg) as the largest and most complex model peptide. Further restrictions, described by **Eq. (1)**, were set by the manufacturers of the HPLC equipment and the analytical POROS CaptureSelect C-tag affinity resin [33,34]. To assess the impact of these factors, the responses listed in Table 3 were weighted according to their importance and goal. The software used **Eq. (2)** to calculate the asymmetry and **Eq. (3)** to determine the plate count [35]. The peaks were measured manually to obtain the data necessary for **Eq. (3)**.

$$15 \bullet X_3 - 0.5 \bullet X_4 \leq 31.250 \quad (1)$$

X_3 Flow rate [mL min^{-1}]
X_4 Column oven temperature [°C]

$$Y_3 = \frac{A_{5\%} + B_{5\%}}{2 \bullet A_{5\%}} \quad (2)$$

$$Y_4 = \frac{41.7 \bullet (t_R / w_{10\%})^2}{B_{10\%}/A_{10\%} + 1.25} \quad (3)$$

Y_3 Asymmetry factor As [-]
Y_4 Plate count N [-]
$A_{5/10\%}$ Distance from the leading edge to the midpoint of the peak at 5 % or 10 % of the peak height [min]
$B_{5/10\%}$ Distance from the midpoint to the tailing edge of the peak at 5 % or 10 % of the peak height [min]
t_R Retention time [min]
$w_{10\%}$ Peak width at 10 % of the peak height [min]

Table 1
. Factors and levels for response surface methodology optimization.

Factor	Unit	Lower level	Upper level
X_1: Glycine concentration	mM	0	50
X_2: pH	–	1.0	2.5
X_3: Flow rate	mL min^{-1}	1.50	2.75
X_4: Column oven temperature	°C	5.0	30.0

Table 2
. Parameter settings for the response surface methodology to investigate the influence of critical process parameters for method optimization.

Run	X_1	X_2	X_3	X_4
1	0	2.5	2.75	20.0
2	50	2.5	2.23	5.0
3	25	2.1	1.40	29.9
4	0	1.0	1.18	12.9
5*	25	1.7	1.95	18.0
6	0	1.0	2.75	30.0
7	50	1.4	1.00	21.3
8	0	1.4	1.89	23.9
9	25	1.0	1.00	30.0
10	50	1.0	2.74	19.7
11	0	2.5	1.82	30.0
12	25	1.0	2.25	5.0
13	37.5	2.1	2.75	30.0
14*	25	1.7	1.95	18.0
15	50	1.0	1.84	30.0
16	50	1.4	1.00	5.0
17	50	2.5	1.00	24.4
18	0	1.7	2.25	5.0
19	37.5	2.1	2.75	30.0
20	0	1.0	1.18	12.9
21	0	2.1	1.35	16.7
22	37.5	2.5	1.39	11.8
23	12.5	2.5	1.00	5.0
24	50	1.4	1.00	5.0
25*	25	1.7	1.95	18.0
26*	25	1.7	1.95	18.0
27	0	1.7	1.00	30.0
28*	25	1.7	1.95	18.0

Glycine concentration (X_1; mM), pH (X_2; –), flow rate (X_3; mL min^{-1}) and temperature (X_4;°C). Center points are marked with an asterisk.

Table 3
. Responses with factors of importance and goal of optimization for response surface methodology optimization.

Response	Unit	Importance factor	Goal
Y_1: Recovery	%	5	Maximize
Y_2: Peak area	mAU min	3	Maximize
Y_3: Asymmetry factor (*As*)	–	2	Minimize
Y_4: Plate count (*N*)	–	1	Maximize

The models were fitted based on regression analysis and analysis of variance (ANOVA), maintaining a hierarchical model structure. Each model was evaluated in confirmation runs (n = 3).

2.4. Method validation

The specificity, range, accuracy and precision of the optimized HPLC method were evaluated according to ICH guideline Q2(R2) on the validation of analytical procedures [36]. The absence of interference from impurities demonstrated the specificity of the method. For this we prepared a product-free cell lysate of *Escherichia coli* Rosetta-gami 2 (DE3) pLysS using BugBuster Mastermix (Merck, Darmstadt, Germany). We also tested recombinant AMP α without a C-tag and bovine serum albumin (BSA; Sigma Aldrich, St. Louis, MO, USA).

2.5. Application of the novel HPLC method

In-process quantification was based on the production and purification of recombinant AMP α_c, which is currently under development. For this purpose, we used product-free lysate and various elution buffer conditions representing the purification process (Table 4). The solutions of these intermediate purification steps were spiked with different amounts of AMP α_c, AMP β_c or AMP γ_c depending on the limit of quantification (LOQ). The peptides were also used to spike ultrapure water as a reference for total recovery.

Table 4
. List of solutions used for in-process quantification with the optimized and validated immunoaffinity HPLC method. The compositions of the product-containing solutions are shown at each step of production and purification.

Step	Solution composition
Cell lysate	Product-free Rosetta-gami 2 (DE3)pLysS cells grown in terrific broth with 34 mg L^{-1} chloramphenicol were enzymatically digested with BugBuster Mastermix
IMAC eluate	20 mM sodium phosphate buffer, 0.5 M NaCl, 0.5 M imidazole, pH 7.4
CaptureSelect C-tag eluates	200 mM phosphate buffer, pH 2
	200 mM phosphate buffer, pH 2, spiked with phosphate buffer to pH 7 with a final phosphate concentration of 200–375 mM
	200 mM glycine, pH 2
	200 mM glycine, pH 2, spiked with phosphate buffer to pH 7 with a final phosphate concentration of 200–375 mM

3. Results and discussion

3.1. Optimization of the HPLC method

Preliminary screening experiments focused on AMP binding to and elution from the new analytical POROS CaptureSelect C-tag affinity resin. We defined the glycine concentration (X_1) and pH (X_2) of the elution buffer as well as the flow rate (X_3) and column oven temperature (X_4) as critical process parameters, which were used as factors to set up the DoE (Tables 1 and 2). To optimize the method, we investigated the recovery (Y_1), peak area (Y_2), peak asymmetry (Y_3) and plate count (Y_4), as shown in Table 5. Some runs resulted in distorted or highly asymmetric elution peaks. To minimize the impact on the statistical modeling of these responses, runs with asymmetry scores > 4 or split peaks were excluded and marked with hashtags [35]. This did not affect the statistical evaluation of the models. To ensure a homogeneous distribution of the externally studentized residuals in the experimental design, we

Table 5
. Responses of the response surface methodology for HPLC optimization.

Run	Y_1	Y_2	Y_3	Y_4
1	98.08	13.12	1.42	28,370
2	98.33	9.67#	7.18	316
3	98.71	22.55	2.20	15,504
4	98.53	26.20	2.26	12,998
5*	98.85	18.25	2.00	23,571
6	98.35	11.45	1.60	31,232
7	98.97	30.75	2.79	10,096
8	98.98	16.67	1.90	24,320
9	98.64	27.19	2.51#	9178#
10	98.94	11.17	1.61	26,047
11	97.58	18.29	1.60	14,762
12	98.56	12.13	1.82	17,610
13	98.50	12.34	1.69	33,298
14*	98.91	18.29	2.02	23,571
15	98.67	16.73	2.01	19,543
16	98.79	29.98	3.06	6805
17	98.18	27.85	3.96	5480
18	98.83	18.11	1.54	29,809
19	98.50	12.48	1.67	28,176
20	98.97	26.25	2.43	12,998
21	98.17	23.47	2.24#	10245#
22	98.39	15.80#	4.96	984
23	97.45	24.72	3.29	8200
24	98.76	30.00	2.89	7162
25*	98.92	18.37	2.02	23,571
26*	98.91	18.18	2.03	23,075
27	98.31	26.33	1.03#	22179#
28*	98.97	18.23	1.77	22,178

We monitored recovery (Y_1; %), peak area (Y_2; mAu min), peak asymmetry (Y_3; –), and plate count (Y_4; –). Center points are marked with asterisks. Excluded runs (asymmetry > 4 or split peaks) are marked with hashtags.

applied an inverse square root transformation to the peak asymmetry response $(Y_3)^{-0.5}$. The other responses (Y_1, Y_2 and Y_4) were used as non-transformed values. Quadratic models, calculated by multiple regression analysis, were reduced while maintaining a hierarchical model structure. The results of the ANOVA and other quality criteria for model selection, such as coefficients of determination and adequate precision values, are listed in Tables 6 and 7. Detailed statistical analysis, along with coded and actual equations, is presented in Appendix B Table B1 and Figure B1.

Each response was fitted with a significant model ($p < 0.0001$) and a high coefficient of determination ($R^2 > 0.83$), representing good fits. Furthermore, the differences between adjusted and predicted R^2 values were < 0.2 and the signal-to-noise ratios were > 4, indicating that the initial measurements were close to the model predictions and provided reliable data [37,38]. The replicate and mean points of the RSM provide access to the pure error of the experiments and allow the models to be tested for lack-of-fit [39]. Here, the lack-of-fit p-values for the responses Y_1, Y_3 and Y_4 were > 0.05, indicating a satisfactory fit to the data. The response Y_2 (peak area) showed a significant lack-of-fit ($p < 0.0001$), indicating that the model may be inappropriate or the HPLC method has a high precision. Due to the high repeatability of the method, the variance of the mean and replicate points used to calculate the pure error is low (Table 5). This means that even small deviations can lead to a significant lack-of-fit. For this reason, the confirmation runs were examined in more detail, revealing that, despite this shortcoming, the model was still valid in its point predictions. All predictions were within a 95 % prediction interval except response Y_4 (plate count), where the data fell within a 96 % prediction interval (Appendix B Table B2). Based on these data, the models were considered suitable for prediction within the defined design space.

The relationship between factors affecting the responses is clearly shown in Table 6 and is supported by the model equation in Appendix B Table B1. Y_3 (peak asymmetry) and Y_4 (plate count) were strongly influenced by interactions between factors, whereas Y_1 (recovery) and Y_2 (peak area) showed only a few dominant interaction effects in the models. The significant influence of the quadratic effect of X_2^2 (pH) indicates a pH optimum in the design space. This strong pH dependence was observed in all responses and in preliminary experiments, where a steep decrease in binding affinity was observed at pH < 2.5 (data not shown). This can be explained by the predominantly electrostatic interaction between the C-tag and the ligand (anti-C-tag camelid antibody) immobilized on the analytical POROS CaptureSelect C-tag affinity resin [29]. The C-tag contains two glutamic acid residues, each side chain with a pKa of 4.07, and an alanine residue (free carboxyl group) with a pKa of 2.35 [40]. A decrease in pH leads to the protonation of these functional groups, which appears to affect the interaction and cause product elution [41]. Y_1 (recovery) showed a particularly high pH dependence, with an anticipated recovery > 97 %. For high recovery ($>Y_1$), the optimal factor settings are $X_2 \sim$ pH 1.4 and $X_4 \sim 17$ °C, regardless of X_3 (flow rate), whereas a higher X_1 (glycine concentration) extends the optimal range anticipated by the glycine buffer capacity [40,42]. However, X_3 (flow rate) is an important factor for Y_2 (peak area), where a minimal X_3 should help to maximize Y_2. Multiple dependencies were observed for Y_3 (peak asymmetry) and Y_4 (plate count), with factor interactions showing significant influences for Y_3 and linear effects for Y_4. Some factors showed inverse dependencies on responses. It was therefore necessary to weigh the responses according to their importance for the quantification method (Table 3). The flow rate should be maximized for high throughput and the temperature should be held as close to room temperature as possible to facilitate analysis in non-temperature-controlled column ovens. Furthermore, a high flow rate is recommended for a sharp elution peak [43], which can be directly related to peak asymmetry and plate count via the van Deemter equation [44–46]. Based on these weightings, the responses and factors were optimized using the calculated RSM. Due in part to the opposing dependencies of the responses on certain factors, we anticipate a desirability of < 1. The following optimized factor settings were predicted with a maximum desirability of 0.75: $X_1 = 32$ mM glycine, $X_2 =$ pH 1.54, $X_3 = 1.545$ mL min^{-1} flow rate, and $X_4 = 22$ °C. In confirmation runs (Appendix B Table B2), these elution settings led to satisfactory results for recovery ($Y_1 \sim 98.8$ % ± 0.1 %) and peak area ($Y_2 \sim 22.4 \pm 0.1$ mAU min) as well acceptable results for asymmetry ($Y_3 \sim 2.3 \pm 0.1$) and plate count ($Y_4 \sim 15{,}900 \pm 1.0$). In addition, analysis of the RSM under these optimized settings showed that the method should be robust to small changes in X_1 (glycine concentration), X_2 (pH) and X_4 (temperature), but sensitive to variations in X_3 (flow rate). The method therefore appears to be particularly user-friendly and reproducible.

Table 6
. Analysis of variance of the response surface methodology. The table lists p-values for the models, equation terms, and lack of fit for the responses.

	p-value			
Source	**Y_1**	**Y_2**	**$(Y_3)^{-0.5}$**	**Y_4**
Model	< 0.0001	< 0.0001	< 0.0001	< 0.0001
X_1	0.0014	0.7635*	< 0.0001	< 0.0001
X_2	< 0.0001	0.5782*	< 0.0001	0.0001
X_3	–	< 0.0001	< 0.0001	< 0.0001
X_4	0.9049*	0.5545*	< 0.0001	0.0004
X_1X_2	0.0492	–	< 0.0001	0.0298
X_1X_3	–	0.0174	0.0280	0.0428
X_1X_4	–	–	0.0002	< 0.0001
X_2X_3	–	–	0.0381	–
X_2X_4	–	–	< 0.0001	–
X_3X_4	–	–	0.0226	0.0078
X_1^2	–	–	–	–
X_2^2	< 0.0001	0.0086	0.0002	< 0.0001
X_3^2	–	0.0004	–	–
X_4^2	0.0033	0.1057	–	–
Lack of Fit	0.0804*	< 0.0001	0.5591*	0.1319*

Responses: recovery (Y_1; %), peak area (Y_2; mAu min), peak asymmetry (Y_3; –) and plate count (Y_4; –) with the factors glycine concentration (X_1), pH (X_2), flow rate (X_3) and temperature (X_4). *Non-significant terms are included to maintain the hierarchy.

Table 7
. Model parameters of the response surface methodology. The table lists coefficients of determination and adequate precision values for the responses.

	Model parameter			
Parameter	**Y_1**	**Y_2**	**$(Y_3)^{-0.5}$**	**Y_4**
R^2	0.8361	0.9745	0.9881	0.9753
Adjusted R^2	0.7892	0.9624	0.9781	0.9605
Predicted R^2	0.6678	0.9251	0.9519	0.8945
Adequate precision	15.8418	26.3033	38.6447	24.5679

Responses: recovery (Y_1; %), peak area (Y_2; mAu min), peak asymmetry (Y_3; –), and plate count (Y_4; –).

3.2. Validation of the HPLC method according to ICH Q2(R2)

Following the analysis of process-relevant parameters and DoE-based optimization, we validated the method in terms of specificity, range, accuracy and precision. The validation parameters for the three AMPs according to ICH guideline Q2(R2) are listed in Tables 8 and 9. The underlying calibration and residual plots are shown in Appendix C Figure C1.

The quantification of the AMPs was unaffected by impurities and the column material was found to be C-tag specific. Linearity and working ranges were determined, depending on the AMP. The lower limits were calculated according to the residual standard error and the upper limits were defined by the detector specifications [34]. Linear regression analysis showed a satisfactory correlation coefficient of ≥ 0.999 for all three AMPs [47]. The residuals were randomly distributed over the regression range (no lack-of-fit) and confirmed the linearity of the

Table 8
. Validated parameters of the proposed HPLC method. The table lists the results of tests for specificity, accuracy and precision. Recovery and repeatability tests were carried out at three levels covering the quantification range of AMP α_c, AMP β_c and AMP γ_c. Recovery data are means ± standard deviations and the maximum RSD is given for repeatability.

Parameter	AMP α_c	AMP β_c	AMP γ_c
Specificity	Specific	Specific	Specific
Accuracy			
Recovery [%]	100.1 ± 1.2	100.1 ± 0.5	100.0 ± 0.7
Precision			
Repeatability, RSD [%]	≤ 0.42	≤ 0.50	≤ 0.41
Intra-day variation, RSD [%]	2.2	0.5	0.9
Inter-day variation, RSD [%]	1.9	0.3	0.2

Table 9
. Regression analysis of calibration graphs for AMP α_c, AMP β_c and AMP γ_c (n = 3). Uncertainties of the slope and intercept are shown as standard errors.

Parameter	AMP α_c	AMP β_c	AMP γ_c
Linearity range [µg per injection]	10–65	5–45	15–45
Slope [mAU min µg^{-1}]	0.6067 ± 0.0082	0.8506 ± 0.0024	1.02297 ± 0.0065
Intercept [mAU min]	–1.731 ± 0.332	1.089 ± 0.068	0.79055 ± 0.20555
Pearson correlation coefficient	0.99955	0.99997	0.9999
LOD [µg per injection]	2.1	0.4	0.6
LOQ [µg per injection]	6.5	1.1	1.7
RSD [%]	1.8	0.4	0.6

specific ranges, which are listed in Table 9. The accuracy of the method was determined by recovery over the corresponding working range of each AMP and was within an acceptable range of 100 ± 2 % [47]. In addition to accuracy, precision is also important for a robust analytical method. The reproducibility RSD should be ≤ 0.5 % and the inter-day and intra-day variation should be ≤ 2 % [48]. Almost all of these requirements were met in our study, the exception being a 2.2 % intra-day RSD for AMP α_c. Given the high precision and accuracy of the method, we found this deviation acceptable. Furthermore, the defined LOQ was below the working ranges for all three AMPs. Combined with the high repeatability (RSD ≤ 0.5 %), this indicates the quantification method has a high sensitivity. Despite significant structural differences between the three AMPs, the greatest difference within the validation was the size of the validated working range. This is always a relationship between parameters such as the structural conformation, amino acid sequence and affinity of the product, and also depends on the sensitivity of the detector. In our study, the DoE-optimized method was applicable to three structurally distinct AMPs with satisfactory specificity, linearity, accuracy, and precision.

3.3. HPLC for in-process quantification

Having validated the quantification of C-tagged AMPs, we developed an in-process method suitable for the quantification of peptides at any manufacturing step. This required the demonstration of product recovery and in-process quantification at different stages of the process.

The recovery of AMPs from the cell lysate poses the greatest challenge because cell disruption introduces a range of impurities, such as host cell proteins, lipids and DNA, which can interact with the resin [49]. Lipids bind irreversibly to the analytical POROS CaptureSelect resins [33], which was also the case in our process. In preliminary experiments, we attempted to remove the irreversibly bound impurities from the column by on-column digestion with lipase from porcine pancreas, but this permanently limited the column performance (data not shown). Further preliminary experiments showed that the influence of the lipids was negligible compared to the bound DNA contaminants. DNA molecules are one of the main causes of irreversible fouling of columns and membranes due to their negative charge and size [50,51]. We showed that bound DNA can be partially removed by washing the column in a buffer containing the endonuclease DENARASE (data not shown). However, this step was time consuming. A more effective alternative is to treat the lysate with endonuclease before loading the column, which is the method we used here. The product-spiked solutions used for in-process quantification and the corresponding recovery of the three AMPs are shown in Fig. 1. The recovery of AMP β_c and AMP γ_c in water, endonuclease-treated cell lysate and the IMAC elution buffer fell within the recommended range of 100 ± 2 % [47]. However, AMP α_c fell just outside the recommended range at 102.6 ± 1.3 % in the cell lysate and 97.2 ± 0.3 % in the IMAC buffer. The harshest elution conditions during preparative CaptureSelect C-tag affinity chromatography (200 mM phosphate buffer or glycine at pH 2) reduced the recovery to ≤ 20 % for all AMPs, but neutralization with phosphate buffer increased the recovery of these samples to between 96.0 ± 0.2 % (for AMP α_c in 200 mM glycine buffer, pH 7) and 98.4 ± 0.4 % (for AMP γ_c in phosphate buffer, pH 7). Some samples did not meet the recommended accuracy limits. Specifically, those prepared at pH 2 were not compatible with the analytical method and should be neutralized beforehand to increase recovery. As described above, the interaction between the ligand and the C-tag is mainly electrostatic nature and therefore pH dependent [29]. Because the samples are applied to the column in a highly concentrated acidic buffer (pH < 2.5), the peptide cannot bind to the column due to the protonated C-tag [40,41]. Neutralization of these samples overcomes this problem but dilutes the sample, so the product content in the initial solution must be high enough for measurements within the specified working ranges. This should not be a major problem during purification and concentration steps such as affinity chromatography, but should be taken into account.

We demonstrated that lysate impurities and acidic sample buffers led to deviations in the process but can be overcome by the pre-treatment of samples. In contrast, 0.5 M sodium chloride with 0.5 M imidazole (IMAC buffer) showed negligible effects, despite acting as matrix effect substances in ELISAs [52,53]. However, due to the electrostatic interaction between ligand and C-tag, we expect high salt concentrations to interfere with detection by reducing the binding affinity [29]. This assumption is supported by the CaptureSelect C-tagXL column in preparative purification processes, where the product is eluted under neutral conditions with high salt concentrations of 2 M $MgCl_2$ at pH 7.4 [17]. We assume that this would lead to a systemic error depending on the buffer. Furthermore, if enough of the product is bound to the column, the error can be calculated specifically for the process. For example, the standard should be measured in the appropriate buffer beforehand to determine the analytical error.

However, given the overall low error of the proposed quantification method and its high precision, the additional error of a low recovery (≤4% in our method) might still be acceptable compared to current alternative immunoassays, which have an accepted coefficient of variation of ≤ 15 % [54]. Measurement time may vary depending on specific parameters and conditions such as the chromatography system, column size and detection method. In our case, a throughput of 2.5 min per sample was possible, which is comparable to the well-known high-throughput technology of an analytical protein A chromatography column [55].

4. Conclusion

We optimized and validated a novel quantification method for C-tagged AMPs using POROS CaptureSelect C-tag affinity resin. The optimized parameters, including glycine concentration, pH, flow rate and column oven temperature, were determined using RSM and were established as method standards. We achieved a product recovery of

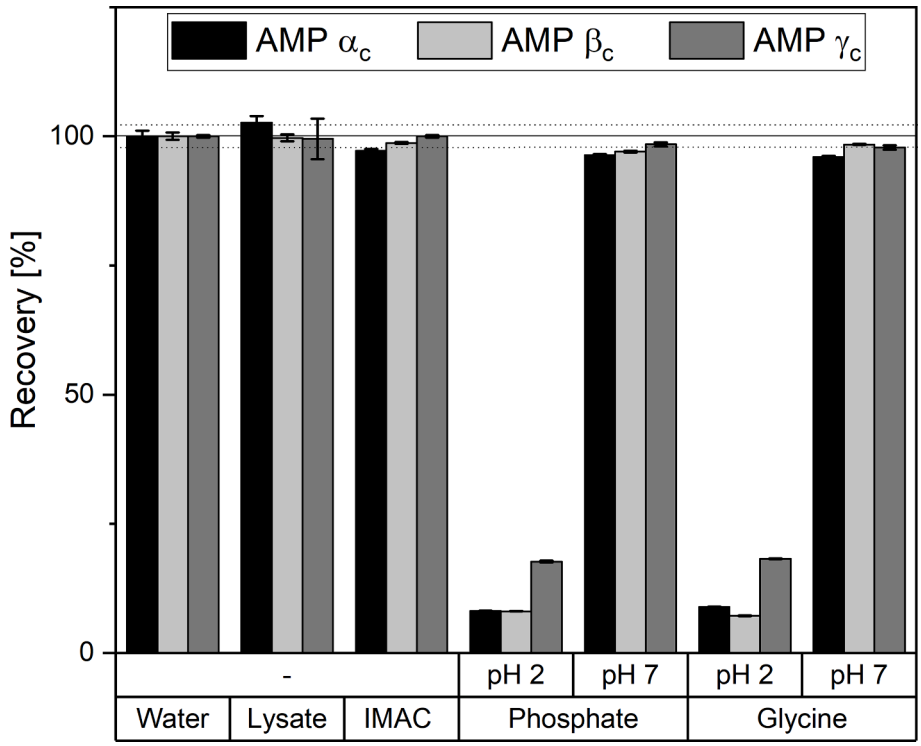

Fig. 1. Recovery of the products AMP α_c, AMP β_c and AMP γ_c in ultra-pure water correlated to endonuclease-treated cell lysate and the process buffers for IMAC (20 mM sodium phosphate buffer, 0.5 M NaCl, 0.5 M imidazole, pH 7.4; 200 mM phosphate buffer pH 2 and 7; 200 mM glycine pH 2 and 7). Horizontal line shows 100 % recovery and dotted lines represent ± 2 % of the recommended limit value.

98.8 ± 0.1 %, confirming the method's accuracy. We also validated the method according to ICH guideline Q2(R2), ensuring its specificity, linearity, accuracy and precision for the quantification of the model AMPs [36]. The application of this quantification method to a production process for recombinant AMPs demonstrated its suitability for accurate product quantification at multiple process steps. In particular, the method achieved the reliable quantification of neutral or neutralized samples with a recovery error ≤ 4 %. Our quantification method supports the use of the C-tag as a platform technology for the production and detection of recombinant proteins. Traditionally, the quantification of C-tagged products has required colorimetric assays, densitometric analysis or ELISA with custom antibodies [14–18,22–24]. As described above, colorimetric assays and densitometric analysis are not sufficient to quantify the product due to their lack of selectivity and precision [19,20]. The current product-specific ELISA is a good method for quantification but the POROS CaptureSelect C-tag affinity resin could achieve further improvement. In the ELISA method for the RfRH5 vaccine, the 96-well plates are loaded approximately 40 times with different solutions and incubation times of 17 h were reported (assuming overnight means 12 h), which is time-consuming and labor-intensive [14,15,22]. Compared to our method, the ELISA samples were also diluted or pre-treated, which can take the same amount of time. However, this calculation must be based on the number of samples to be analyzed. In addition, it may be possible to combine the pipetting steps of different samples to save time in the ELISA and in our method [52]. For economic comparisons, it is not possible to calculate the cost of the POROS CaptureSelect C-tag affinity resin because it is not currently available on the market. However, the antibodies used in the ELISAs were prepared specifically for each product, and were then used in large quantities for plate coating before they were washed off and thus discarded [14,15,22]. In contrast, the single-domain anti-C-tag camelid antibody immobilized on the POROS resin is stable and reusable [29–32]. Both methods could be used for high-throughput quantification, but our method makes it possible to purify, detect and monitor different C-tagged proteins throughout the production process. Overall, the optimized and validated quantification method using analytical C-tag affinity resin provides a valuable tool for the accurate quantification of C-tagged proteins in research projects and industrial processes.

CRediT authorship contribution statement

Carolin A. Lappöhn: Conceptualization, Data curation, Formal analysis, Funding acquisition, Investigation, Methodology, Project administration, Resources, Software, Supervision, Validation, Visualization, Writing – original draft, Writing – review & editing. **Lea Maerz:** Data curation, Formal analysis, Investigation, Methodology, Software, Validation, Visualization, Writing – review & editing. **Robin Stei:** Data curation, Formal analysis, Investigation, Methodology, Validation. **Linus G. Weber:** Data curation, Formal analysis, Investigation, Methodology, Validation. **Michael W. Wolff:** Conceptualization, Funding acquisition, Project administration, Resources, Supervision.

Declaration of Competing Interest

The authors declare that they have no known competing financial interests or personal relationships that could have appeared to influence the work reported in this paper.

Data availability

Data will be made available on request.

Acknowledgments

The authors would like to thank Peter Czermak for technical support and Richard M. Twyman for editing the manuscript. The manuscript is part of Carolin A. Lappöhn's dissertation at the Graduate Centre for Engineering Sciences under the aegis of the Justus-Liebig-University

Giessen, Germany, in cooperation with the University of Applied Sciences Mittelhessen, Giessen, Germany.

Funding

C. Lappoehn was financially supported by the Johannes Hübner Foundation with a doctoral scholarship. This work was financially supported by the strategic research fund of the University of Applied Sciences Mittelhessen, Giessen, Germany.

Appendix A. Supplementary data

Supplementary data to this article can be found online at https://doi.org/10.1016/j.jchromb.2023.123899.

References

[1] World Health Organization, Prioritization of Pathogens to Guide Discovery, Research and Development of New Antibiotics for Drug-Resistant Bacterial Infections, Including Tuberculosis, Doc. No: WHO/EMP/IAU/2017.12 (2017). https://apps.who.int/iris/handle/10665/311820, 2017 (accessed 09 February 2022).

[2] M. Naghav, Global burden of bacterial antimicrobial resistance in 2019: a systematic analysis, Lancet 399 (2022) (2019) 629–655, https://doi.org/10.1016/S0140-6736(21)02724-0.

[3] T. Mestrovic, G. Robles Aguilar, L.R. Swetschinski, K.S. Ikuta, A.P. Gray, N. Davis Weaver, C. Han, E.E. Wool, A. Gershberg Hayoon, S.I. Hay, C. Dolecek, B. Sartorius, C.J.L. Murray, I.Y. Addo, B.O. Ahinkorah, A. Ahmed, M.A. Aldeyab, K. Allel, R. Ancuceanu, A.E. Anyasodor, M. Ausloos, F. Barra, A.S. Bhagavathula, D. Bhandari, S. Bhaskar, N. Cruz-Martins, A. Dastiridou, K. Dokova, E. Dubljanin, O.C. Durojaiye, A.F. Fagbamigbe, S. Ferrero, P.A. Gaal, V.B. Gupta, V.K. Gupta, V.K. Gupta, C. Herteliu, S. Hussain, I.M. Ilic, M.D. Ilic, E. Jamshidi, T. Joo, A. Karch, A. Kisa, S. Kisa, T. Kostyanev, H.H. Kyu, J. Lám, G. Lopes, A.G. Mathioudakis, A.F.A. Mentis, I.M. Michalek, M.A. Moni, C.E. Moore, F. Mulita, I. Negoi, R.I. Negoi, T. Palicz, A. Pana, J. Perdigão, I.R. Petcu, N. Rabiee, D.L. Rawaf, S. Rawaf, M.Z. Shakhmardanov, A. Sheikh, L.M.L.R. Silva, V.Y. Skryabin, A.A. Skryabina, B. Socea, A. Stergachis, T.Z. Stoeva, C.D. Sumi, A. Thiyagarajan, M.R. Tovani-Palone, M. Yesiltepe, S. Bin Zaman, M. Naghavi, The burden of bacterial antimicrobial resistance in the WHO European region in 2019: a cross-country systematic analysis, Lancet Public Heal. 7 (2022) e897–e913. https://doi.org/10.1016/S2468-2667(22)00225-0.

[4] L. Zhang, R.L. Gallo, Antimicrobial peptides, Cell Press, Current Biology 26 (2016) 14–19, https://doi.org/10.1007/978-3-319-29785-9_6.

[5] I. Arash, R.L. Gallo, Antimicrobial peptides, Am. Acad. Dermatology. 52 (2005) 381–390, https://doi.org/10.1007/978-3-319-29785-9_6.

[6] M.D. Seo, H.S. Won, J.H. Kim, T. Mishig-Ochir, B.J. Lee, Antimicrobial peptides for therapeutic applications: A review, Molecules 17 (2012) 12276–12286, https://doi.org/10.3390/molecules171012276.

[7] C. Li, T. Haug, O.B. Styrvold, T.O. Jørgensen, K. Stensvåg, Strongylocins, novel antimicrobial peptides from the green sea urchin, *Strongylocentrotus droebachiensis*, Developmental and Comparative Immunology 32 (2008) 1430–1440, https://doi.org/10.1016/j.dci.2008.06.013.

[8] N.S. Parachin, K.C. Mulder, A.A.B. Viana, S.C. Dias, O.L. Franco, Expression systems for heterologous production of antimicrobial peptides, Peptides 38 (2012) 446–456, https://doi.org/10.1016/j.peptides.2012.09.020.

[9] J.P. Bradshaw, Cationic Antimicrobial Peptides: Issues for Potential Clinical Use, BioDrugs 17 (2003) 233–240, https://doi.org/10.2165/00063030-200317040-00002.

[10] Z. Zheng, N. Tharmalingam, Q. Liu, E. Jayamani, W. Kim, B.B. Fuchs, R. Zhang, A. Vilcinskas, E. Mylonakis, Synergistic Efficacy of Aedes aegypti Antimicrobial Peptide Cecropin A2 and Tetracycline against *Pseudomonas aeruginosa*, Antimicrobial Agents and Chemotherapy 61 (2017) 1–15, https://doi.org/10.1128/AAC.00686-17.

[11] H. Müller, D. Salzig, P. Czermak, Considerations for the process development of insect-derived antimicrobial peptide production, Biotechnology Progress 31 (2015) 1–11, https://doi.org/10.1002/btpr.2002.

[12] J. Huang, S.N. Stanislav, A. Koide, R.S. Rock, S. Koide, A peptide tag system for facile purification and single-molecule immobilization, Biochemistry 48 (2009) 11834–11836, https://doi.org/10.1021/bi901756n.A.

[13] Life technologies, Product Information Sheet: CaptureSelect ™ C-tag Affinity Matrix, Pub. No. MAN0010706. https://assets.thermofisher.com/TFS-Assets/LSG/manuals/MAN0010706_CapSelect_Ctag_PI.pdf , 2014 (accessed 22 March 2023).

[14] J. Jin, K.A. Hjerrild, S.E. Silk, R.E. Brown, G.M. Labbé, J.M. Marshall, K.E. Wright, S. Bezemer, S.B. Clemmensen, S. Biswas, Y. Li, A. El-Turabi, A.D. Douglas, P. Hermans, F.J. Detmers, W.A. de Jongh, M.K. Higgins, R. Ashfield, S.J. Draper, Accelerating the clinical development of protein-based vaccines for malaria by efficient purification using a four amino acid C-terminal 'C-tag', International Journal for Parasitology 47 (2017) 435–446, https://doi.org/10.1016/j.ijpara.2016.12.001.

[15] J. Jin, R.D. Tarrant, E.J. Bolam, P. Angell-Manning, M. Soegaard, D.J. Pattinson, P. Dulal, S.E. Silk, J.M. Marshall, R.A. Dabbs, F.L. Nugent, J.R. Barrett, K. A. Hjerrild, L. Poulsen, T. Jørgensen, T. Brenner, I.N. Baleanu, H.M. Parracho, A. Tahiri-Alaoui, G. Whale, S. Moyle, R.O. Payne, A.M. Minassian, M.K. Higgins, F. J. Detmers, A.M. Lawrie, A.D. Douglas, R. Smith, W.A. de Jongh, E. Berrie, R. Ashfield, S.J. Draper, Production, quality control, stability, and potency of cGMP-produced *Plasmodium falciparum* RH5.1 protein vaccine expressed in *Drosophila* S2 cells, npj Vaccines 3 (2018) 1–13, https://doi.org/10.1038/s41541-018-0071-7.

[16] C. Fougeroux, M. Idorn, V. Soroka, S.K. Myeni, R. Dagil, C.M. Janitzek, K. Aves, E. W. Horsted, J. Dorosz, S. Clemmensen, L. Fredsgaard, S. Thrane, E.E. Vidal-calvo, T.M. Hulen, S. Choudhary, M. Theisen, S. Singh, A. Garcia-, L. Van Oosten, G. Pijlman, B. Hierzberger, T. Domeyer, W. Blanka, M. Skrzypczak, L.F. Andersson, T.J. Dalebout, H. Ullum, L.S. Reinert, M. Kikkert, T.G. Theander, M.A. Nielsen, A. Salanti, F. Adam, A. Aps, M. Sciences, H. Hospital, Capsid-like particles decorated with the SARS2-CoV-2 receptor-binding domain elicit strong virus neutralization activity, Nature Communications 12 (2021), https://doi.org/10.1038/s41467-020-20251-8.

[17] M.S. Khan, E. Kim, A. McPherson, F.J. Weisel, S. Huang, T.W. Kenniston, E. Percivalle, I. Cassaniti, F. Baldanti, M. Meisel, A. Gambotto, Adenovirus-vectored SARS-CoV-2 vaccine expressing S1-N fusion protein, Antib. Ther. 5 (2022) 177–191.

[18] S. Djender, A. Beugnet, A. Schneider, A. de Marco, The Biotechnological Applications of Recombinant Single-Domain Antibodies are Optimized by the C-Terminal Fusion to the EPEA Sequence (C Tag), Antibodies 3 (2014) 182–191, https://doi.org/10.3390/antib3020182.

[19] S. Grotefend, L. Kaminski, S. Wroblewitz, S. El Deeb, N. Kühn, S. Reichl, M. Limberger, S. Watt, H. Wätzig, Protein quantitation using various modes of high performance liquid chromatography, Journal of Pharmaceutical and Biomedical Analysis 71 (2012) 127–138, https://doi.org/10.1016/j.jpba.2012.08.024.

[20] S. Schröder, H. Zhang, E.S. Yeung, L. Jänsch, C. Zabel, H. Wätzig, Quantitative gel electrophoresis: sources of variation, Journal of Proteome Research 7 (2008) 1226–1234, https://doi.org/10.1021/pr700589s.

[21] J. Horak, A. Ronacher, W. Lindner, Quantification of immunoglobulin G and characterization of process related impurities using coupled Protein A and size exclusion high performance liquid chromatography, Journal of Chromatography. A 1217 (2010) 5092–5102, https://doi.org/10.1016/j.chroma.2010.06.007.

[22] K.A. Hjerrild, J. Jin, K.E. Wright, R.E. Brown, J.M. Marshall, G.M. Labbé, S.E. Silk, C.J. Cherry, S.B. Clemmensen, T. Jørgensen, J.J. Illingworth, D.G.W. Alanine, K. H. Milne, R. Ashfield, W.A. De Jongh, A.D. Douglas, M.K. Higgins, S.J. Draper, Production of full-length soluble *Plasmodium falciparum* RH5 protein vaccine using a *Drosophila melanogaster* Schneider 2 stable cell line system, Scientific Reports 6 (2016) 1–15, https://doi.org/10.1038/srep30357.

[23] A.D. Douglas, A.R. Williams, J.J. Illingworth, G. Kamuyu, S. Biswas, A.L. Goodman, D.H. Wyllie, C. Crosnier, K. Miura, G.J. Wright, C.A. Long, F.H. Osier, K. Marsh, A. V. Turner, A.V.S. Hill, S.J. Draper, The blood-stage malaria antigen PfRH5 is susceptible to vaccine-inducible cross-strain neutralizing antibody, Nature Communications 2 (2011), https://doi.org/10.1038/ncomms1615.

[24] A.D. Douglas, A.R. Williams, E. Knuepfer, J.J. Illingworth, J.M. Furze, C. Crosnier, P. Choudhary, L.Y. Bustamante, S.E. Zakutansky, D.K. Awuah, D.G.W. Alanine, M. Theron, A. Worth, R. Shimkets, J.C. Rayner, A.A. Holder, G.J. Wright, S. J. Draper, Neutralization of *Plasmodium falciparum* Merozoites by Antibodies against PfRH5, Journal of Immunology 192 (2014) 245–258, https://doi.org/10.4049/jimmunol.1302045.

[25] S. Sakamoto, W. Putalun, S. Vimolmangkang, W. Phoolcharoen, Y. Shoyama, H. Tanaka, S. Morimoto, Enzyme-linked immunosorbent assay for the quantitative/qualitative analysis of plant secondary metabolites, Journal of Natural Medicines 72 (2018) 32–42, https://doi.org/10.1007/s11418-017-1144-z.

[26] J. Corrales, W.L. Gordon, E.J. Noga, Development of an ELISA for quantification of the antimicrobial peptide piscidin 4 and its application to assess stress in fish, Fish & Shellfish Immunology 27 (2009) 154–163, https://doi.org/10.1016/j.fsi.2009.02.023.

[27] S.S. Omar, M.A. Haddad, S. Parisi, Validation of HPLC and Enzyme-Linked Immunosorbent Assay (ELISA) techniques for detection and quantification of aflatoxins in different food samples, Foods. 9 (2020), https://doi.org/10.3390/foods9050661.

[28] V. Dohnal, V. Dvořák, F. Malíř, V. Ostrý, T. Roubal, A comparison of ELISA and HPLC methods for determination of ochratoxin A in human blood serum in the Czech Republic, Food and Chemical Toxicology 62 (2013) 427–431, https://doi.org/10.1016/j.fct.2013.09.010.

[29] E.J. De Genst, T. Guilliams, J. Wellens, E.M. Day, C.A. Waudby, S. Meehan, M. Dumoulin, S.T.D. Hsu, N. Cremades, K.H.G. Verschueren, E. Pardon, L. Wyns, J. Steyaert, J. Christodoulou, C.M. Dobson, Structure and properties of a complex of α-synuclein and a single-domain camelid antibody, Journal of Molecular Biology 402 (2010) 326–343, https://doi.org/10.1016/j.jmb.2010.07.001.

[30] S. Muyldermans, T.N. Baral, V.C. Retamozzo, P. De Baetselier, E. De Genst, J. Kinne, H. Leonhardt, S. Magez, V.K. Nguyen, H. Revets, U. Rothbauer, B. Stijlemans, S. Tillib, U. Wernery, L. Wyns, G. Hassanzadeh-Ghassabeh, D. Saerens, Camelid immunoglobulins and nanobody technology, Veterinary Immunology and Immunopathology 128 (2009) 178–183, https://doi.org/10.1016/j.vetimm.2008.10.299.

[31] E. De Genst, D. Saerens, S. Muyldermans, K. Conrath, Antibody repertoire development in camelids, Developmental and Comparative Immunology 30 (2006) 187–198, https://doi.org/10.1016/j.dci.2005.06.010.

[32] P. Holliger, P.J. Hudson, Engineered antibody fragments and the rise of single domains, Nature Biotechnology 23 (2005) 1126–1136, https://doi.org/10.1038/nbt1142.
[33] ThermoScientific, POROS™ A and G Affinity Columns POROS™ CaptureSelect ™ Affinity Columns Product Information Sheet, Prod. Inf. Sheet. Pub. No. 8-0003-40-1093. https://assets.thermofisher.com/TFS-Assets/LSG/manuals/80003401093_POROSAGC_PI.pdf. , 2018 (accessed 13 March 2023).
[34] ThermoScientific, Dionex Softron GmbH - Part of Thermo Fisher Scientific Inc. Dionex UltiMate 3000 Series – Diode Array Detectors DAD-3000(RS) and MWD-3000(RS), Oper. Instr. (Revision 1.4) Doc. No. 4820.8250. https://assets.thermofisher.com/TFS-Assets/CMD/man , 2013 (accessed 08 August 2022).
[35] J.P. Foley, J.G. Dorsey, Equations for Calculation of Chromatographic Figures of Merit for Ideal and Skewed Peaks, Analytical Chemistry 55 (1983) 730–737, https://doi.org/10.1021/ac00255a033.
[36] International Council for Harmonisation of technical Requirements for Pharmaceuticals for Human Use, Validation of analytical procedures: ICH guidelines Q2(R2), https://www.Ema.Europa.Eu/En/Documents/Scientific-Guideline/Ich-Guideline-Q2r2-Validation-Analytical-Procedures-Step-2b_en.Pdf. , 2022 (accessed 13 March 2023).
[37] P.J.W. Mark, J. Anderson, DOE simplified: Practical tools for effective experimentation, third ed., CRC Press, London, 2017.
[38] R.J. Del Vecchio, Understanding design of experiments: a primer for technologists, Hanser/Gardner, Munich, 2007.
[39] R.B. Patel, N.M. Patel, M.R. Patel, A.B. Solanki, Optimization of robust HPLC method for quantitation of ambroxol hydrochloride and roxithromycin using a DoE approach, Journal of Chromatographic Science 55 (2017) 275–283, https://doi.org/10.1093/chromsci/bmw182.
[40] S. Bräse, J. Bülle, A. Hüttermann, Organische und bioorganische Chemie: Das Basiswissen für Master- und Diplomprüfungen, first ed., Wiley, 2008.
[41] E. Sada, S. Katoh, Y. Sohma, Effects of histidine residues on adsorption equilibrium of peptide antibodies, Journal of Immunological Methods 130 (1990) 33–37, https://doi.org/10.1016/0022-1759(90)90296-8.
[42] M.A. Firer, Efficient elution of functional proteins in affinity chromatography, Journal of Biochemical and Biophysical Methods 49 (2001) 433–442, https://doi.org/10.1016/S0165-022X(01)00211-1.
[43] R.L. Fahrner, H.V. Iyer, G.S. Blank, The optimal flow rate and column length for maximum production rate of protein A affinity chromatography, Bioprocess Engineering 21 (1999) 287–292, https://doi.org/10.1007/s004490050677.
[44] L. Nováková, H. Vlčková, A review of current trends and advances in modern bio-analytical methods: Chromatography and sample preparation, Analytica Chimica Acta 656 (2009) 8–35, https://doi.org/10.1016/j.aca.2009.10.004.
[45] J.J. van Deemter, F.J. Zuiderweg, A. Klinkenberg, Longitudinal diffusion and resistance to mass transfer as causes of nonideality in chromatography, Chemical Engineering Science 5 (1956) 271–289, https://doi.org/10.1016/0009-2509(96)81813-6.
[46] J.C. Giddings, Dynamics of Chromatography. Part. I: Principles and Theory, Marcel Dekker, Berichte der Bunsengesellschaft für physikalische Chemie, New York, 1965.
[47] S. Ghulam, Step-by-step analytical methods validation and protocol in the quality system compliance industry, J. Valid. Technol. (2005), https://doi.org/10.1590/s0034-89102006000700002.
[48] R.O.V. and R. Breno M. Marson, Victor Concentino, Allan M. Junkert, Mariana M. Fachi, Pontarolo, VALIDATION OF ANALYTICAL METHODS IN A PHARMACEUTICAL QUALITY SYSTEM: AN OVERVIEW FOCUSED ON HPLC METHODS, Quim. Nov. 43 (2020) 1190–1203. https://doi.org/10.21577/0100-4042.20170589.
[49] M. Pathak, A.S. Rathore, Mechanistic understanding of fouling of protein A chromatography resin, Journal of Chromatography. A 1459 (2016) 78–88, https://doi.org/10.1016/j.chroma.2016.06.084.
[50] P. Gerster, E.M. Kopecky, N. Hammerschmidt, M. Klausberger, F. Krammer, R. Grabherr, C. Mersich, L. Urbas, P. Kramberger, T. Paril, M. Schreiner, K. Nöbauer, E. Razzazi-Fazeli, A. Jungbauer, Purification of infective baculoviruses by monoliths, Journal of Chromatography. A 1290 (2013) 36–45, https://doi.org/10.1016/j.chroma.2013.03.047.
[51] D.J. Roush, Y. Lu, Advances in primary recovery: Centrifugation and membrane technology, Biotechnology Progress 24 (2008) 488–495, https://doi.org/10.1021/bp070414x.
[52] F. Rubio, L.J. Veldhuis, B.S. Clegg, J.R. Fleeker, J.C. Hall, Comparison of a direct ELISA and an HPLC method for glyphosate determinations in water, Journal of Agricultural and Food Chemistry 51 (2003) 691–696, https://doi.org/10.1021/jf020761g.
[53] A. Kummer, E.C.Y. Li-Chan, Application of an ELISA-elution assay as a screening tool for dissociation of yolk antibody-antigen complexes, Journal of Immunological Methods 211 (1998) 125–137, https://doi.org/10.1016/S0022-1759(97)00199-3.
[54] S. Aydin, A short history, principles, and types of ELISA, and our laboratory experience with peptide/protein analyses using ELISA, Peptides 72 (2015) 4–15, https://doi.org/10.1016/j.peptides.2015.04.012.
[55] Tosoh Bioscience, Fast Monoclonal Antibody Titer Determination with TSKgel Protein A-5PW, Appl. Note. A16L08A, https://theanalyticalscientist.com/fileadmin/tas/i. https://www.separations.eu.tosohbioscience.com/solutions/hplc-products/protein-a. , 2019 (accessed 23 March 2022).

CHAPTER 4: Summary and future perspectives

This dissertation project aimed to develop and establish a platform technology for the production of AMPs. Given the small size of AMPs, this platform was constructed and investigated using a small fusion tag, the C-tag. The work was divided into several steps, focusing on heterologous production, purification, and analytics in the context of the C-tag.

In the first step, IMPI was selected as a model AMP because it has a complex structure, and yields have previously been low. It was successfully produced in a genetically modified *E. coli* strain with the C-tag, resulting in a significant 7.6-fold increase in expression levels compared to its non-tagged counterpart. By adjusting process parameters such as the induction time, inducer concentration, and temperature, the yield was increased by a factor of 10. The final yield was 30-fold higher than that of any process described in the literature. Furthermore, the C-tag could be used to capture the product efficiently, resulting in 86.4 ± 5.0% recovery and 77 ± 10% purity. Notably, the C-tag did not affect IMPI activity, eliminating the need for tag removal and thus reducing costs and time.

Subsequently, these insights were used to establish an analytical method, which is necessary to detect and quantify the product throughout the production process. In this context, a C-tag-specific resin under development by Thermo Fisher Scientific was used for analytical affinity chromatography. Process-relevant parameters such as buffer concentration, pH, flow rate, and column temperature were identified and optimized by statistical experimental designs. This enabled the elution of ~98.8 ± 0.1% of the product from the column matrix, ensuring accurate quantification. Further validation of this method confirmed its high specificity, linearity, accuracy, and precision. It was subsequently used for the characterization and evaluation of product samples during the manufacturing process. Quantification was less accurate if the pH of the sample fell below 2, but this could be mitigated by neutralization. The measurement time of 2.5 min per sample is suitable for the high-throughput quantification of C-tagged AMPs.

Although these results represent a significant step toward a platform technology for the heterologous expression and purification of AMPs, it has only been demonstrated for a single AMP. To be defined as a platform, similar performance must be achieved with at

least two additional structurally diverse AMPs, potentially from non-microbial expression hosts, to accommodate variations in expression levels and the removal of other impurities using the C-tag. Furthermore, the post-capture purification steps need to be studied in more detail. As we learn more about the interactions between microorganisms and AMPs, the significance of the C-terminus may also become clearer. In this work, none of the AMPs lost activity when the C-terminus was covered by the C-tag, but further work on AMP mechanisms of action may reveal additional insights. For the production of IMPI, the addition of the C-tag led to higher yields, which could be improved further by initial process optimization. In a controlled bioreactor system with additional optimized process parameters, even higher yields are anticipated. The influence of N-terminal fusion tags should also be investigated.

The platform concept based on the C-tag has also been supported by the development of an analytical method. In the future, this system will enable the quantification of not only AMPs but also other C-tagged products. This platform offers a significant advantage over current methods for small-scale, high-throughput applications, but large-scale processes must be carefully evaluated to determine whether the cost of product-specific antibodies is justified by the increase in process performance. Depending on the load of impurities, the lifespan of the affinity column could be a decisive cost factor.

APPENDIX

List of own publications and presentations related to the dissertation

Paper

Lappöhn, C.A., Oestreich, A.M., Stei, R., Weber, L.G., Maerz, L., Wolff, M.W. Process intensification for the production of a C-tagged antimicrobial peptide in *Escherichia coli* - First steps toward a platform technology. J. Biosci. Bioeng. 136, 5 (2023) doi:10.1016/j.jbiosc.2023.09.003.

Lappöhn, C.A., Maerz, L., Stei, R., Weber, L.G., Wolff, M.W. Optimization and validation of analytical affinity chromatography for the in-process monitoring and quantification of peptides containing a C-tag. J. Chromatogr. B, Anal. Technol. Biomed. life Sci. 1229, 123899 (2023) doi:10.1016/j.jchromb.2023.123899.

Conference contributions

Lappöhn, C.A., Wolff, M.W.: Economic purification platform for antimicrobial peptides based on small molecular fusion tags, online, European Federation of Biotechnology 2021.

Lappöhn, C.A., Wolff, M.W.: An Economic Purification Platform for Insect-Derived Antimicrobial Peptides, online, INSECTA Conference 2021.

Lappöhn, C.A., Stei, R., Weber, L.G., Maerz, L., Wolff, M.W.: Optimized Production Platform for the Insect Metalloproteinase Inhibitor (IMPI), Gießen, INSECTA Conference 2022. (Best Poster Award)

Others

Lappöhn, C.A., Stei, R., Weber, L.G., Maerz, L., Wolff, M.W.: Entwicklung und Etablierung einer Plattformtechnologie zur Herstellung antimikrobieller Peptide, Gießen, Interdisziplinäres Promovierenden-Kolloquium der THM, 2022.

Significance of final theses

Some of the results presented below were obtained as part of student research projects. Conception and planning of the experiments, evaluation and validation of the results as well as their visualization were carried out by Carolin Anna Lappöhn. The analysis and practical work was carried out in part by the students and in part by Carolin Anna Lappöhn.

Master's thesis by Robin Stei: "Entwicklung und Charakterisierung eines chromatographischen Aufreinigungsprozesses zur rekombinanten Produktion antimikrobieller Peptide (AMP)"

Master thesis by Lea Maerz: "Optimization and validation of an analytical affinity chromatography for in-process quantification of C-tagged antimicrobial peptides"

Master's thesis by Linus Georg Weber: "Establishment and optimization of the chromatographic downstream process of a recombinantly produced antimicrobial peptide"

Bachelor's thesis by Daria Dudnik: "Optimierung der rekombinanten Herstellung des Insektenmetalloproteinase-Inhibitors in *Escherichia coli*"

Research and development project by Robin Stei: "IMPI Produktion in Rosetta-gami 2"

Research and development project by Linus Georg Weber: "Optimierung der rekombinanten Proteinproduktion in *Escherichia coli* Rosetta-gami 2"

Research and development project by Daria Dudnik: "Expressionsstammscreening zur Herstellung eines antimikrobiellen Peptides

SUPPLEMENTARY MATERIAL

Supplementary Material: Production and purification of an insect-derived AMP

Lappöhn, C.A., Oestreich, A.M., Stei, R., Weber, L.G., Maerz, L., Wolff, M.W. Process intensification for the production of a C-tagged antimicrobial peptide in *Escherichia coli* - First steps toward a platform technology. J. Biosci. Bioeng. 136, 5 (2023) doi:10.1016/j.jbiosc.2023.09.003

Supplementary Materials Text S1:

2.1.1 Strains

E. coli NEB10β

Chemically competent *E. coli* from New England Biolabs.
Genotype: Δ(ara-leu) 7697 araD139 fhuA ΔlacX74 galK16 galE15 e14$^-$ ϕ80dlacZΔM15 recA1 relA1 endA1 nupG rpsL (Str^R) rph spoT1 Δ(mrr-hsdRMS-mcrBC).

E. coli Rosetta-gami 2(DE3) pLysS

Including vector pLysSRARE2. Chemically competent *E. coli* from Merck.
Genotype: Δ(ara–leu)7697 ΔlacX74 ΔphoA PvuII phoR araD139 ahpC galE galK rpsL(DE3) F′[lac$^+$ lacI^q pro] gor522:Tn10 trxB pLysSRARE2 (Cam^R Str^R Tet^R).

2.1.2 Plasmid constructs, primers and PCR conditions

pGG117 (4516bp)

lacI. pILV5. Gentamicin resistance. tAOD. pUC origin. RBS. His_6 tag. Trx. Thr. IMPI. T7 promoter/terminator

pGG117C (4528bp)

lacI. pILV5. Gentamicin resistance. tAOD. pUC origin. RBS. His_6 tag. Trx. Thr. IMPI. C-tag (EPEA). T7 promoter/terminator

Primers used for Q5 site-directed mutagenesis:

Q5SDM_GG117_F 5′-GAA GCG TAA TGG GTA ATT GAT TAA TAC CTA G-3′ T_m = 72 °C
Q5SDM_GG117_R 5′-CGG TTC GCT ACG GAT TTT CGG ACA G-3′ T_m = 65 °C

2.1.3. Product characteristics

Expression product: His_6-Trx-Thr-IMPI-C

Amino acid sequence:
HHHHHHSESDKIIHLTDDSFDTDVLKADGAILVDFWAEWCGPCKMIAPILDEIADEYQGKLTVAKL
NIDQNPGTAPKYGIRGIPTLLLFKNGEVAATKVGALSKGQLKEFLDANLAEQGGGSLVPRGSIVLI
CNGGHEYYECGGACDNVCADLHIQNKTNCPIINVRCNDKCYCEDGYARDVNGKCIPIKDCPKIRS
EPEA
Number of amino acids: 201
Molecular weight: 21901.85 Da
Grand average of hydropathicity (GRAVY): –0.298
Theoretical pI: 5.41

Expression product: His_6-Trx-Thr-IMPI

Amino acid sequence:
HHHHHHSESDKIIHLTDDSFDTDVLKADGAILVDFWAEWCGPCKMIAPILDEIADEYQGKLTVAKL
NIDQNPGTAPKYGIRGIPTLLLFKNGEVAATKVGALSKGQLKEFLDANLAEQGGGSLVPRGSIVLI
CNGGHEYYECGGACDNVCADLHIQNKTNCPIINVRCNDKCYCEDGYARDVNGKCIPIKDCPKIRS
Number of amino acids: 197
Molecular weight: 21475.43 Da
Grand average of hydropathicity (GRAVY): –0.269
Theoretical pI: 5.67

IMPI

Amino acid sequence:
IVLICNGGHEYYECGGACDNVCADLHIQNKTNCPIINVRCNDKCYCEDGYARDVNGKCIPIKDCP
KIRS
Number of amino acids: 69
Molecular weight: 7653.76 Da

Grand average of hydropathicity (GRAVY): –0.319

IMPI+C-tag

Amino acid sequence:
IVLICNGGHEYYECGGACDNVCADLHIQNKTNCPIINVRCNDKCYCEDGYARDVNGKCIPIKDCP
KIRSEPEA
Number of amino acids: 73
Molecular weight: 8080.19 Da
Grand average of hydropathicity (GRAVY): –0.395

BR029C

Amino acid sequence:
KWKIFKKIEKAGRNIRDGIIKAGPAVSVVGEAATIYKTGEPEA
Number of amino acids: 43
Molecular weight: 4641.40 Da
HPLC purity: 90.0%

BR029H

Amino acid sequence:
KWKIFKKIEKAGRNIRDGIIKAGPAVSVVGEAATIYKTGHHHHHH
Number of amino acids: 45
Molecular weight: 5037.81 Da
HPLC purity: 99.9%

C-tag

Amino acid sequence: EPEA
Number of amino acids: 4
Molecular weight: 444.44 Da
Grand average of hydropathicity (GRAVY): –0.45
Theoretical pI: 3.80

Supplementary Materials Text S2:

2. Production of the in-house IMPIC standard

2.1. Strain and plasmid constructs

E. coli Rosetta-gami 2(DE3) pLysS and pGG117C (see Supplementary Text S1)

2.2. Cultivation and IMPI expression

RG2 pGG117C cells were cultivated in terrific broth supplemented with 34 mg L^{-1} chloramphenicol and 15 mg L^{-1} gentamicin. The optimized cultivation parameters were applied, starting from cryo-cultures (ΔOD_{600} = 0.2 at 32 °C). When the ΔOD_{600} reached 2.8, we added 1.4 mM IPTG and continued cultivation for another 4 h.

2.3. Cell harvest and disruption

The cells were harvested by centrifugation (16,000 g, 4 °C, 5 min) 4 h post-induction and were diluted with PBS (20% w/v biomass) and disrupted by two cycles of high-pressure homogenization (~2000 bar). The cell lysate was clarified by centrifugation (16,000 g, 4 °C, 1 h) and passed through a 0.45-µm cellulose acetate filter (Avantor, Radnor, PA, USA). For specificity studies, a product-free RG2 cell lysate was prepared by enzymatic disruption using BugBuster master mix followed by DNA digestion with 250 U mL^{-1} DENARASE (c-LEcta, Leipzig, Germany).

2.4. Immobilized metal ion affinity chromatography (IMAC)

A 1-mL HisTrap FF crude column was mounted on an ÄKTA fast protein liquid chromatography (FPLC) system and was flushed with 10 column volumes (CV) of equilibration buffer (20 mM sodium phosphate buffer, 500 mM NaCl, 20 mM imidazole, pH 7.4). We then loaded 25 ml of clarified lysate supplemented with 20 mM imidazole at a flow rate of 150 cm h^{-1}. The column was washed with 10 CV of equilibration buffer, followed by elution in 5 CV elution buffer (20 mM sodium phosphate buffer, 500 mM NaCl, 500 mM imidazole, pH 7.4). The elution peak was detected by measuring the absorbance at 280 nm.

2.5. Purification of the IMPIC standard by reversed-phased chromatography

The IMAC eluate was purified by RP-FPLC using a 3-mL RESCOURCE column (Cytiva). The column was equilibrated with 10 CV 95% (v/v) ultrapure water/acetonitrile and 0.1% trifluoroacetic acid (TFA) at a flow rate of 3 cm h^{-1}. After loading each 2-mL sample, we applied a linear gradient from 5% to 95% acetonitrile over 9 CV. Product-containing fractions were collected, pooled, and freeze-dried (0.2 bar, –52 °C) using an Alpha 1-4 LD plus device (Martin Christ Gefriertrocknungsanlagen, Osterode am Harz, Germany). The purified AMP was resuspended in methanol, centrifuged (20,000 g, 4 °C, 10 min) and evaporated. The standard was dissolved in ultrapure water and freeze-dried before use.

2.6. Analytical reversed-phased chromatography

Samples were prepared using an XSelect Peptide CSH C18 Column (130 Å, 2.5 µm, 2.1 × 150 mm; Waters, Framlington, MA, USA) mounted on an Ultimate 3000 UHPLC System RS (Thermo Fisher Scientific) with Chromeleon v7.2 SR4 software (Thermo Fisher Scientific) to determine the purity of the lyophilized IMPIC standard. A 30-min gradient was established at a flow rate of 0.40 mL min^{-1} from 95% water + 5% acetonitrile (HPLC-grade, Carl Roth) + 0.1% trifluoroacetic acid (TFA; LC-MS grade, Carl Roth) to 5% water + 95% acetonitrile + 0.1% TFA. The RS diode array detector was used at wavelengths of 214 / 220 / 254 / 280 nm.

2.7. SDS-PAGE and western blot

Samples were mixed with 4× Laemmli sample buffer containing 5% 2-mercaptoethanol and were heated at 95 °C for 5 min. Aprotinin (≥ 3.0 PEU mg^{-1}) was used as the quantification standard. Samples were loaded onto a 4–20% TGX Stain-Free Gel alongside Precision Plus Protein Unstained Standard. Gels were visualized and assessed by densitometry using the ChemiDoc MP system (Software Image Lab v5.2). Gels were stained using the Pierce Silver Stain Kit.

For western blotting, proteins were transferred from gels to a TransferPac Midi 0.2 µm polyvinylidene diflouride (PVDF) membrane using the Trans-Blot Turbo Transfer System at 2.5 A and 25 V for 7 min. The membrane was then blocked with 5% BSA in PBS for 2 h and washed three times in 0.1% (v/v) Tween-20/PBS. We then incubated the membrane for 2 h in the HRP-conjugated anti-His_5 primary antibody (diluted 1:5000) or HRP-conjugated anti-IMPI(I38V) (diluted 1:10,000) and the Precision Protein StrepTactin alkaline phosphatase (AP) conjugate in 0.05% (v/v) Tween-20/PBS. The signal was visualized using the ChemiDoc MP system as described above.

2.8. Bradford assay

A transparent 96-well plate (Bio-Tek Instruments) was used to measure total protein compared to 0.05 to 0.95 g L^{-1} of standard (BSA) and a blank. Bradford reagent (0.1 g L^{-1} Coomassie Brilliant Blue, 4.75% (v/v) ethanol, 10% (v/v) phosphoric acid) was passed through a 0.45-µm cellulose acetate filter before centrifugation (5000 g, 5 min, room temperature) and stored in the dark. We then added 270 µL Bradford reagent to each well and incubated in a Synergy HT plate reader for 5 min at 30 °C. We measured the absorbance at 450 and 595 nm and calculated the ratio. The RSD was 3%.

Supplementary Materials Figure S1:

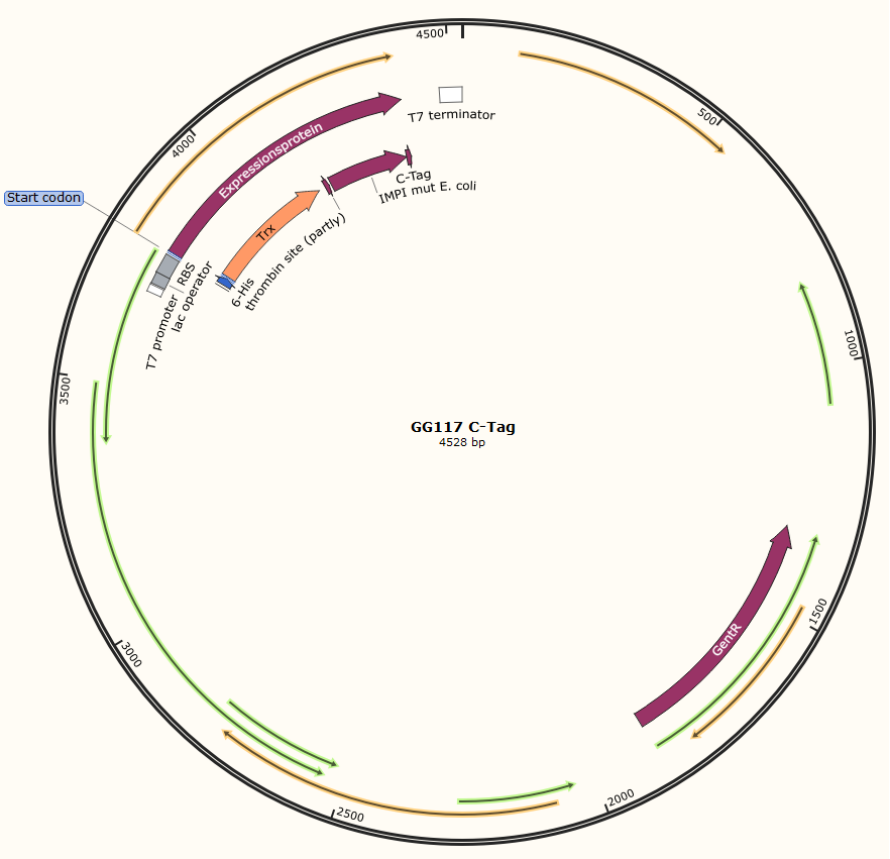

Figure S1: Schematic representation of pGG117C. Abbreviations: lacI (Lac promoter/operator); $Gent^R$ (gentamicin resistance); pUC origin (replication origin); RBS (ribosome binding site); 6-His (His_6 tag); Trx (thioredoxin); Thr (thrombin cleavage site); IMPI (insect metalloproteinase inhibitor); C-tag (EPEA); T7 promoter/terminator

Supplementary Materials Figure S2:

3.1 Effect of the C-tag on cell growth and IMPI production

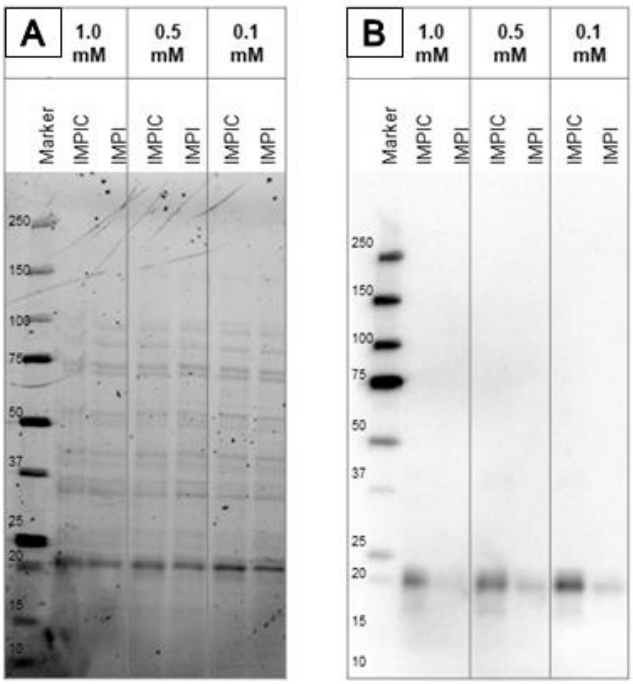

Figure S2: Comparison of three different IPTG concentrations (1.0, 0.5 and 0.1 mM) in RG2 pGG117 cell lysates containing IMPI and RG2 pGG117C cell lysates containing IMPIC. The Precision Plus Protein Unstained Standard was used as a marker, and samples were normalized to ΔOD_{600} = 1.7. (A) SDS-PAGE in 4–20% TGX Stain-Free gels. (B) Western blot probed with the anti-His_5-HRP conjugate and StrepTactin AP. IMPI and IMPIC are both visible as bands at ~20 kDa.

Supplementary Materials Figure S3:

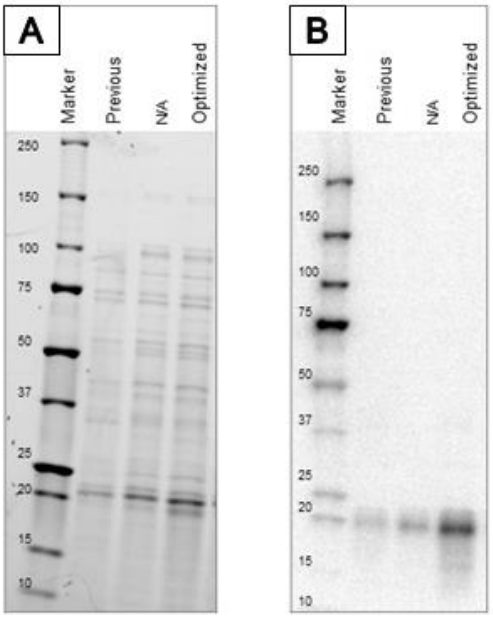

Figure S3: Comparison of initial cultivation conditions (37 °C, 1.0 mM IPTG at ΔOD_{600} = 1.0) with the optimized process (32 °C, 1.4 mM IPTG at ΔOD_{600} = 2.8) in RG2 pGG117C cell lysates containing IMPIC. The Precision Plus Protein Unstained Standard was used as a marker, and samples were normalized to ΔOD_{600} = 1.7. (A) SDS-PAGE in 4–20% TGX Stain-Free gels. (B) Western blot probed with the anti-His_5-HRP conjugate and StrepTactin AP. IMPI and IMPIC are both visible as bands at ~20 kDa.

Supplementary Materials FigureS4:

3.3 Comparison of IMPI activity after C-terminal modification

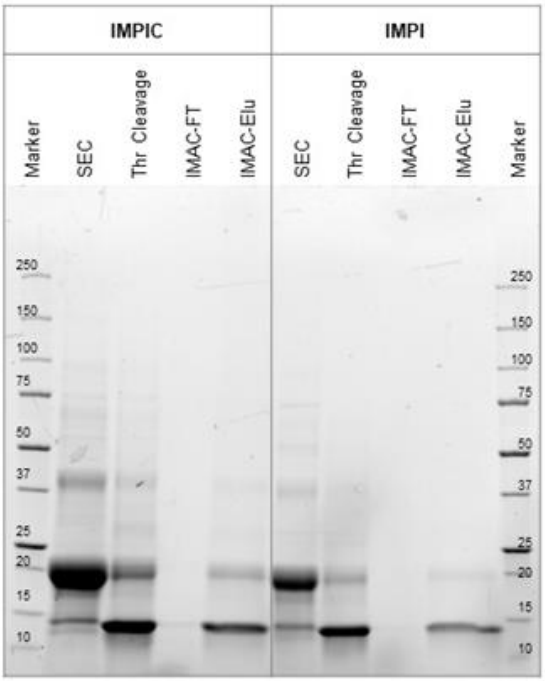

Figure S4: Purification of IMPIC and IMPI. The process consisted of size exclusion chromatography (SEC) and buffer exchange of the products (N-terminal His_6 tag; expected at ~20 kDa), followed by thrombin digestion into the cleavage products (N-terminal His_6 tag, fusion part, expected at ~ 4 kDa, IMPI/IMPIC expected at ~8 kDa). The flow-through (IMAC-FT) fraction is expected to contain the product and the eluate (IMAC-Elu) the residual fusion component. SDS-PAGE in 4–20% TGX Stain-Free gels with Precision Plus Protein Unstained Standard used as a marker.

Supplementary Materials FigureS5:

3.3 Comparison of IMPI activity after C-terminal modification

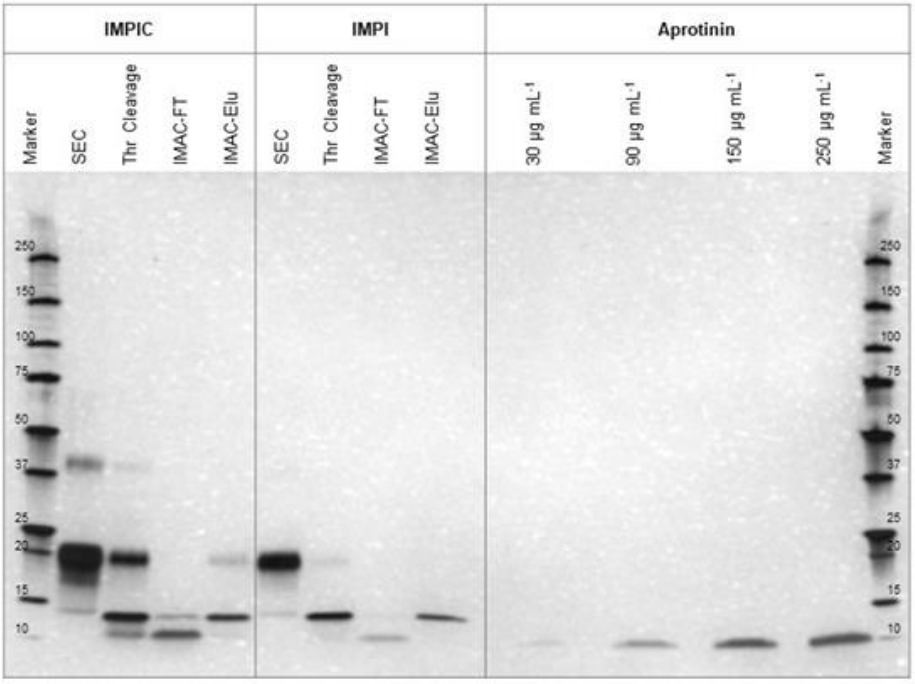

Figure S5: Purification of IMPIC and IMPI. The process consisted of size exclusion chromatography (SEC) and buffer exchange of the products (N-terminal His_6 tag; expected at ~20 kDa), followed by thrombin digestion into the cleavage products (N-terminal His_6 tag, fusion part, expected at ~4 kDa, IMPI/IMPIC expected at ~8 kDa). The flow-through (IMAC-FT) fraction is expected to contain the product and the eluate (IMAC-Elu) the residual fusion component. SDS-PAGE in 4–20% TGX Stain-Free gels followed by silver staining. Aprotinin (30/90/150/250 µg mL^{-1}) was used as a semi-quantitative standard and Precision Plus Protein Unstained Standard used as a marker.

Supplementary Materials FigureS6:

3.3 Comparison of IMPI activity after C-terminal modification

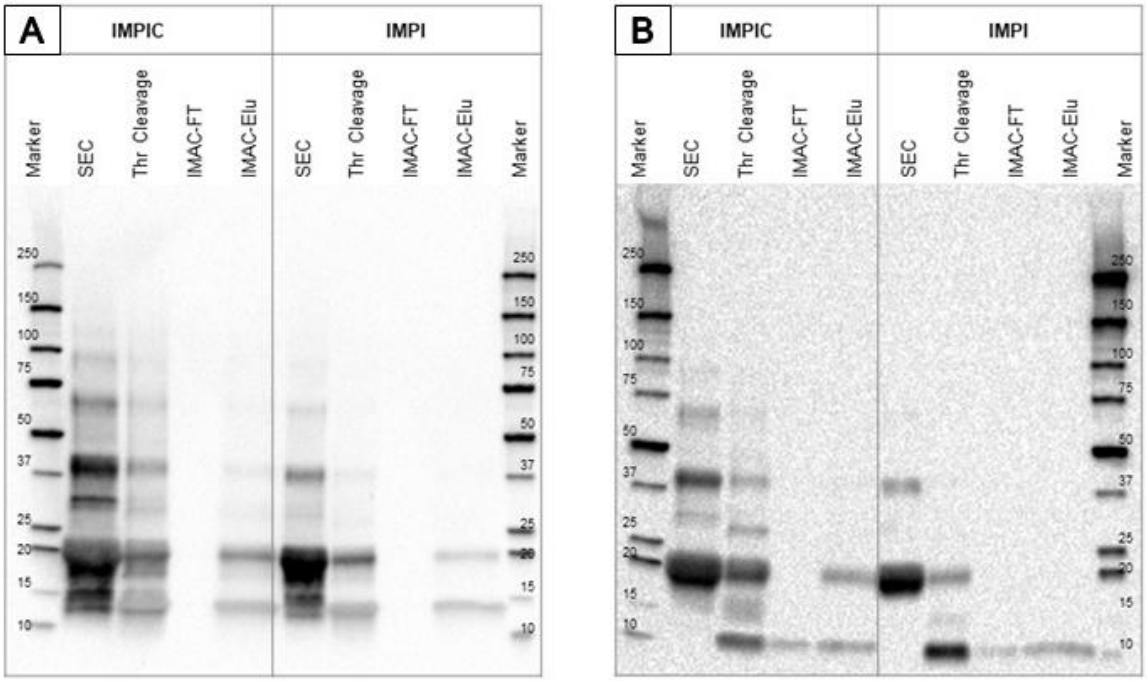

Figure S6: Purification of IMPIC and IMPI. The process consisted of size exclusion chromatography (SEC) and buffer exchange of the products (N-terminal His_6 tag; expected at ~20 kDa), followed by thrombin digestion into the cleavage products (N-terminal His_6 tag, fusion part, expected at ~ 4 kDa, IMPI/IMPIC expected at ~8 kDa). The flow-through (IMAC-FT) fraction is expected to contain the product and the eluate (IMAC-Elu) the residual fusion component. Precision Plus Protein Unstained Standard was used as marker. (A) Western blot probed with the anti-His_5-HRP conjugate and StrepTactin AP. (B) Western blot probed with the anti-IMPI-HRP conjugate and StrepTactin AP.

Supplementary Materials Table S1:

3.2 Experimental design for production process intensification

Table S1: Analysis of variance (ANOVA) of the reduced quadratic response surface model. X_1 = induction time (h), X_2 = IPTG concentration (mM), X_3 = temperature (°C).

Source	Sum of squares	df	Mean square	F-value	p-value
Model	12.300	7	1.7600	44.070	< 0.0001
X_1	0.0000	1	0.0000	0.0004	0.9842
X_2	0.0204	1	0.0204	0.5125	0.4851
X_3	2.9200	1	2.9200	73.240	< 0.0001
X_1X_3	0.4865	1	0.4865	12.200	0.0033
X_2X_3	1.8800	1	1.8800	47.200	< 0.0001
X_1^2	1.4000	1	1.4000	35.200	< 0.0001
X_2^2	4.1800	1	4.1800	104.970	< 0.0001
Residual	0.5979	15	0.0399		
Lack of fit	0.4044	8	0.0505	1.83	0.2206
Pure error	0.1935	7	0.0276		
Total	12.90	22			

Supplementary Materials Table S2:

3.2 Experimental design for production process intensification

Table S2: Coefficient in terms of coded factors of the quadratic response surface model. X_1 = induction time (h), X_2 = IPTG concentration (mM), X_3 = temperature (°C).

Factor	Coefficient estimate	df	Standard error	95% CI Low	95% CI High	VIF
Intercept	4.95	1	0.078	4.79	5.12	
X_1	-0.0012	1	0.0586	-0.126	0.1237	1.03
X_2	0.0415	1	0.0579	-0.082	0.1649	1.03
X_3	-0.4956	1	0.0579	-0.619	-0.3722	1.02
X_1X_3	-0.2734	1	0.0783	-0.4403	-0.1066	1.05
X_2X_3	-0.5189	1	0.0755	-0.6798	-0.3579	1.05
X_1^2	-0.5575	1	0.094	-0.7578	-0.3572	1.07
X_2^2	-0.9781	1	0.0955	-1.18	-0.7746	1.09

Supplementary Material: Detection and quantification of AMPs

Lappöhn, C.A., Maerz, L., Stei, R., Weber, L.G., Wolff, M.W. Optimization and validation of analytical affinity chromatography for the in-process monitoring and quantification of peptides containing a C-tag. J. Chromatogr. B, Anal. Technol. Biomed. life Sci. 1229, 123899 (2023) doi:10.1016/j.jchromb.2023.123899

Appendix A

Text A1

1. Peptide standards

Recombinant AMP α_c

Sequence:
HHHHHHSESDKIIHLTDDSFDTDVLKADGAILVDFWAEWCGPCKMIAPILDEIADEYQGKLTVAKL
NIDQNPGTAPKYGIRGIPTLLLFKNGEVAATKVGALSKGQLKEFLDANLAEQGGGSLVPRGSIVLI
CNGGHEYYECGGACDNVCADLHIQNKTNCPIINVRCNDKCYCEDGYARDVNGKCIPIKDCPKIRS
EPEA
Number of amino acids: 201
Molecular weight: 21901.85 Da
Grand average of hydropathicity (GRAVY): –0.298
Theoretical pI: 5.41
HPLC purity: > 90%

AMP β_c (chemically synthesized by GenScript Biotech)

Sequence: KWKIFKKIEKAGRNIRDGIIKAGPAVSVVGEAATIYKTGEPEA
Number of amino acids: 43
Molecular weight: 4641.40 Da
GRAVY: –0.319
Theoretical pI: 9.78
HPLC purity: 90.0%

AMP γ_c (kindly provided by Lena Stillger/Prof. Dr.-Ing. Dirk Holtmann, Institute of Bioprocess Engineering and Pharmaceutical Technology, University of Applied Sciences Mittelhessen, Giessen, Germany)

Sequence: KKLLKWLKKLLEPEA
Number of amino acids: 15
Molecular weight: 1837.32 Da
GRAVY: –0.547
Theoretical pI: 9.83
HPLC purity: > 90%

Appendix A

Text A2

2. Production of the recombinant peptide standard AMP α_c

2.1. Strain and plasmid constructs

E. coli NEB10β

Chemically competent *E. coli* from New England Biolabs (Ipswich, MA, USA)
Genotype: Δ(ara-leu) 7697 araD139 fhuA ΔlacX74 galK16 galE15 e14- ϕ80dlacZΔM15 recA1 relA1 endA1 nupG rpsL (Str^R) rph spoT1 Δ(mrr-hsdRMS-mcrBC)

E. coli Rosetta-gami 2(DE3) pLysS

Including vector pLysSRARE2, chemically competent *E. coli* from Merck
Genotype: Δ(ara–leu)7697 ΔlacX74 ΔphoA PvuII phoR araD139 ahpC galE galK rpsL(DE3) F'[lac+ lacI q pro] gor522:Tn10 trxB pLysSRARE2 (Cam^R, Str^R, Tet^R)

pGG117 (4516bp)

lacI, pILV5, gentamicin resistance, tAOD, pUC origin, RBS, His_6 tag, Trx, Thr, IMPI, T7 promoter/terminator

pGG117C (4528bp)

lacI, pILV5, gentamicin resistance, tAOD, pUC origin, RBS, His_6 tag, Trx, Thr, IMPI, C-tag (EPEA), T7 promoter/terminator

Primers used for Q5 site-directed mutagenesis:

Q5SDM_GG117_F 5′-GAA GCG TAA TGG GTA ATT GAT TAA TAC CTA G-3′ T_m = 72 °C
Q5SDM_GG117_R 5′-CGG TTC GCT ACG GAT TTT CGG ACA G-3′ T_m = 65 °C

Table A.1: PCR conditions for Q5 site-directed mutagenesis of pGG117 with Q5 mutagenesis primers Q5SDM_GG117_F and Q5SDM_GG117_R to produce pGG117C.

Temperature	Time	Cycle
98 °C	30 s	1
98 °C	10 s	35
66 °C	30 s	
72 °C	7 min	
72 °C	2 min	1
4 °C	storage	1

The Rosetta-gami 2(DE3)pLysS (ΔtrxB/Δgor mutant) (RG2) strain from Merck was used as an expression system with plasmid GG117C (4528 bp), constructed by Golden Gate cloning and Q5 mutagenesis [32]. This system was used to express the insect metalloprotease inhibitor, known as IMPI(I38V) and here described as AMP α_c, as a fusion product. The fusion product AMP α_c consists of an N-terminal His_6 tag, a thioredoxin (Trx) tag, a thrombin cleavage site (Thr), the IMPI coding sequence, and a C-terminal C-tag consisting of four amino acids (EPEA).

2.2. Cultivation and AMP production

RG2 GG117C cells were cultivated in terrific broth (Carl Roth, Karlsruhe, Germany) supplemented with 34 $mg \cdot L^{-1}$ chloramphenicol and 15 $mg \cdot L^{-1}$ gentamicin. The cultivation parameters were applied, starting from cryo-cultures (ΔOD_{600} = 0.2 at 32 °C). When the ΔOD_{600} reached 3.0, we added 1.5 mM IPTG (Sigma-Aldrich) and continued cultivation for another 4 h.

Appendix A

2.3. Cell harvest and disruption

The cells were harvested by centrifugation (16,000 g, 4 °C, 5 min) 4 h post-induction and were diluted with PBS (20% w/v biomass) and homogenized at 500 bar during the first pass and at 1500 bar during the second and third passes. The cell lysate was clarified by centrifugation (16,000 g, 4 °C, 1 h) and passed through a 0.45-µm cellulose acetate filter (Avantor, Radnor, PA, USA). For specificity studies, a product-free RG2 cell lysate was prepared by enzymatic disruption using BugBuster master mix followed by DNA digestion with 250 U mL^{-1} DENARASE (c-LEcta, Leipzig, Germany).

2.4. Immobilized metal-chelate affinity chromatography (IMAC)

A 1-mL HisTrap FF crude column was mounted on an ÄKTA fast protein liquid chromatography (FPLC) system and was flushed with 10 column volumes (CV) of equilibration buffer (20 mM sodium phosphate buffer, 500 mM NaCl, 20 mM imidazole, pH 7.4). We then loaded 25 ml of clarified lysate supplemented with 20 mM imidazole at a flow rate of 150 cm h^{-1}. The column was washed with 10 CV of equilibration buffer, followed by elution in 5 CV elution buffer (20 mM sodium phosphate buffer, 500 mM NaCl, 500 mM imidazole, pH 7.4). The elution peak was detected by measuring the absorbance at 280 nm.

2.5. Purification of AMP α_c by reversed-phase HPLC

The IMAC eluate was purified by RP-FPLC using a 3-mL RESCOURCE column (Cytiva, Marlborough, MA, USA). The column was equilibrated with 10 CV 95% (v/v) ultrapure water/acetonitrile and 0.1% trifluoroacetic acid (TFA) at a flow rate of 3 cm h^{-1}. After loading each 2-mL sample, we applied a linear gradient from 5% to 95% acetonitrile over 9 CV. Product-containing fractions were collected, pooled, and freeze-dried (0.2 bar, –52 °C) using an Alpha 1-4 LD plus device (Martin Christ Gefriertrocknungsanlagen, Osterode am Harz, Germany). The purified AMP was resuspended in methanol, centrifuged (20,000 g, 4 °C, 10 min) and evaporated. The standard was dissolved in ultrapure water and freeze-dried before use.

2.6. Analytical reversed-phase chromatography

Samples were prepared using an XSelect Peptide CSH C18 Column (130 Å, 2.5 µm, 2.1 × 150 mm; Waters, Framlington, MA, USA) mounted on an Ultimate 3000 UHPLC System RS (Thermo Fisher Scientific) with Chromeleon v7.2 SR4 software (Thermo Fisher Scientific) to determine the purity of the lyophilized AMP α_c standard. A 30-min gradient was established at a flow rate of 0.40 mL min^{-1} from 95% water + 5% acetonitrile (HPLC-grade, Carl Roth) + 0.1% trifluoroacetic acid (TFA; LC-MS grade, Carl Roth) to 5% water + 95% acetonitrile + 0.1% TFA. The RS diode array detector was used at wavelengths of 214 / 220 / 254 / 280 nm.

2.7. SDS-PAGE and western blot

Samples were mixed with 4× Laemmli sample buffer containing 5% 2-mercaptoethanol and were heated at 95 °C for 5 min. Aprotinin (≥ 3.0 PEU mg^{-1}) was used as the quantification standard. Samples were loaded onto a 4–20% TGX Stain-Free Gel alongside Precision Plus Protein Unstained Standard. Gels were visualized and assessed by densitometry using the ChemiDoc MP system (Software Image Lab v5.2). Gels were stained using the Pierce Silver Stain Kit. For western blotting, proteins were transferred from gels to a TransferPac Midi 0.2 µm polyvinylidene diflouride (PVDF) membrane using the Trans-Blot Turbo Transfer System at 2.5 A and 25 V for 7 min. The membrane was then blocked with 5% BSA in PBS for 2 h and washed three times in 0.1% (v/v) Tween-20/PBS. We then incubated the membrane for 2 h in the HRP-conjugated anti-His_5 primary antibody (diluted 1:5000) or HRP-conjugated anti-IMPI(I38V) (diluted 1:10,000) and the Precision Protein StrepTactin alkaline phosphatase (AP) conjugate in 0.05% (v/v) Tween-20/PBS. The signal was visualized using the ChemiDoc MP system as described above.

Appendix B

3.1. Optimization of the HPLC method by design of experiments

Table B1: Coefficient of coded factors / coded equation – coefficient estimate (Coded) with standard error (SE) and actual equations (Actual) – of the response surface methodology for the responses.

	Equation of the response					
	Y_1			Y_2		
Factor	**Coded**	**SE**	**Actual**	**Coded**	**SE**	**Actual**
Intercept	98.92	0.0644	97.00224	19.13	0.4675	35.49063
X_1	0.1688	0.0459	-0.004467	-0.1052*	0.3441*	0.087263*
X_2	-0.3374	0.0484	2.03802	-0.2090*	0.3687*	10.83540*
X_3	-	-	-	-7.85	0.3457	-21.07616
X_4	-0.0059*	0.0485*	0.057276*	-0.2159*	0.3582*	0.192380*
X_1X_2	0.1202	0.0576	0.006411	-	-	-
X_1X_3	-	-	-	-1.07	0.4053	-0.048785
X_1X_4	-	-	-	-	-	-
X_2X_3	-	-	-	-	-	-
X_2X_4	-	-	-	-	-	-
X_3X_4	-	-	-	-	-	-
X_1^2	-	-	-	-	-	-
X_2^2	-0.4256	0.0800	-0.756627	-1.79	0.6020	-3.17544
X_3^2	-	-	-	2.72	0.6220	3.55305
X_4^2	-0.2578	0.0778	-0.001650	-0.9360	0.5478	-0.005990

	$(Y_3)^{-0.5}$			Y_4		
Factor	**Coded**	**SE**	**Actual**	**Coded**	**SE**	**Actual**
Intercept	0.6993	0.0060	0.454564	12665,64	637.56	-21179.1212
X_1	-0.0692	0.0048	0.002459	-4031,34	515.83	-122.73641
X_2	-0.0471	0.0048	0.226101	-2711.88	528.99	40825.68391
X_3	0.0790	0.0056	0.120828	8622.61	610.05	7888.11377
X_4	0.0338	0.0053	-0.013235	2616.59	575.16	-529.05308
X_1X_2	-0.0617	0.0056	-0.003292	-1473.08	613.70	-78.56407
X_1X_3	-0.0161	0.0065	-0.000735	-1577.47	712.62	-72.11299
X_1X_4	0.0341	0.0066	0.000109	4181.82	723.01	13.38182
X_2X_3	-0.0155	0.0067	-0.023678	-	-	-
X_2X_4	0.0540	0.0067	0.005756	-	-	-
X_3X_4	0.0183	0.0071	0.001674	2355.70	767.03	215.37841
X_1^2	-	-	-	-	-	-
X_2^2	-0.0423	0.0083	-0.075137	-6826.73	876.02	-12136.4046
X_3^2	-	-	-	-	-	-
X_4^2	-	-	-	-	-	-

*Responses: recovery (Y_1; %), peak area (Y_2; mAu min), peak asymmetry (Y_3; –), and plate count N (Y_4; -) with the factors glycine concentration (X_1), pH (X_2), flow rate (X_3) and temperature (X_4). *Non-significant terms are included to maintain the model hierarchy.*

Appendix B

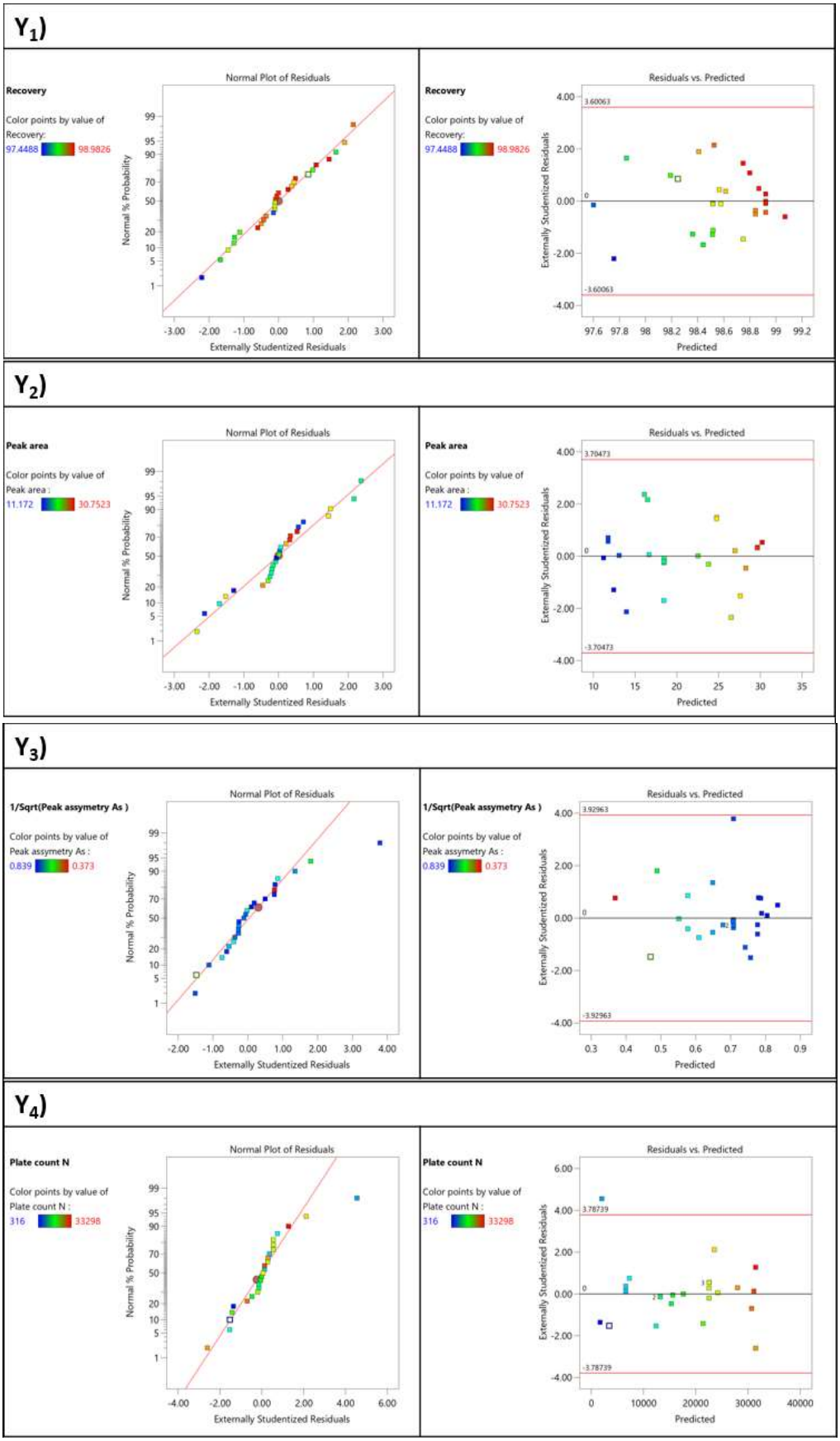

Figure B1: Normal plot of the residuals and residuals vs predicted plot of the response surface methodology for the responses recovery (Y_1; %), peak area (Y_2; mAu min), peak asymmetry (Y_3; –) and plate count N (Y_4; –).

Appendix B

Table B2: Results of the confirmation runs at the factor setting of 32 mM glycine, pH = 1.54, flow rate = 1.545 mL min^{-1}, and 22 °C of the response surface methodology.

Response	Predicted mean	Standard deviation	95 % PI low	Data mean	95 % PI high
Y_1	98.9809	0.185281	98.7243	98.79	99.2376
Y_2	22.2784	1.2272	20.4988	22.41	24.0581
Y_3	2.2149	0.114591	2.04809	2.31	2.39292
Y_4	18834.7	1914.71	16046.1	15901	21623.4

The data are means (n = 3) of the responses recovery (Y_1; %), peak area (Y_2; mAu min), peak asymmetry (Y_3; –), and plate count N (Y_4; –), the predicted mean with standard deviation, and the lower and upper limits of the 95% prediction interval (95% PI low/high).

Appendix C

3.2. Validation of the HPLC method using ICH Guideline Q2(R2)

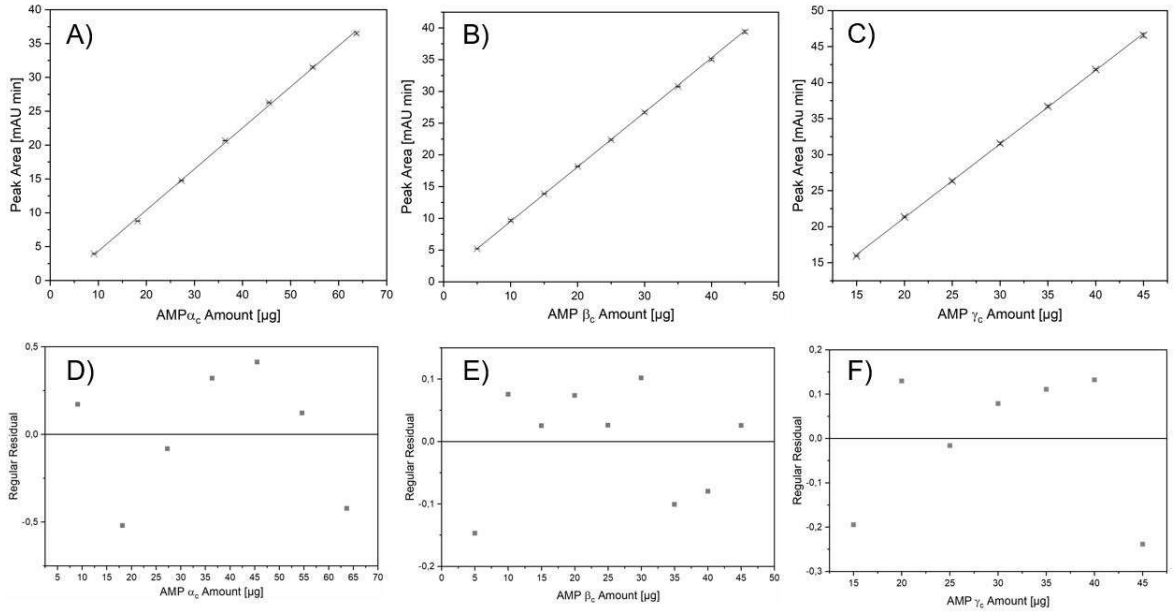

Figure C1: Calibration and residual plots of AMP α_c, AMP β_c and AMP γ_c. Graphs (A), (B) and (C) show the peak area [mAU min] over the peptide amount [µg]. The error bars indicate standard deviations (n = 3). Data points are gray crossed distributed along the calibration line. Graphs (D), (E) and (F) plot the regular residuals (gray squares) against the peptide amount [µg] and a zero line.